Polymer nanoparticles and their supracolloidal monolithic structures for applications in separation science

By

Aminreza Khodabandeh PhD

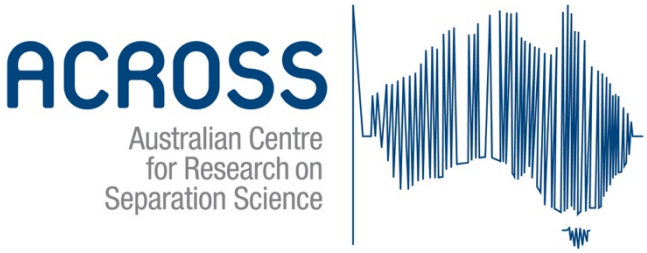

School of Physical Sciences

University of Tasmania

December 2016

Declaration

This thesis contains no material which has been accepted for a degree or diploma by the University or any other institution, except by way of background information and duly acknowledged in the thesis, and to the best of the my knowledge and belief no material previously published or written by another person except where due acknowledgement is made in the text of the thesis, nor does the thesis contain any material that infringes copyright.

The publishers of the papers in this thesis hold the copyright for that content, and access to the material should be sought from the respective journals. The remaining non published content of the thesis may be made available for loan and limited copying and communication in accordance with the Copyright Act 1968.

The research associated with this thesis abides by the international and Australian codes on human and animal experimentation, the guidelines by the Australian Government's Office of the Gene Technology Regulator and the rulings of the Safety, Ethics and Institutional Biosafety Committees of the University

Aminreza Khodabandeh
December 2016

Acknowledgements

I feel very fortunate to have worked under the direction of Prof. Emily Hilder for the past four years. During my time at UTAS, Emily gave me room to improvise and allowed me to develop as a researcher through experimentation. Throughout my PhD candidature I have been assisted, advised and guided by my co-supervisors Dr. R. Dario Arrua and Dr. Stuart Thickett. I have been extremely lucky to have a supervisory team who cared so much about my work, and who responded to my questions and queries so promptly. I also want to thank Prof. Stefan Bon from the University of Warwick for his continued encouragement and help through out my PhD who without there would probably be no completed thesis. I would like to acknowledge the support of Australian Government for providing me with funding.

There is not really space to properly thank everyone but I would like to mention my very bestest friends who have been there for me over my time in Hobart, amongst others and in no particular order; Julie Viecieli, Geoff Howard, Sir Max Bingham, Dr. Esme Candish, Dr. Tom Karazian, Dr. Sara Sandron, Dr. Joan Marc Cabot Canyelles, Dr. Sinéad Ní Chiardubháin, Dr. María Florencia Torres, Cecil, Rahbar, Marina, Chris D, Adam, Chris T, Ben, Daniel, Ali, Reyne, Andrew and Brendon. My living in Hobart has been made all the more enjoyable.

It was a pleasure to be a member of the Australian Center for research on separation science (ACROSS). I would like to thank all members of the center; the students, post docs and staffs for offering their assistance and friendships throughout my candidature.

My sincere gratitude goes to all of the technical staff in the School of Physical Sciences, and Central Science Laboratory (UTAS) for all of their

expertise and help. I would like to thank in particular Dr. Karsten Gömann and Dr. Sandrin Feig for assistance with scanning electron microscopy as well as Dr. James Horne for assistance with NMR, A/Prof. Noel Davies for assistance with Mass- Spectroscopy (Central Science Laboratory, University of Tasmania) and Dr. Thomas Rodemann for the RAMAN and FTIR analysis carried out and all the help and input given in the work.

Last but not least, I would like to thank my beloved family, my wonderful parents, Mehdi and Fateme, my brothers Reza and Vahid that have supported me constantly throughout my studies and in all other areas of my life.

Without the love and support of my amazing wife Maryam none of what I have achieved would have been possible. She has been a rock of wisdom, intelligence, kindness and, although she would not admit it, patience. I look forward to the rest of our adventure together.

Statement of co-authorship

The following people and institutions contributed to the publication of work undertaken as part of this thesis:

Aminreza Khodabandeh, School of Physical Sciences, UTAS = Candidate

R. Dario Arrua, School of Physical Sciences, UTAS = Author 1

Stuart C. Thickett, School of Physical Sciences, UTAS = Author 2

Stefan A.F. Bon, Department of Chemistry, University of Warwick, United Kingdom= Author 3

Chris T. Desire, School of Physical Sciences, UTAS = Author 4

Fotouh R. Mansour, School of Physical Sciences, UTAS = Author 5

Thomas Rodemann, Central Science Laboratory, UTAS = Author 6

Bryan R. Coad, Future Industries Institute, UniSA = Author 7

Takuji Ohigashi, Institute for Molecular Science, Okazaki, Japan = Author 8

Nobuhiro Kosugi, Institute for Molecular Science, Okazaki, Japan = Author 9

Emily F. Hilder, School of Physical Sciences, UTAS = Author 10

Author details and their roles:

Paper 1 < Preparation of inverse polymerized high internal phase emulsions using an amphiphilic macro-RAFT agent as sole stabilizer>

Located in **chapter 2**

Candidate was the primary author (65%) with author 2 (5%). Author 1, 3 and 10 (10% respectively) contributed to the idea, and its formalisation and development. Author 4 assisted with refinement and presentation. Author 6 provided assistance with specialised instrumentation.

Paper 2 < PEO-based brush-type amphiphilic macro-RAFT agents and their assembled polyHIPE monolithic structures for applications in separation science >

Located in **chapter 3**

Candidate was the primary author (65%) with author 5 (5 %). Author 1, 2 and 10 (10 % respectively) contributed to the idea, and its formalisation and development.

Paper 3 < Morphology control in polymerised high internal phase emulsion templated via macro-RAFT agent composition: Visualizing surface chemistry>

Located in **chapter 4**

Candidate was the primary author (65%) with author 1 (15 %). Author 2 and 10 (10% respectively) assisted with refinement and presentation. Author 6, 7, 8 and 9 provided assistance with specialised instrumentation.

We the undersigned agree with the above stated "proportion of work undertaken" for each of the above published (or submitted) peer-reviewed manuscripts contributing to this thesis:

Signed: Candidate _____

Author 1 _____

Author 2 _____

Author 3 _____

Author 4 _____

Author 5 _____

Author 6 _____

Author7 _____

Author8 _____

Author 9 _____

Author 10 _____

Date: 1st December 2016

Statement of co-authorship

Aminreza Khodabandeh, School of Physical Sciences, UTAS = Candidate

R. Dario Arrua, School of Physical Sciences, UTAS = Author 1

Stuart C. Thickett, School of Physical Sciences, UTAS = Author 2

Stefan A.F. Bon, Department of Chemistry, University of Warwick, United Kingdom= Author 3

Chris T. Desire, School of Physical Sciences, UTAS = Author 4

Fotouh R. Mansour, School of Physical Sciences, UTAS = Author 5

Thomas Rodemann, Central Science Laboratory, UTAS = Author 6

Bryan R. Coad, Future Industries Institute, UniSA = Author 7

Takuji Ohigashi, Institute for Molecular Science, Okazaki, Japan = Author 8

Nobuhiro Kosugi, Institute for Molecular Science, Okazaki, Japan = Author 9

Emily F. Hilder, School of Physical Sciences, UTAS = Author 10

Author details and their roles:

Paper 1 < Preparation of inverse polymerized high internal phase emulsions using an amphiphilic macro-RAFT agent as sole stabilizer>

Located in **chapter 2**

Candidate was the primary author (65%) with author 2 (5%). Author 1, 3 and 10 (10% respectively) contributed to the idea, and its formalisation and

development. Author 4 assisted with refinement and presentation. Author 6 provided assistance with specialised instrumentation.

Paper 2 < PEO-based brush-type amphiphilic macro-RAFT agents and their assembled polyHIPE monolithic structures for applications in separation science >

Located in **chapter 3**

Candidate was the primary author (65%) with author 5 (5 %). Author 1, 2 and 10 (10 % respectively) contributed to the idea, and its formalisation and development.

Paper 3 < Morphology control in polymerised high internal phase emulsion templated via macro-RAFT agent composition: Visualizing surface chemistry>

Located in **chapter 4**

Candidate was the primary author (65%) with author 1 (15 %). Author 2 and 10 (10% respectively) assisted with refinement and presentation. Author 6, 7, 8 and 9 provided assistance with specialised instrumentation.

We the undersigned agree with the above stated "proportion of work undertaken" for each of the above published (or submitted) peer-reviewed manuscripts contributing to this thesis:

Signed: –

Emily Hilder
Supervisor
School of Physical Sciences
University of Tasmania

John Dickey
Head of School
School of Physical Sciences
University of Tasmania

21/4/17

List of publications and presentations

1. Khodabandeh, A., Arrua, R. D., Desire, C. T., Rodemann, T., Bon, S. A. F., Thickett S. C., & Hilder, E. F. 2016. Preparation of inverse polymerized high internal phase emulsions using an amphiphilic macro-RAFT agent as sole stabilizer. Polymer Chemistry (**Chapter 2**).

2. Khodabandeh, A., Arrua, R. D., Mansour, F. R., Thickett S. C., & Hilder, E. F. 2016. PEO-based brush-type amphiphilic macro-RAFT agents and their assembled polyHIPE monolithic structures for applications in separation science. Nature - Scientific Reports (**Chapter 3**).

3. Khodabandeh, A., Arrua, R. D., Coad, B. R., Rodemann, T., Ohigashi, T., Kosugi, N., Thickett S. C., & Hilder, E. F. 2016. Morphology control in polymerised high internal phase emulsion templated via macro-RAFT agent composition: Visualizing surface chemistry. Polymer Chemistry (*In preparation)* (**Chapter 4**).

4. Khodabandeh, A., Arrua, R. D., Desire, C.T., Bon, S. A. F., & Hilder, E. F. 2013. High internal phase emulsions stabilized by both functionalized polymeric nanoparticles and polymeric surfactants: First step to prepare new class of separation media (Poster presentation). **HPLC 2013** - 40th International Symposium on High Performance Liquid Phase Separations and Related Techniques. Hobart, Australia.

5. Khodabandeh, A., Arrua, R. D., Desire, C. T., Rodemann, T., & Hilder, E. F. 2014. High internal phase emulsions stabilized by functionalized copolymer: Effect of emulsion formulation on the pore structure of polyHIPEs (Oral presentation). **MACRO 2014** - 46th IUPAC world polymer congress. Chiang Mai, Thailand.

6. Khodabandeh, A., Desire, C. T., Arrua, R. D., & Hilder, E. F. 2014. High internal phase emulsions stabilized from a functionalized macro-RAFT agent (Poster presentation). **RACI workshop on polymer nanoparticles, self-assembly and colloids**. Sydney, Australia.

7. Khodabandeh, A., Arrua, R. D., Desire, C.T., Bon, S. A. F., & Hilder, E. F. 2014. (Oral presentation). **RACI National Congress 2014**. High internal phase emulsions stabilized from a functionalized Macro-RAFT agent. Adelaide, Australia.

8. Khodabandeh, A., Arrua, R. D., Desire, C.T., Bon, S. A. F., & Hilder, E. F. 2014. (Poster presentation). **ACIS 2015** - Australian Colloid and

Interface Symposium. Amphiphilic macro-RAFT agent as a sole emulsifier for stabilized an inverse high internal phase emulsion. Hobart, Australia.

9. Khodabandeh, A., Arrua, R. D., Mansour, F. R., Thickett S. C., & Hilder, E. F. 2016. (Oral presentation). **AnaChem 2016** - RACI Analytical and Environmental Chemistry Division meeting. PEO-based brush-type amphiphilic macro-RAFT agents and their assembled polyHIPE monolithic structures for applications in separation science. Adelaide, Australia.

10. Khodabandeh, A., Arrua, R. D., Rodemann, T., Thickett S. C., & Hilder, E. F. 2016. (Oral presentation). **36th APS** - Australasian Polymer Symposium. High internal phase emulsions stabilized by functionalized copolymer: Effect of emulsion formulation and RAFT end-group on the pore structure of polyHIPEs. Mantra Lorne, Australia.

Abstract

Porous polymers generated from high internal phase emulsions (HIPEs), having interconnected open-void morphology, low density and high porosity up to 95%, are finding various applications including separation science due to their exceptional properties, such as tunable pore size and surface characters.

A new class of polyHIPE materials has been prepared using HIPE template stabilized by a series of tailor-made polymeric surfactant as sole stabilizer. These polymeric surfactants were synthesized by radical addition-fragmentation chain transfer (RAFT) polymerization, which from the obtained copolymer is called an amphiphilic macro-RAFT agent.

The first section focuses on the preparation and characterization of functionalized polyHIPE materials prepared via HIPE-template stabilized by an anionic polymeric surfactant. The presence of these amphiphilic species allowed the successful preparation of a polyHIPE upon polymerization. The effect of concentration of macro-RAFT agent, pH, initiator, hexadecane as an organic modifier and the polymerization temperature on the morphology of the resulting porous materials was investigated. A strategy for preparation of functional polyHIPEs and a tool to transfer the RAFT moiety to the surface by introducing macro-RAFT agent was established.

Upon development of various new polyHIPE materials, an inverse high internal phase emulsion was introduced to a capillary format as a ‘column housing’. The influence of the PEO-based brush-type amphiphilic macro-RAFT agents on the morphology and surface chemistry of the resulting macroporous polymers is discussed in detail. Using nano-liquid

chromatography, it is shown that the polyHIPE are decorated with different microenvironments amongst the voids or domains of the monolithic structure. This is the first reported use of a hydrophilic polyHIPE in a capillary format as a stationary phase and also the first demonstration of the role of the RAFT group of the emulsifier in the attachment of the obtained polyHIPE to the inner surface of a capillary format column.

Furthermore, polyHIPE materials have also been prepared by using water in oil template using macro-RAFT agent as polymeric surfactant, while the RAFT part of the macro-RAFT agent is placed in the oil phase (monomer phase). The obtained polyHIPE is a tough material with a close structure. The pore structure of polyHIPEs was closed. Further study shows that by removing the RAFT-end group of the polymeric surfactant, the obtained polyHIPE possess an open structure with voids. The effect of the RAFT part of the polymeric surfactant on the surface chemistry of the polyHIPE is discussed. Novel technology was developed to allow straightforward functionalization of the obtained polyHIPE via surfactant-assisted functionalization strategy for application in separation science as a new functionalized stationary phase.

Table of content

List of abbreviations

Acronym	Representation
AIBN	2,2'-azo-bis-isobutironitrile
AAm	acylamide
MeCN	Acetonitrile
APS	Ammonium persulfate As Peak asymmetry
ATR-FTIR	attenuated total reflectance fourier transform infrared
BET	Brunauer, Emmett and Teller
CEC	Capillary electrochromatography
DI	Deionised
DVB	divinyl benzene
FESEM	Field Emission Scanning Electron Microscope
FTIR	Fourier transform infrared spectroscopy
HILIC	Hydrophilic interaction liquid chromatography
HIPE	High internal phase emulsions
HLB	Hydrophilic-lipophilic balance
k'	Retention/Capacity factor
Kd	Distribution coefficient
KPS	Potassium persulfate L Length of column
LC	Liquid chromatography
MeOH	Methanol
MPa	Mega Pascal
N	Number of theoretical plates
nc	Number of carbons
o/w	Oil in water
P	poly

Acronym	Representation
PDI	Polydispersity index
PEGDA	poly(ethylene glycol) diacrylate
PolyHIPEs	polymeric high internal phase emulsions
PSt	Polystyrene
Qb	quasi-block
RAFT polymerization	Reversible addition−fragmentation chain-transfer polymerization
RP-HPLC	Reversed phase high performance liquid chromatography
SEC	Size-exclusion chromatography
SEM	scanning electron microscopy
STXM	Scanning transmission X-ray microscopy
Sty	Styrene
TGA	Thermal gravimetric analysis
UV	Ultraviolet
VPBA	(4-Vinylphenyl) boronic acid
w/o	water in oil emulsion

Preface

Porous polymer monoliths are a category of materials developed more than 20 years ago [1-5]. Monolithic polymeric materials with well-defined pore properties and surfaces are excellent materials for chromatographic separation media, ion exchange resins, and catalyst supports, due to their relatively easy preparation as well as high gas/liquid permeability without loss of reparation efficiency [6-10].

The greatest changes in separation selectivity can be achieved by changing the properties of the stationary phase, in particular the surface chemistry with which analytes can potentially interact. With respect to the monolith surface, the desired surface chemistry of the monoliths can be achieved using two basic approaches: copolymerization of monomers containing the preferred functionalities and post-polymerization modifications. While the first approach is a simple single step, functionalities are distributed throughout the bulk and some of them may not be accessible. In the second approach, pores of a monolith prepared from monomers containing reactive group are filled with the reagent. After the reaction is completed, the monolith is flushed with a solvent to remove all un-reacted components. However, it has become clear that in some cases surface-functional materials are evenly dispersed throughout the structure rather than expressed on the surface, which is most desirable for chromatographic applications [11].

A range of approaches have been explored in order to obtain homogeneous and highly ordered structures for separation media [5]. Polymerised high internal phase emulsions (polyHIPEs) consists of a highly porous structure with interconnected spherical voids [12]. Because of these features, polyHIPEs appear to be a new generation of materials for use as a stationary

phase in separation science. An important difference between these supports and conventional monoliths (in separation science) is that polyHIPEs can easily be prepared in analytical scale separation columns as the weight fraction of monomer used is low and consequently the heat produced during the polymerisation reaction is easily dissipated by the solvent phase [13].

A scanning electron microscopy (SEM) image of a typical PolyHIPE material is shown in **Figure 1**, where the highly interconnected void network can clearly be seen. In the literature [14-16], "voids" or "pores" are referred to the spherical cavities created by the emulsion droplets and terms "windows" or "pore throats" are referred to interconnecting holes. One of the keys in the preparation of polyHIPEs is in many cases the stability of the initial emulsion and the surfactants used to stabilize the systems.

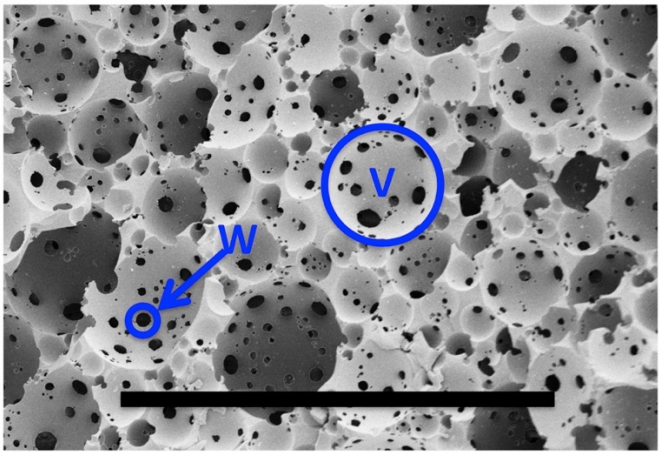

Figure 1. SEM of a typical PolyHIPE material. **V** indicates void, **W** indicates window. The scale bar is 50 μm.

There are a few examples in which the polyHIPE monolithic structure can be used as separation media in high-pressure liquid chromatography (HPLC) [17, 18]. All demonstrated examples consist of polymers that are hydrophobic in nature, which limits their applications to separation of non-polar analytes in reversed phase (RP) mode. As a consequence,

manipulating the surface chemistry of the polyHIPE structure is highly desirable to explore the application of these materials under different chromatographic modes.

There is a rich diversity of approaches for the preparation of monolithic structures (See **Table 1)**. One developed approach to stabilize a polyHIPE is the "surfactant free" concept [19]. This concept, usually referred to as a "Pickering emulsion", is an emulsion stabilized by solid particles (micrometer- or nanometer-scale) that preferentially migrate to the interface. By using particles bearing specific functionality, the surface of the resulting polyHIPE could be homogeneously decorated by desired functional group.

Table 1. Advantages and disadvantages of PolyHIPE versus monolithic polymer

Conventional PolyHIPE	Pickering- PolyHIPE	Monolithic polymer
Positive attributes		
Permeable to gases and wetting liquids (due to their highly interconnected struture) [6]	Decorating the polymer surface with Functional Nanoparticles	Study on the preparation, structures and application in separation science for more than two decades [3, 17, 20-25]
Uniform porous structure: Void sizes between 1 and 20 µm and interconnectivity by windows, which are around 20–50% of the void diameter [12, 26]	Enhance the thermal and mechanical properties of PolyHIPE [27]	Relatively easy preparation [28]
Easy preparation, facile control of void size [17]	High surface area available for reactivity	High permeability [29]
Negative attributes		
Poor mechanical stability [12]	Low permeability due to closed structure	Some limitation in modification of surface [30]
Low surface area (Conventional PolyHIPE)	Closed-cell voids ranging from 200 to 700µm [31, 32]	Some problem related to heterogeneity of structure

Despite successful preparation of the functionalized Pickering- PolyHIPE, the application of these types of materials is restricted as the void or domain

possess closed structure, especially for flow-through applications. Using surfactants and nano-fillers as Pickering stabilizers have a synergistic effect and the obtained polyHIPEs possess open structure [33, 34]. As an alternative method, tailor-made polymeric nanoparticles can be used for functionalization of polyHIPE monoliths by simple embedded strategy [35, 36]. While this could be considered for preparation of a functionalized polyHIPE, a large portion of the polymeric nanoparticles is expected to be fully embedded inside the polymer wall, thereby making only a small contribution to the surface chemistry. Novel polymerization methods are needed to improve the structural homogeneity of the monolith while the surface chemistry is modified, in order to establish a desired chromatographic selectivity and appropriate flow permeability. This could be achieved by using tailor-made reactive polymeric surfactant.

Scope of this thesis

The main aim of this study is to develop a polymeric surfactant-assisted functionalization strategy to design supracolloidal monolithic structures for applications in separation science. The polymerized high internal phase emulsion stabilized by a diblock copolymer will provide different surface chemistry in the resulting monolithic structure as well as a control over the interconnectivity. These polyHIPE materials can be tailored for application to a specific analytical problem, which has important implications for rapid and high-throughput screening of small molecules. Their interconnected structure allows the convective flow of the mobile phase through the separation medium, producing low-pressure drops at high flow rates as well as fast mass transfer of the solutes to the stationary phase.

The following steps constitute the main frame of the project:

1) Synthesis functional amphiphilic copolymer by RAFT technology
2) Stabilization of HIPE by tailored-made polymeric Surfactants

3) Immobilized functional amphiphilic macro-RAFT agent in HIPE (High Internal Phase Emulsion)
4) Evaluation PolyHIPE as Stationary Phase for separation science

The first chapter of this thesis covers some of the theory and concepts of emulsion preparation in addition to a brief introduction on the theory and concept of the "Reversible Addition-Fragmentation chain Transfer" (RAFT) technology, which will be used regularly for synthesis throughout this thesis. The RAFT technology allows the synthesis of amphiphilic block polymers (or macro-RAFT agents) required for the fabrication of HIPEs, with the sequential polymerization of two monomers of opposing lyophilicity (e.g. a hydrophilic monomer and then a hydrophobic monomer).

The second chapter of this thesis deals with preparing anionic amphiphilic macro-RAFT agents to be used as sole stabilizer for an inverse HIPE-template (oil in water). A strategy for preparation of functional polyHIPEs and a tool to transfer the RAFT moiety to the surface by introducing macro-RAFT agent was established. The third chapter examines the surface chemistry of the obtained polyHIPE using nano-liquid chromatography. PolyHIPE monoliths, in a capillary format, was investigated and characterised to evaluate their suitability for separation of small molecules. The final chapter investigates the role of the RAFT-end group of the amphiphilic macro-RAFT agent on the morphology and surface chemistry of the obtained polyHIPE via water in oil emulsion templating.

References

1. Svec, F., *Porous polymer monoliths: amazingly wide variety of techniques enabling their preparation.* J Chromatogr A, 2010. **1217**(6): p. 902-24.

2. Aoki, H., et al., *Polymer-based monolithic columns in capillary format tailored by using controlled in situ polymerization.* J Sep Sci, 2009. **32**(3): p. 341-58.
3. Nordborg, A., E.F. Hilder, and P.R. Haddad, *Monolithic phases for ion chromatography.* Annu Rev Anal Chem, 2011. **4**: p. 197-226.
4. Hemström, P., et al., *Polymer-based monolithic microcolumns for hydrophobic interaction chromatography of proteins.* J Sep Sci, 2006. **29**(1): p. 25-32.
5. Billen, J. and G. Desmet, *Understanding and design of existing and future chromatographic support formats.* J Chromatogr A, 2007. **1168**(1-2): p. 73-99.
6. Manley, S.S., et al., *New insights into the relationship between internal phase level of emulsion templates and gas–liquid permeability of interconnected macroporous polymers.* Soft Matter, 2009. **5**(23): p. 4780-4787.
7. Hilder, E.F., F. Svec, and J.M.J. Fréchet, *Development and application of polymeric monolithic stationary phases for capillary electrochromatography.* J Chromatogr A, 2004. **1044**(1-2): p. 3-22.
8. Schaller, D., E.F. Hilder, and P.R. Haddad, *Monolithic stationary phases for fast ion chromatography and capillary electrochromatography of inorganic ions.* J Sep Sci, 2006. **29**(12): p. 1705-1719.
9. Arrua, R.D., et al., *Review of recent advances in the preparation of organic polymer monoliths for liquid chromatography of large molecules.* Anal Chim Acta, 2012. **738**: p. 1-12.
10. Potter, O.G. and E.F. Hilder, *Porous polymer monoliths for extraction: diverse applications and platforms.* J Sep Sci, 2008. **31**(11): p. 1881-906.

11. Svec, F. and Y. Lv, *Advances and recent trends in the field of monolithic columns for chromatography.* Anal Chem, 2015. **87**(1): p. 250-273.
12. Cameron, N.R. and D.C. Sherrington, *High internal phase emulsions (HIPEs) — Structure, properties and use in polymer preparation.* Adv. Polym. Sci., 1996. **126**: p. 163-214.
13. Levkin, P.A., F. Svec, and J.M. Frechet, *Porous polymer coatings: a versatile approach to superhydrophobic surfaces.* Advanced Functional Materials, 2009. **19**(12): p. 1993-1998.
14. Kimmins, S.D. and N.R. Cameron, *Functional Porous Polymers by Emulsion Templating: Recent Advances.* Adv. Funct. Mater., 2011. **21**(2): p. 211-225.
15. Zhang, H. and A.I. Cooper, *Synthesis and applications of emulsion-templated porous materials.* Soft Matter, 2005. **1**(2): p. 107-113.
16. Cameron, N.R., *High internal phase emulsion templating as a route to well-defined porous polymers.* Polymer, 2005. **46**(5): p. 1439-1449.
17. Arrua, R.D., T.J. Causon, and E.F. Hilder, *Recent developments and future possibilities for polymer monoliths in separation science.* Analyst, 2012. **137**(22): p. 5179-5189.
18. Choudhury, S., D. Connolly, and B. White, *Supermacroporous polyHIPE and cryogel monolithic materials as stationary phases in separation science: a review.* Anal. Methods, 2015. **7**(17): p. 6967-6982.
19. Colver, P.J. and S.A.F. Bon, *Cellular Polymer Monoliths Made via Pickering High Internal Phase Emulsions.* Chem. Mater., 2007. **19**(7): p. 1537-1539.
20. Nischang, I., O. Brueggemann, and F. Svec, *Advances in the preparation of porous polymer monoliths in capillaries and*

microfluidic chips with focus on morphological aspects. Anal Bioanal Chem, 2010. **397**(3): p. 953-960.

21. Krenkova, J. and F. Svec, *Less common applications of monoliths: IV. Recent developments in immobilized enzyme reactors for proteomics and biotechnology.* J Sep Sci, 2009. **32**(5-6): p. 706-718.
22. Svec, F. and A.A. Kurganov, *Less common applications of monoliths. III. Gas chromatography.* J Chromatogr A, 2008. **1184**(1-2): p. 281-295.
23. Svec, F., *Less common applications of monoliths: preconcentration and solid-phase extraction.* J Chromatogr B, 2006. **841**(1-2): p. 52-64.
24. Tennikova, T.B. and F. Švec, *Chapter 16 Theoretical Aspects of Separation using Short Monolithic Beds*, in *Journal of Chromatography Library*, T.B.T. František Švec and D. Zdeněk, Editors. 2003, Elsevier. p. 351-371.
25. Švec, F. and T.B. Tennikova, *Chapter 1 Historical Review*, in *Journal of Chromatography Library*, T.B.T. František Švec and D. Zdeněk, Editors. 2003, Elsevier. p. 1-15.
26. Hainey, P., et al., *Synthesis and ultrastructural studies of styrene-divinylbenzene polyhipe polymers.* Macromolecules, 1991. **24**(1): p. 117-121.
27. Gurevitch, I. and M.S. Silverstein, *Polymerized pickering HIPEs: Effects of synthesis parameters on porous structure.* J. Polym. Sci., Part A: Polym. Chem., 2010. **48**(7): p. 1516-1525.
28. Svec, F. and C.G. Huber, *Monolithic Materials: Promises, Challenges, Achievements.* Anal Chem, 2006. **78**(7): p. 2100-2107.
29. Buchmeiser, M.R., *Polymeric monolithic materials: Syntheses, properties, functionalization and applications.* Polymer, 2007. **48**(8): p. 2187-2198.

30. Nesterenko, E.P., et al., *Nano-particle modified stationary phases for high-performance liquid chromatography.* Analyst, 2013. **138**(15): p. 4229-4254.
31. Ikem, V.O., A. Menner, and A. Bismarck, *High internal phase emulsions stabilized solely by functionalized silica particles.* Angew Chem Int Ed Engl, 2008. **47**(43): p. 8277-8279.
32. Menner, A., et al., *High internal phase emulsion templates solely stabilised by functionalised titania nanoparticles.* Chem. Commun., 2007. **43**(41): p. 4274-4276.
33. Ikem, V.O., A. Menner, and A. Bismarck, *Tailoring the mechanical performance of highly permeable macroporous polymers synthesized via Pickering emulsion templating.* Soft Matter, 2011. **7**(14): p. 6571.
34. Ikem, V.O., et al., *Highly permeable macroporous polymers synthesized from pickering medium and high internal phase emulsion templates.* Adv Mater, 2010. **22**(32): p. 3588-3592.
35. Dario Arrua, R., et al., *Monolithic cryopolymers with embedded nanoparticles. I. Capillary liquid chromatography of proteins using neutral embedded nanoparticles.* J Chromatogr A, 2013. **1273**: p. 26-33.
36. Arrua, R.D., P.R. Haddad, and E.F. Hilder, *Monolithic cryopolymers with embedded nanoparticles. II. Capillary liquid chromatography of proteins using charged embedded nanoparticles.* J Chromatogr A, 2013. **1311**: p. 121-6.

1. Introduction

1.1 Introduction structure

This introduction consists of two sections. The first section will cover some of the theory and concepts of emulsion preparation, specifically high internal phase emulsions (HIPEs). The second section will briefly cover the "Reversible Addition-Fragmentation chain Transfer" (RAFT) technology, which will be used regularly for synthesis throughout this thesis. A particular focus will be placed on the preparation of amphiphilic polymeric copolymer under RAFT control.

1.2 High Internal Phase Emulsion Templating

High internal phase emulsions (HIPEs) are concentrated mixtures of liquid droplets dispersed in another liquid, defined by a minimum droplet volume fraction of 74% [1]. This amount represents the most efficient packing arrangement viable for identical spheres [2]. Due to higher levels of the internal phase in a HIPE, the droplets of internal phase become distorted and are deformed into polyhedra, which was first stated by Kepler (known as Kepler's conjecture) [3]. In a HIPE, the continuous phase forms a network of thin liquid film separating the dispersed phase. A well-known example of a HIPE is mayonnaise. Vegetable oil as internal phase in mayonnaise, emulsified in the external phase (vinegar), using the lecithin in egg yolk as the emulsifier [4].

In 1974, Lissant *et al.* [5] coined the phrase, "HIPEs" for emulsions. They showed using scanning electron microscopy that the droplets were polyhedral and relatively monodisperse in size [6]. The most studied system comprises of styrene and divinylbenzene (DVB), which was patented by

Barby and Haq (Unilever) in 1982 [7]. In the literature this kind of emulsion also has a number of other names, such as high internal phase ratio emulsions (HIPRE) [5, 8], hydrocarbon gels [9], concentrated emulsions [6, 10], and gel emulsions [11, 12].

The type of HIPE that is formed depends on numerous factors including temperature, electrolyte concentration, proportions of components, nature of components and surfactant structure. The simple HIPE structures are droplets of water, in case of water-in-oil (w/o) emulsions or droplets of oil, in case of oil-in-water (o/w) emulsions.

HIPEs were originally investigated as a method for entrapping volatile, toxic solvents in non-Newtonian formulations for such applications as cleaning wax or sulfur from oil and gas wells and for transporting bulk solids [13-16]. The most common use of HIPEs is the formation of PolyHIPEs [1]. In this case, the continuous phase must consist of cross-linker(s) and/or an electrolyte solution. Minimum requirements needed for preparation of water-in-oil high internal phase emulsion (known as a conventional or normal HIPE) are: aqueous phase with electrolyte (liquid at least 74% for droplets), monomer, initiator and cross-linker, and emulsifier. A stable HIPE can be used as a precursor for preparing a homogeneous polyHIPE monolithic structure.

1.2.1 Stability of high internal phase emulsion

An emulsion is defined as a mixture of two immiscible liquids, where one phase is dispersed as droplets within the other. HIPEs are generally formed by the controlled addition of the internal phase to the external phase (which also contains the surfactant), under constant stirring. Only a few of the available surfactants are able to keep the major internal phase dispersed

within the minor external phase [17]. Surfactant molecules placed at the interface of the two phases provide stability and prevent the two phases separating by reducing the overall interfacial tension. Based on the nature of the dispersed phase, emulsions can be oil-in-water (o/w), water-in-oil (w/o) or oil-in-oil (o/o) [18]. The liquid in which the surfactant has a higher solubility tends to be the continuous phase, meaning that w/o emulsions persists in the presence of oil soluble surfactant and are rapidly destroyed in the presence of a water-soluble surfactant. Conversely, o/w emulsions persist in the presence of water-soluble surfactants. This is a model which predicts emulsion morphology based on surfactant affinity to the continuous phase (Bancroft's rule) [19].

Emulsion stability is a kinetic concept. As it can be seen in **Figure 1.1**, after the preparation of emulsion, several breakdown processes may occur due to a series of processes at the microscopic level that depend on the particle size distribution and the density difference between the internal and the external phase. The four main ways in which an emulsion may become unstable are creaming (or sedimentation) [18], aggregation (flocculation) [20], coalescence and Ostwald ripening [21]. An emulsion that is stable against coalescence and aggregation is referred to as a kinetically stable emulsion.

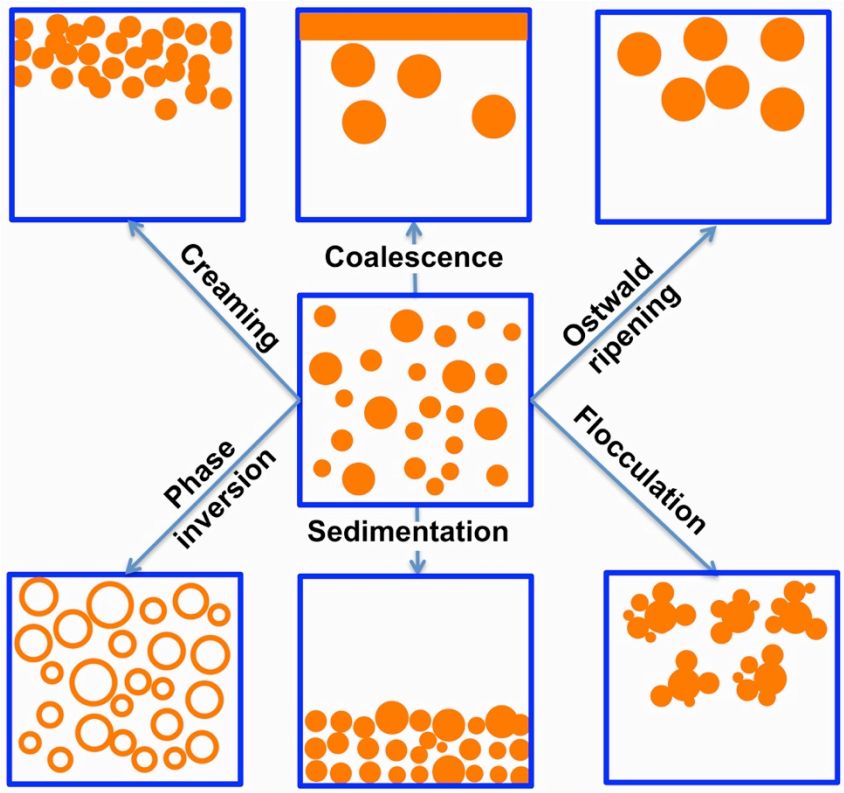

Figure 1.1. Schematic of emulsion breakdown processes.

There are two major studied mechanisms for minimizing the interfacial area: coalescence and Ostwald ripening [21]. Ostwald ripening consists of a diffusive transfer of the dispersed phase from smaller to larger droplets and it is determined by the solubility of the dispersed droplets in the continuous phase and the particle size distribution. Coalescence is the formation of larger droplets by merging of smaller ones where small droplets come into the contact by thinning and finally dissolution of the liquid surfactant film that covers them [22].

Describing each method of breakdown is non-trivial and requires analysis of all possible surface forces that have a rule in a particular physical phenomenon [18]. For an emulsion system such as a HIPE, the degree of

kinetic stability is very important. Typically, this is influenced by a number of factors such as molecular structures of the components, the surfactant type, the dispersed phase content, the temperature and the presence of stabilizing salts. Among them, the nature of the surfactant is critical to the stability of a major phase dispersed within a minor phase [4].

1.2.1.1 Surfactant as emulsifiers in HIPEs

Surface-active agents (usually referred to as surfactants) are amphipathic molecules that consist of a hydrophilic group (water-loving) and at least a hydrophobic group (lipophilic group). Surfactants can be either nonionic or ionic in nature, depending on their ionization and dissociation in water [23].

HIPEs are commonly stabilized by surfactants [24]. To achieve a stable HIPE, the surfactant must rapidly adsorb at the interface, and must lower the interfacial tension between the phases to form a rigid interfacial film [25]. The polymerization of the continuous phase of HIPEs leads to porous polymeric monoliths with open-cellular structure [26]. Typically, a surfactant stabilized HIPE results in a conventional polyHIPE structure with pore sizes ranging from 1 and 20 μm [27]. There are only a limited number of emulsifiers able to stabilize the HIPE, such as SPAN 80[1] [28] or a mixture of nonionic, anionic, and cationic surfactants: SPAN 20[2], DDBSS[3], and CTAB[4] [29, 30]. Between them, Sorbitan monooleate (Span 80) is the most commonly used emulsifier for w/o HIPE stabilization [2].

Another important class of surfactants are polymeric surfactants [31]. Various polymeric surfactants have been introduced under special trade names, such as Hypermers®, Pluronics® and Synperonic® [23, 32]. The

[1]Sorbitan monooleate
[2]Sorbitan monolaureate
[3]Dodecyl benzenesulfonic acid sodium salt
[4]Cetyltrim ethylammonium bromide

non-ionic polymeric surfactants, Hypermer 1070 [33-35], Hypermer B246 SF [24, 36, 37], and Hypermer 2296 [38-42] were successfully used to stabilize HIPEs. Several block and graft copolymers are produced with trademarks Pluronics® or Synperonic PE ® with structure PEO[5]-PPO[6]-PEO with different chain lengths of the blocks. The hydrophobic PPO chain anchors to the hydrophobic surface, leaving the two PEO chains dangling in the aqueous solution and providing thereby a steric stabilization. Yao *et al.* stabilized HIPEs using a triblock copolymer surfactant Pluronics®) consisting of PEO end blocks and a PPO midblock [43].

The selection of different surfactants in the preparation of either o/w or w/o emulsions is often still made on an empirical basis. For selecting an emulsifier for any emulsion system, there are two concepts that help us to find a stable emulsion: Hydrophilic-Lipophilic Balance (HLB) concept [44] and Phase Inversion Temperature (PIT) concept [18]. Even after 60 years and numerous limitations, Griffin's HLB is still the most commonly used surfactant property to predict surfactant performance.

1.2.1.1.1 Hydrophilic-Lipophilic Balance (HLB) Concept

The concept of HLB (hydrophile -lipophile balance) was first introduced by Griffin based on the surfactant solubility in water and, consequently its tendency to be dissolved by oils [45]. Surfactants are assigned a HLB value ranging from 0 - 40, and it is related to the balance between the hydrophilic and hydrophobic portions of the molecule. Where a surfactant of intermediate value is required, two surfactants of a higher and lower value than the one that is required can be combined (Formula (1)):

$$HLB_{mix} = \Sigma X_i HLB_i \qquad (1)$$

[5] poly(ethylene oxide) (PEO)
[6] poly(propylene oxide) (PPO)

For all emulsions there will be an optimum HLB value. The HLB range over which w/o emulsions can be formed is very narrow and it has been shown that variation of surfactant HLB value within this range has little influence on emulsion stability [46]. In addition, a mixture of oil soluble surfactant and water soluble surfactant often more effectively stabilizes emulsions than a single surfactant [47].

A few years after Griffin, J. T. Davis created a method that extended the calculation of HLB to ionic surfactants [48]. The Davis system assigns positive or negative numerical values to diverse chemical groups based on their hydrophilic or hydrophobic potency. Other methods have been developed in attempts to improve upon the HLB system that Griffin originated [49]. The balance of the hydrophilic and lipophilic groups is often the most important surfactant property in determining surfactant performance. For example, a nonionic surfactant with a low HLB, such as Span 80 with HLB of 4.3, is needed to form a stable w/o HIPE.

The HLB value also can be determined experimentally [50, 51]. HLB values for surfactants with unknown HLB values can be compared to surfactant standards with known HLB values or estimated by observing how the surfactant disperses in water (no dispersion = 1 to 3; poor dispersion = 3 to 6; unstable milky dispersion = 6 to 8; stable milky dispersion = 8 to 10; translucent to clear dispersion = 10 to 13; and clear solution > 13) [48]. **Table 1.1** provides general guidance for matching surfactant HLB values with surfactant applications. Generally, surfactants with HLB > 7 tend to form o/w emulsions and those with HLB < 7 tend to form w/o emulsions. An example of how the HLB value can sometimes be misleading is that o/w emulsions could be effectively stabilized by using a polymeric surfactant with low HLB value [52].

Table1.1. General guide for matching surfactant HLB to surfactant application [23]

Application	HLB Range
Mixing unlike oils	1 to 3
Water-in-oil emulsions	4 to 11
Antifoam	4 to 8
Wetting	7 to 12
Self-emulsifying oils	7 to 10
Oil-in-water emulsions	10 to 16
Detergent	12 to 15
Solubilize oils and microemulsions	13 to 18
Stabilizer	16 to 20

1.2.1.2 Particle as emulsifier in HIPE (Pickering-HIPE)

A different approach to stabilizing HIPE was developed by using a "surfactant free" concept [53]. This concept is usually referred to as Pickering emulsion, is an emulsion stabilized by solid particles (micrometer- or nanometer-scale) that preferentially migrate to the interface. In contrast to conventional polyHIPEs, Pickering-polyHIPEs have larger voids but closed-cell voids ranging from 200 to 700 μm [42]. The first paper describing the concept of particle-stabilized, or Pickering emulsions as a template to manufacture polyHIPEs was published by Colver *et al*. [54]. The particles used as stabilizers in Pickering emulsions are generally perceived to be irreversibly trapped at the liquid-liquid interface [55]. These characteristics can produce a number of benefits in polyHIPE manufacturing, not totally achievable when using conventional low-molecular-weight surfactants. For example, this method has been improved the mechanical strength of polyHIPEs [56]. Among the particles that used in

Pickering stabilized emulsion, the most improvement on mechanical stability effective was observed with incorporating inorganic components [33, 57, 58].

The use of particles to stabilize the emulsion polymerization mixture has some other advantages such as the possibility to functionalize the cell walls of the porous polymers with a layer of solid nanoparticles bearing different functional groups [54]. In general, these particles could contain functional groups for substrate, for example, for the ion exchange interaction [59]. Moreover, individual cell walls of the polyHIPE will allow functionalization of different types of particles via one simple synthetic procedure. These different micro-environments could create great potential benefit, especially in the design of porous monoliths for multistep reactions.

The Pickering HIPE tends to form closed-cell porous material and occasionally only a few pore throats can be formed while drying, which unfortunately limits the application of Pickering-polyHIPEs [60].

1.2.2 Polymerized high internal phase emulsion (polyHIPE)

The emulsion structure at the gel point of polymerization is a template for the pore structure of the resultant macroporous polymer, commonly called a polyHIPE after the internal phase is removed as visualized in **Figure 1.2**. The water-in-oil high internal phase emulsion is referred as “normal HIPEs” and if the oil phase is replaced by a hydrophobic monomer the “normal polyHIPEs” would be synthesized [17].

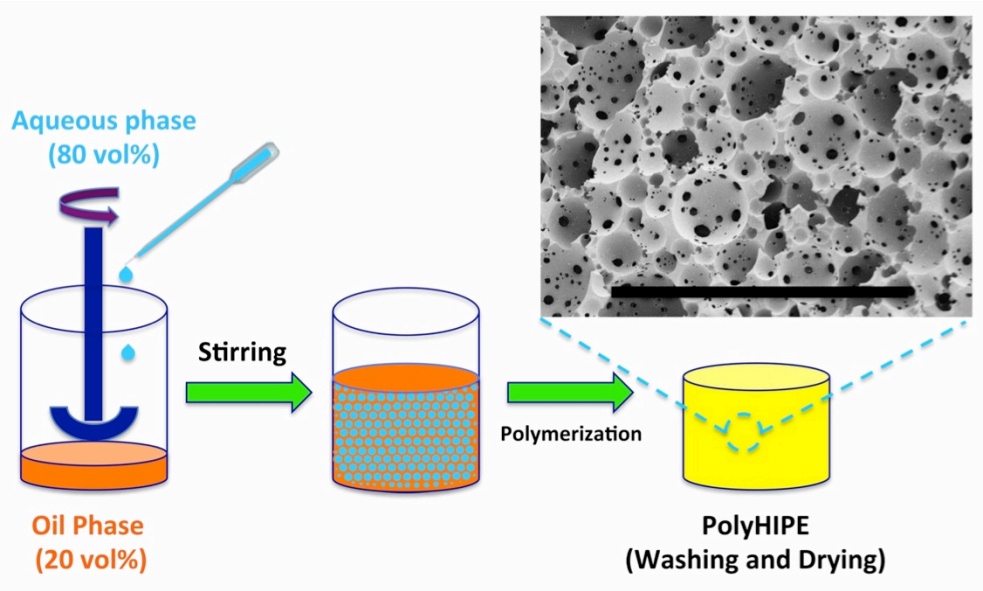

Figure 1.2. Schematic of polyHIPE preparation. The scale bar is 50μm.

1.2.2.1 PolyHIPE morphology

Porous polymer materials are generally formed via templates of water droplets (usually range from 5 to 100 μm)-in- an oily monomer phase (continuous phase) and the emulsion stabilized with surfactants. The surfactant content is often more important in determining the porous structure than the internal phase content. In 1988, a closed-cell structure was produced at surfactant contents below 5% of the external phase, while at around 7 % of surfactant; a highly interconnected open-cell structure was produced. It was indicated that open or closed structure is largely depended on the amount of added surfactant during HIPE formation [61].

Resulting polyHIPE materials typically possess an open pore system, meaning that voids which arise as a result of extraction of internal phase after the polymerisation of continuous phase are connected via smaller windows [26]. Increasing the proportion of surfactant causes the thinning of monomer layer between droplets and at some critical point of added

surfactant the monomer layer becomes very thin. The polymer film shrinks slightly because of monolith volume contraction and consecutively breaks between neighboring former droplets to form windows. Another explanation is that the window is obtained by drying in vacuum or extraction of polyHIPE after polymerization [62]. Gitli *et al.* indicated that the holes are formed during polymerization since bi-continuous phase structures have been observed in polyHIPE that have not undergone post-polymerization processing [63].

Various factors affect the droplet size of the dispersed phase. In the earlier work in polyHIPE, the void size decreased with divinylbenzaene (DVB) content, reflecting the greater hydrophobicity of DVB. In addition, the addition of a salt to dispersed phase can also reduce the void size by an order of magnitude [64].

In 2006, Carnachan *et al.* [65] changed the temperature of the internal aqueous phase to control the porous structure as well as adding organic additives. The coarsening of the emulsion results from an enhancement in Ostwald ripening. They used NMR[7] technique for finding rates of diffusion of water through the continuous phase.

1.2.2.2 PolyHIPE surface area

A possible disadvantage of conventional polyHIPEs is that they exhibit only modest surface areas around 5–20 m^2/g due to fact that the voids in polyHIPEs are tens of micrometers in diameter and the walls are essentially "solid" [1]. Conventional polyHIPE densities are around 0.1 g/cm^3. However different research groups have reported the preparation of polyHIPEs with high surface by adding a porogen to the external phase. The mechanism was based on the phase separation that some voids were

[7] Nuclear Magnetic Resonance

obtained within the developing polymer matrix and resulting in surface areas up to 700 m^2/g [27, 29, 66-68]. A reduction in overall density was observed, for instance, polyHIPEs with densities as low as 0.0126 g/cm^3 have been synthesized through variations in the emulsifier type, the emulsifier content, and the porogen content [69].

The wall structure can be affected by porogens which can often resemble the assembly of particles rather than a smooth polymeric wall [67]. The possible reason for this kind of wall is related to the formation and the phase separation of porogen-swollen microgel particles during polymerization. This kind of "particle assembly" structure for polyHIPE is also seen for hydrophilic polyHIPEs synthesized from an aqueous solution of monomers. In this case, water acts as the swelling porogen [70].

Jerabek *et al.* [71] prepared a swollen polyHIPE and indicated that the porosity can be significantly greater than that of a dried polyHIPE. The extremely high surface areas (up to 1200 m^2/g) in polyHIPE were generated by internal and external electrophiles under catalysis of a Lewis acid leading to hyper-crosslinked polymers [72].

1.2.2.3 Mechanical Stability

Many groups have tried to improve the relatively poor mechanical properties of polyHIPEs, specifically the modulus and the toughness, which range with Young's modulus between 3-6 MPa, to enhance their suitability for particular applications. With increasing the density by increasing the volume fraction of monomer will yield a significant increase in modulus. For example, relatively tough porous polymers were synthesized using relatively low internal phase contents of around 60% with densities around 0.4 g/cm^3 [37].

Different initiators can change the mechanical stability. Williams *et. al.* [64] showed that polystyrene-based polyHIPEs initiated using KPS [8] in the internal aqueous phase had a higher modulus than identical formulations initiated using AIBN[9] in the external organic phase. It was found that by changing the locus of initiation, both macromolecular and porous structures will be affected and eventually the modulus will be changed [63, 73, 74].

There are a large number of polyHIPE-based systems in which the synthesis of interpenetrating polymer networks [75], organic–inorganic hybrids [76, 77], ring opening metathesis polymerization [78, 79] and nanocomposites [80-85] have been used to enhance polyHIPE mechanical properties. A great mechanical stability of polyHIPEs was obtained when the ring opening metathesis is utilized for preparation of the polymer. While using a surfactant for stabilizing the emulsion often producing a brittle material, the obtained polyHIPE material of poly(dicyclopentadiene) (pDCPD) with 80% porosity demonstrate very good mechanical properties [78]. Within the same group, the ring opening metathesis polymerization was utilized for preparation of polyMIPEs (medium internal phase emulsions) and HIPEs with different internal phase fractions ranging from 50 to 80 v% [79]. These obtained materials show open porous architectures. After the oxidation step, the E-moduli of polyHIPE is the highest Young's modulus reported so far in the literature.

For improving the mechanical stability of polyHIPE, reversible addition fragmentation chain transfer (RAFT) technology was used to synthesize polyHIPEs based upon polystyrene (PSt) [86]. While the RAFT-synthesized polyHIPEs from practically identical HIPEs exhibited similar porous microstructures, the modulus and crush strengths of the polyHIPEs

[8] Potassium persulfate
[9] 2,2′-Azobis(2-methylpropionitrile)

synthesized under RAFT control were 3-fold those of the conventional polyHIPEs.

The same research group reported the use of a w/o miniemulsion template method with internal phase contents down to 40% was used for the RAFT synthesis of porous PSt-based monoliths with highly interconnected porous structures (voids around 300 nm and windows of around 100 nm) [87]. The miniemulsion-template material produced an increase of around 40-fold in modulus and in crush strength as well as reducing the porosity from 80% in a conventional polyHIPE to 47% in a RAFT synthesized polyHIPE. The RAFT technology is discussed in more detail in the following section.

1.2.2.4 Hydrophilic polyHIPEs

A water-in-oil high internal phase are normally classified as "Normal" HIPE and oil-in-water are considered as "Inverse" HIPE [88]. There are several reports on the preparation of hydrophilic polyHIPE foams using o/w template and related chemistries are well researched, including acrylic acid (AA) [89], cross-linked polyacrylamide [90-95], cross-linked PHEA[10] and PHMA[11] [90], polysaccharide [96], 2-hydroxyethyl methacrylate (HEMA) [70, 97] or N -isopropyl acrylamide (NIPAM) [98, 99]. However, the hydrophilic polyHIPE can be obtained by sulfonation of the corresponding hydrophobic materials or by the production of highly porous polymers with ionic or polar groups [100].

The relatively poor mechanical stability of oil-in-water polyHIPE as well as relatively limited synthesis windows for many systems generally produces hydrophilic polyHIPEs with low porosities. To overcome these problems, in 2010 Silverstein *et al.* synthesized a hydrophobic t-butyl acrylate-based

[10] Poly(hydroxylethyl acrylate)
[11] poly(hydroxyethyl methacrylates)

polyHIPE and then hydrolyzed the t-butyl groups to carboxylic acid, transforming it into a relatively hydrophilic PAA like polyHIPE [101].

1.2.2.5 Application of PolyHIPE in separation science

PolyHIPEs have high porosities and because of this high interconnectivity, [28, 61, 102] they are permeable to gases and wetting liquids [103]. Studies have demonstrated their great potential as separation media [104, 105]. While the monolithic polyHIPEs have found application as media for cell growth [106] and as solid supports for catalysis and solid phase synthesis [107], there are few reports using them for analytical chromatography with moderate performance demonstrated in capillary electrochromatography (CEC) mode and high performance liquid chromatography (HPLC) mainly related to the separations of proteins and other biological molecules [108]. This is largely due to problems in dealing with shrinkage from the column wall in analytical columns as well as low specific surface area and low mechanical strength.

In 2009, for HPLC application, fairly rigid PGMA-based polyHIPEs were synthesized by adding w/o HIPEs (80% internal phase) to a stainless steel HPLC column using a polymeric surfactant (Pluronic® F127) as stabilizer [43]. The epoxy groups were converted to weak anion-exchange functionalities. Fairly good separation of a protein mixture containing lysozyme, bovine serum albumin, ovalbumin and pepsin was observed. Almost baseline separation was completed in about 1 min at 6 ml/min. In contrast with conventional organic based monoliths, separation by these supports was not comparable and the pore size distribution curves for these supports were broader.

The absorption of metal ions (Ag, Cu, Cr) was investigated by PGMA-based polyHIPEs from w/o HIPEs (85% internal phase) functionalized with

various amines [109]. The most efficient absorption was observed for silver. The authors of this work concluded that 2-phenylimidazole proved most effective amine for separation of these ions.

Tunc *et al.* prepared a poly (isodecylacrylate-co-divinyl benzene)HIPE monolithic column used for the separation of alkylbenzenes and a good resolution demonstrated in CEC mode [110]. In this work, they prepared polyHIPE monolithic columns by the *in situ* polymerization of isodecylacrylate (IDA) and divinylbenzene (DVB) in the continuous phase of a HIPE. With different initiator concentration, different size spherical voids of polyHIPE were obtained and the columns were successfully used for the separation of alkyl benzenes.

1.3 Synthesis of amphiphilic polymer by reversible addition fragmentation chain transfer (RAFT)

Reversible deactivation radical polymerization (RDRP) is among the most rapidly developing areas of chemistry, with the number of publications approximately doubling each year. Reversible addition-fragmentation chain transfer (RAFT) mediated polymerization is one of a number of RDRP that was developed over the last two decades [111-117]. The first RAFT polymerization using thiocarbonylthio compounds was reported by the Commonwealth Scientific and Industrial Research Organization (CSIRO) in 1998 [118]. RAFT is now a well-established technique for living free-radical polymerization.

This type of polymerization can be stopped and restarted at anytime. In other words, these polymerizations stop only when there is no more monomer. The polymerization can continue upon the addition of more monomer, enabling block copolymers to be prepared in a straightforward

manner. This pioneering technology enables the synthesis of tailored polymers with unprecedented control over composition and architecture.

The RAFT mechanism and the appropriate RAFT agent structures have been recently detailed in a number of review articles [111-113, 119, 120]. Briefly, during a RAFT process, the oligomeric radicals formed at the initiation stage of polymerization add to the highly reactive C=S bond of the RAFT agents (**Figure 1.3**).

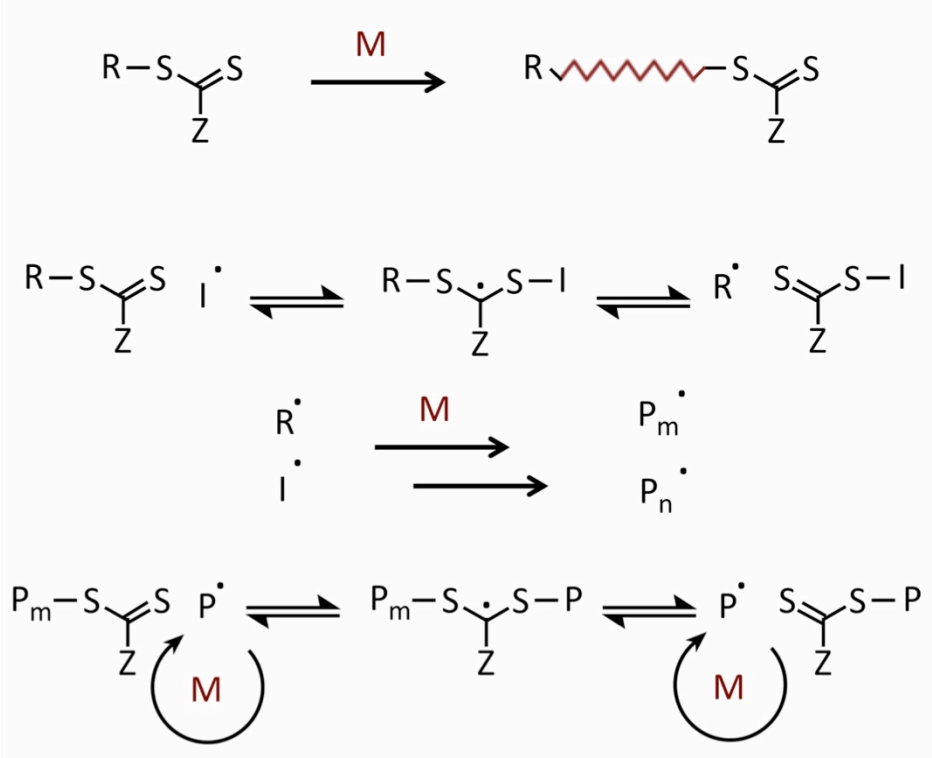

Figure 1.3. Overall RAFT process. The RAFT mechanism. Initiation, propagation, and equlibria providing chain transfer. I: initiator fragment; M: monomer; P: polymer chains. The top schematics show the overall reaction providing polymers with defined R and dithioester Z end groups.

Fragmentation of these radical intermediates results in the formation of oligomeric RAFT agents and R group radicals. The R group should be both a good homolytic leaving group and be able to initiate the growth of polymer chains. The growing polymeric radicals add to the polymeric RAFT agents forming stabilized radical intermediates, following by the fragmentation to the polymeric RAFT agents and polymeric radicals. At the end of polymerization, dormant polymeric RAFT agents together with terminated polymeric radicals are obtained.

Propagation occurs with the polymeric radical, whose "active" lifetime is comparable to or shorter than the time it takes to add one monomer unit. This time is very brief compared to the time that the chains reside in their dormant state, i.e. the time they spend as non-propagating $S=C(Z)SP_n$ entities.

The RAFT technology allows control of chain length, the molecular weight distribution and its polydispersity, chain architecture (e.g. a gradient monomer sequence) and topology. Numerous novel polymer molecules and structures have been produced [121-125].

1.3.1 Synthesis of block copolymers using RAFT polymerization

Amphiphilic block copolymers consist of connected polymeric sequences that differ in nature: A hydrophobic block that is insoluble in aqueous phase and a water-soluble hydrophilic block which hydrophobic block covalently attached to a hydrophilic segment. Amphiphilic copolymers behave similarly to low-molecular-weight surfactants; however, polymeric surfactants have much lower diffusion coefficients and critical micelle concentrations than "classic" surfactants in general. The synthesis of different kind of polymeric surfactants as well as properties and applications of them has been recently described in great detail elsewhere [126].

The use of amphiphilic block copolymers dramatically enhanced the solubilization capacity of medium-chain surfactants. These polymeric surfactants successfully employed in variety of applications, such as emulsifiers, dispersion stabilizers, and wetting agents. A low molecular weight dispersity is considered as an essential factor for enhancing the performance [127]. The RAFT technology is one of the most extensively studied controlled radical polymerization methods that has been used to prepare well-defined polymeric materials such as well-defined block copolymers [128-130]. Control over the length of each block is possible [131], and this provides an additional control over the behavior of the macro-RAFT agent (**Figure 1.4**). A comprehensive tutorial review about using RAFT agent for preparation of block copolymers has been published by Keddie [132].

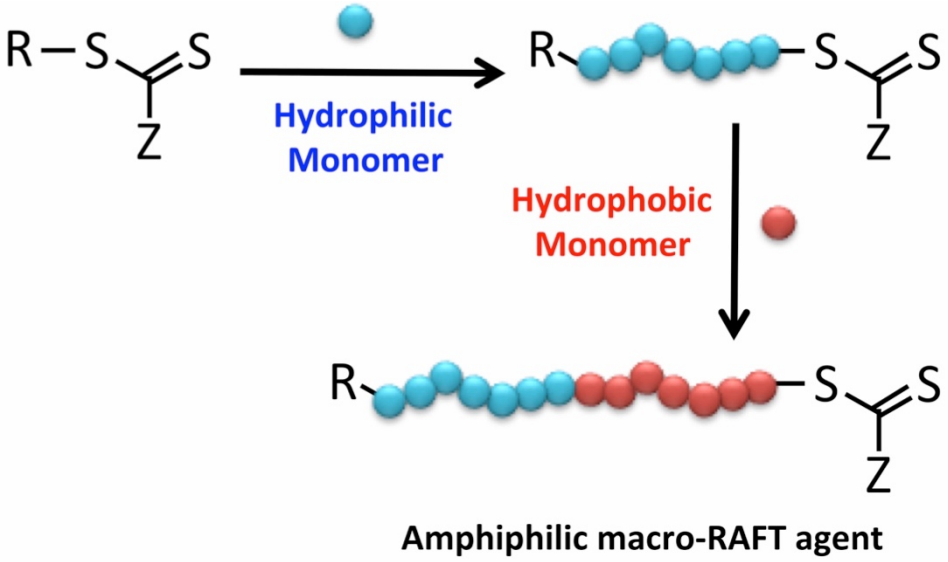

Figure 1.4. Schematic representation of the RAFT polymerization approach towards copolymerization of a hydrophilic and a hydrophobic monomer.

Recently, a new one-pot polymerization method (shown in Figure 1.5) has been developed for the preparation of (quasi) block copolymers via RAFT polymerization. This approach has been utilized to achieve the synthesis of block-like copolymers using sequential monomer addition with view to industrial application. The conversion of monomer in the first step is lower than 100% prior to a second monomer being incorporated without purification of the macro-RAFT agent.

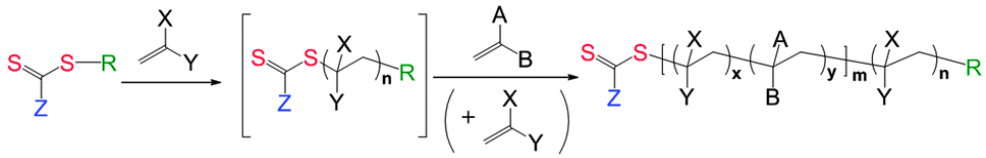

Figure 1.5. Overall synthesis of quasi-block copolymers (reprinted with permission from Ref [132])

This protocol was successfully utilized for the preparation of polymer materials in organic solution, sequential aqueous solution/emulsion as well as in supercritical carbon dioxide [133-135]. Generally, it is assumed that the residual monomers from the initial polymerization are consumed in the second step of quasi-block synthesis. This incorporation may alter the properties of the obtained block-copolymer, particularly for polymeric surfactants [126].

1.4 References

1. Cameron, N.R. and D.C. Sherrington, *High internal phase emulsions (HIPEs) — Structure, properties and use in polymer preparation.* Adv. Polym. Sci., 1996. **126**: p. 163-214.
2. Silverstein, M.S., *Emulsion-templated porous polymers: A retrospective perspective.* Polymer, 2014. **55**(1): p. 304-320.

3. Hales, T.C., *Historical Overview of the Kepler Conjecture.* Discrete & Computational Geometry, 2006. **36**(1): p. 5-20.
4. Cameron, N.R., P. Krajnc, and M.S. Silverstein, *Colloidal Templating*, in *Porous Polymers*. 2011, John Wiley & Sons, Inc. p. 119-172.
5. Lissant, K.J., et al., *Structure of high-internal-phase-ratio emulsions.* J. Colloid Interface Sci., 1974. **47**(2): p. 416-423.
6. Lissant, K.J. and K.G. Mayhan, *A study of medium and high internal phase ratio water/polymer emulsions.* J. Colloid Interface Sci., 1973. **42**(1): p. 201-208.
7. Barby, D. and Z. Haq, *Low density porous cross-linked polymeric materials and their preparation.* EP0060138, 1982.
8. Lissant, K.J., *The geometry of high-internal-phase-ratio emulsions.* J. Colloid Interface Sci., 1966. **22**(5): p. 462-468.
9. Kunieda, H., et al., *The formation of gel-emulsions in a water/nonionic surfactant/oil system.* Colloids Surf., 1987. **24**(2-3): p. 225-237.
10. Ruckenstein, E. and J.S. Park, *Hydrophilic-hydrophobic polymer composites.* J. Polym. Sci., Polym. Lett. Ed., 1988. **26**(12): p. 529-536.
11. Kunieda, H., et al., *The structure of gel-emulsions in a water/ nonionic surfactant/oil system.* Colloids Surf., 1990. **47**: p. 35-43.
12. Kunieda, H., N. Yano, and C. Solans, *The stability of gel—emulsions in a water/nonionic surfactant/oil system.* Colloids Surf., 1989. **36**(3): p. 313-322.
13. Lissant, K.J., *U.S. Pat. 3523826* P. Corp, Editor. 1970.
14. Lissant, K.J., *U. S. Pat. 3617095*, P. Corp, Editor. 1971.
15. Lissant, K.J., *U.S. Pat. 3700594*, P. Corp, Editor. 1972.
16. Lissant, K.J., *U.S. Pat. 3732166*, P. Corp., Editor. 1973

17. Silverstein, M.S., *PolyHIPEs: Recent advances in emulsion-templated porous polymers.* Prog. Polym. Sci., 2014. **39**(1): p. 199-234.
18. Tadros, T.F., *Applications of Surfactants in Emulsion Formation and Stabilisation*, in *Applied Surfactants*. 2005, Wiley-VCH Verlag GmbH & Co. KGaA. p. 115-185.
19. Bancroft, W.D., *The Theory of Emulsification, I.* J. Phys. Chem., 1911. **16**(3): p. 177-233.
20. Langmuir, I., *The mechanism of the surface phenomena of flotation.* Trans. Faraday Soc., 1920. **15**(June): p. 62-74.
21. Bhakta, A. and E. Ruckenstein, *Ostwald ripening: A stochastic approach.* The Journal of Chemical Physics, 1995. **103**(16): p. 7120-7135.
22. Vincent, B., *Colloidal Aspects of Emulsion Polymerisation*, in *Chemistry and Technology of Emulsion Polymerisation*. 2013, John Wiley & Sons Ltd. p. 167-186.
23. Tadros, T.F., *Surfactants in Foams*, in *Applied Surfactants*. 2005, Wiley-VCH Verlag GmbH & Co. KGaA. p. 259-284.
24. Menner, A., et al., *Particle-stabilized surfactant-free medium internal phase emulsions as templates for porous nanocomposite materials: poly-Pickering-Foams.* Langmuir, 2007. **23**(5): p. 2398-2403.
25. Ford, R.E. and C.G.L. Furmidge, *Studies at phase interfaces.* J. Colloid Interface Sci., 1966. **22**(4): p. 331-341.
26. Cameron, N.R., et al., *Study of the formation of the open-cellular morphology of poly(styrene/divinylbenzene) polyHIPE materials by cryo-SEM.* Colloid Polym. Sci., 1996. **274**(6): p. 592-595.

27. Hainey, P., et al., *Synthesis and ultrastructural studies of styrene-divinylbenzene polyhipe polymers.* Macromolecules, 1991. **24**(1): p. 117-121.
28. Williams, J.M., *High internal phase water-in-oil emulsions: Influence of surfactants and cosurfactants on emulsion stability and foam quality.* Langmuir, 1991. **7**(7): p. 1370-1377.
29. Barbetta, A. and N.R. Cameron, *Morphology and surface area of emulsion-derived (PolyHIPE) solid foams prepared with oil-phase soluble porogenic solvents: Span 80 as surfactant.* Macromolecules, 2004. **37**(9): p. 3188-3201.
30. Zhang, S., J. Chen, and V.T. Perchyonok, *Stability of high internal phase emulsions with sole cationic surfactant and its tailoring morphology of porous polymers based on the emulsions.* Polymer, 2009. **50**(7): p. 1723-1731.
31. Pons, R., *Polymeric Surfactants as Emulsion Stabilizers*, in *Amphiphilic Block Copolymers*, P.A. Lindman, Editor. 2000, Elsevier Science B.V.: Amsterdam. p. 409-422.
32. Tadros, T., *Polymeric surfactants in disperse systems.* Adv Colloid Interface Sci, 2009. **147-148**: p. 281-299.
33. Haibach, K., et al., *Tailoring mechanical properties of highly porous polymer foams: Silica particle reinforced polymer foams via emulsion templating.* Polymer, 2006. **47**(13): p. 4513-4519.
34. Menner, A., R. Powell, and A. Bismarck, *Open porous polymer foams via inverse emulsion polymerization: Should the definition of high internal phase (ratio) emulsions be extended?* Macromolecules, 2006. **39**(6): p. 2034-2035.
35. Menner, A., R. Powell, and A. Bismarck, *A new route to carbon black filled polyHIPEs.* Soft Matter, 2006. **2**(4): p. 337-342.

36. Cummins, D., et al., *Synthesis of Functional Photopolymerized Macroporous PolyHIPEs by Atom Transfer Radical Polymerization Surface Grafting.* Chem. Mater., 2007. **19**(22): p. 5285-5292.
37. Menner, A., et al., *Tough reinforced open porous polymer foams via concentrated emulsion templating.* Polymer, 2006. **47**(22): p. 7628-7635.
38. Menner, A., et al., *Nanocomposite foams obtained by polymerization of high internal phase emulsions.* J. Polym. Sci., Part A: Polym. Chem., 2008. **46**(16): p. 5708-5714.
39. Manley, S.S., et al., *New insights into the relationship between internal phase level of emulsion templates and gas–liquid permeability of interconnected macroporous polymers.* Soft Matter, 2009. **5**(23): p. 4780-4787.
40. Wong, L.L., et al., *Hierarchical polymerized high internal phase emulsions synthesized from surfactant-stabilized emulsion templates.* Langmuir, 2013. **29**(20): p. 5952-5961.
41. Kimmins, S.D., P. Wyman, and N.R. Cameron, *Photopolymerised methacrylate-based emulsion-templated porous polymers.* React. Funct. Polym., 2012. **72**(12): p. 947-954.
42. Menner, A., et al., *High internal phase emulsion templates solely stabilised by functionalised titania nanoparticles.* Chem. Commun., 2007. **43**(41): p. 4274-4276.
43. Yao, C., et al., *A novel glycidyl methacrylate-based monolith with sub-micron skeletons and well-defined macropores.* J. Mater. Chem., 2009. **19**(6): p. 767-772.
44. Griffin, W.C., *Calculation of HLB values of non-ionic durfactants.* Am Perfumer Essent Oil Rev, 1955. **65**: p. 26-29.
45. Griffin, W.C., *Classification of surface-active agents by HLB.* Am Perfumer Essent Oil Rev, 1949. **1**(5): p. 311-326.

46. Boyd, J., C. Parkinson, and P. Sherman, *Factors affecting emulsion stability, and the HLB concept.* J. Colloid Interface Sci., 1972. **41**(2): p. 359-370.
47. Atwood, D. and A.T. Florence, *Surfactant systems*. 1985, NewYork: Chapman and Hall.
48. *Chapter 3 Hydrophile-lipophile balance of surfactants*, in *Studies in Interface Science*, M.K. Pyotr, Editor. 2000, Elsevier. p. 146-266.
49. Burguera, J.L. and M. Burguera, *Analytical applications of emulsions and microemulsions.* Talanta, 2012. **96**: p. 11-20.
50. Ben-Et, G. and D. Tatarsky, *Application of NMR for the determination of HLB values of nonionic surfactants.* Journal of the American Oil Chemists' Society, 1972. **49**(8): p. 499-500.
51. Robbers, J.E. and V.N. Bhatia, *Technique for the Rapid Determination of HLB and Required-HLB Values.* J. Pharm. Sci., 1961. **50**(8): p. 708-709.
52. Pons, R., C. Solans, and T.F. Tadros, *Rheological behavior of highly concentrated oil-in-water (o/w) emulsions.* Langmuir, 1995. **11**(6): p. 1966-1971.
53. Pickering, S.U., *CXCVI. - Emulsions.* Journal of the Chemical Society, Transactions, 1907. **91**: p. 2001-2021.
54. Colver, P.J. and S.A.F. Bon, *Cellular Polymer Monoliths Made via Pickering High Internal Phase Emulsions.* Chem. Mater., 2007. **19**(7): p. 1537-1539.
55. Pieranski, P., *Two-Dimensional Interfacial Colloidal Crystals.* Phys. Rev. Lett., 1980. **45**(7): p. 569-572.
56. Wang, T., et al., *Soft polymer and nano-clay supracolloidal particles in adhesives: Synergistic effects on mechanical properties.* Soft Matter, 2009. **5**(20): p. 3842-3849.

57. Ranting, W.U., A. Menner, and A. Bismarck, *Tough Interconnected polymerized medium and high internal phase emulsions reinforced by silica particles.* Journal of Polymer Science, Part A: Polymer Chemistry, 2010. **48**(9): p. 1979-1989.
58. Wu, R., A. Menner, and A. Bismarck, *Tough interconnected polymerized medium and high internal phase emulsions reinforced by silica particles.* J. Polym. Sci., Part A: Polym. Chem., 2010. **48**(9): p. 1979-1989.
59. Nordborg, A. and E.F. Hilder, *Recent advances in polymer monoliths for ion-exchange chromatography.* Anal Bioanal Chem, 2009. **394**(1): p. 71-84.
60. Zhu, Y., et al., *High internal phase emulsions prepared with poly(urethane urea) aqueous nanodispersion at different temperatures.* J. Polym. Sci., Part A: Polym. Chem., 2010. **48**(19): p. 4356-4360.
61. Williams, J.M. and D.A. Wrobleski, *Spatial distribution of the phases in water-in-oil emulsions. Open and closed microcellular foams from cross-linked polystyrene.* Langmuir, 1988. **4**(3): p. 656-662.
62. Menner, A. and A. Bismarck, *New Evidence for the Mechanism of the Pore Formation in Polymerising High Internal Phase Emulsions or Why polyHIPEs Have an Interconnected Pore Network Structure.* Macromol. Symp., 2006. **242**(1): p. 19-24.
63. Gitli, T. and M.S. Silverstein, *Bicontinuous hydrogel–hydrophobic polymer systems through emulsion templated simultaneous polymerizations.* Soft Matter, 2008. **4**(12): p. 2475-2485.
64. Williams, J.M., A.J. Gray, and M.H. Wilkerson, *Emulsion Stability and Rigid Foams from Styrene or Divinylbenzene Water-in-Oil Emulsions.* Langmuir, 1990. **6**(2): p. 437-444.

65. Carnachan, R.J., et al., *Tailoring the morphology of emulsion-templated porous polymers.* Soft Matter, 2006. **2**(7): p. 608-616.
66. Sergienko, A.Y., et al., *Polymerized high internal phase emulsions containing a porogen: Specific surface area and sorption.* J. Appl. Polym. Sci., 2004. **94**(5): p. 2233-2239.
67. Cameron, N.R. and A. Barbetta, *The influence of porogen type on the porosity, surface area and morphology of poly(divinylbenzene) PolyHIPE foams.* J. Mater. Chem., 2000. **10**(11): p. 2466-2471.
68. Barbetta, A. and N.R. Cameron, *Morphology and surface area of emulsion-derived (PolyHIPE) solid foams prepared with oil-phase soluble porogenic solvents: Three-component surfactant system.* Macromolecules, 2004. **37**(9): p. 3202-3213.
69. Richez, A., et al., *Preparation of ultra-low-density microcellular materials.* J. Appl. Polym. Sci., 2005. **96**(6): p. 2053-2063.
70. Kulygin, O. and M.S. Silverstein, *Porous poly(2-hydroxyethyl methacrylate) hydrogels synthesized within high internal phase emulsions.* Soft Matter, 2007. **3**(12): p. 1525-1529.
71. Jerabek, K., et al., *Porogenic solvents influence on morphology of 4-vinylbenzyl chloride based polyHIPEs.* Macromolecules, 2008. **41**(10): p. 3543-3546.
72. Schwab, M.G., et al., *High surface area polyHIPEs with hierarchical pore system.* Soft Matter, 2009. **5**(5): p. 1055-1059.
73. Livshin, S. and M.S. Silverstein, *Cross-linker flexibility in porous crystalline polymers synthesized from long side-chain monomers through emulsion templating.* Soft Matter, 2008. **4**(8): p. 1630-1638.
74. Livshin, S. and M.S. Silverstein, *Crystallinity and cross-linking in porous polymers synthesized from long side chain monomers through emulsion templating.* Macromolecules, 2008. **41**(11): p. 3930-3938.

75. Lépine, O., M. Birot, and H. Deleuze, *Preparation of macrocellular PU–PS interpenetrating networks.* Polymer, 2005. **46**(23): p. 9653-9663.
76. Brun, N., et al., *Hybrid foams, colloids and beyond: from design to applications.* Chem Soc Rev, 2011. **40**(2): p. 771-788.
77. Tai, H., A. Sergienko, and M.S. Silverstein, *Organic-inorganic networks in foams from high internal phase emulsion polymerizations.* Polymer, 2001. **42**(10): p. 4473-4482.
78. Kovacic, S., P. Krajnc, and C. Slugovc, *Inherently reactive polyHIPE material from dicyclopentadiene.* Chem Commun (Camb), 2010. **46**(40): p. 7504-6.
79. Kovačič, S., et al., *Ring opening metathesis polymerisation of emulsion templated dicyclopentadiene giving open porous materials with excellent mechanical properties.* Polymer Chemistry, 2012. **3**(2): p. 325.
80. Normatov, J. and M.S. Silverstein, *Highly porous elastomer-silsesquioxane nanocomposites synthesized within high internal phase emulsions.* J. Polym. Sci., Part A: Polym. Chem., 2008. **46**(7): p. 2357-2366.
81. Normatov, J. and M.S. Silverstein, *Interconnected Silsesquioxane−Organic Networks in Porous Nanocomposites Synthesized within High Internal Phase Emulsions.* Chem. Mater., 2008. **20**(4): p. 1571-1577.
82. Claire Hermant, M., B. Klumperman, and C.E. Koning, *Conductive Pickering-poly(high internal phase emulsion) composite foams prepared with low loadings of single-walled carbon nanotubes.* Chem Comm., 2009(19): p. 2738-2740.
83. Li, T., et al., *Macroporous magnetic poly(styrene–divinylbenzene) nanocomposites prepared via magnetite nanoparticles-stabilized*

high internal phase emulsions. J. Mater. Chem., 2011. **21**(34): p. 12865-12827.

84. Moghbeli, M.R. and M. Shahabi, *Morphology and Mechanical Properties of an Elastomeric Poly(HIPE) Nanocomposite Foam Prepared via an Emulsion Template.* Iran. Polym. J., 2011. **20**(5): p. 343-355.
85. Zheng, Z., et al., *Macroporous graphene oxide-polymer composite prepared through pickering high internal phase emulsions.* ACS Appl Mater Interfaces, 2013. **5**(16): p. 7974-7982.
86. Luo, Y., A.N. Wang, and X. Gao, *Pushing the mechanical strength of PolyHIPEs up to the theoretical limit through living radical polymerization.* Soft Matter, 2012. **8**(6): p. 1824-1830.
87. Luo, Y.W., A.N. Wang, and X. Gao, *Miniemulsion template polymerization to prepare a sub-micrometer porous polymeric monolith with an inter-connected structure and very high mechanical strength.* Soft Matter, 2012. **8**(29): p. 7547-7551.
88. Pulko, I. and P. Krajnc, *High internal phase emulsion templating--a path to hierarchically porous functional polymers.* Macromol Rapid Commun, 2012. **33**(20): p. 1731-1746.
89. Krajnc, P., D. Štefanec, and I. Pulko, *Acrylic Acid "Reversed" PolyHIPEs.* Macromol Rapid Commun, 2005. **26**(16): p. 1289-1293.
90. Butler, R., I. Hopkinson, and A.I. Cooper, *Synthesis of Porous Emulsion-Templated Polymers Using High Internal Phase CO2-in-Water Emulsions.* Journal of the American Chemical Society, 2003. **125**(47): p. 14473-14481.
91. Zhang, H. and A.I. Cooper, *Synthesis of Monodisperse Emulsion-Templated Polymer Beads by Oil-in-Water-in-Oil (O/W/O) Sedimentation Polymerization.* Chem. Mater., 2002. **14**(10): p. 4017-4020.

92. Butler, R., C.M. Davies, and A.I. Cooper, *Emulsion Templating Using High Internal Phase Supercritical Fluid Emulsions.* Adv. Mater., 2001. **13**(19): p. 1459-1463.
93. Katagawa, N., in *6 218 440.*, US Pat. Appl., Editor. 2001.
94. Zhu, Y., et al., *Hydrophilic porous polymers based on high internal phase emulsions solely stabilized by poly(urethane urea) nanoparticles.* Polymer, 2010. **51**(16): p. 3612-3617.
95. Hua, Y., et al., *Hydrophilic polymer foams with well-defined open-cell structure prepared from pickering high internal phase emulsions.* J. Polym. Sci., Part A: Polym. Chem., 2013. **51**(10): p. 2181-2187.
96. Barbetta, A., et al., *Enzymatic cross-linking versus radical polymerization in the preparation of gelatin PolyHIPEs and their performance as scaffolds in the culture of hepatocytes.* Biomacromolecules, 2006. **7**(11): p. 3059-68.
97. Kovacic, S., D. Stefanec, and P. Krajnc, *Highly porous open-cellular monoliths from 2-hydroxyethyl methacrylate based high internal phase emulsions (HIPEs): Preparation and void size tuning.* Macromolecules, 2007. **40**(22): p. 8056-8060.
98. Zhang, H. and A.I. Cooper, *Thermoresponsive "Particle Pumps": Activated Release of Organic Nanoparticles from Open-Cell Macroporous Polymers.* Adv. Mater., 2007. **19**(18): p. 2439-2444.
99. Grant, N.C., A.I. Cooper, and H. Zhang, *Uploading and temperature-controlled release of polymeric colloids via hydrophilic emulsion-templated porous polymers.* ACS Appl Mater Interfaces, 2010. **2**(5): p. 1400-1406.
100. K. Jomes, et al., in *4 611 014.*, US Pat. Appl., Editor. 1986
101. Livshin, S. and M.S. Silverstein, *Enhancing hydrophilicity in a hydrophobic porous emulsion-templated polyacrylate.* J. Polym. Sci., Part A: Polym. Chem., 2009. **47**(18): p. 4840-4845.

102. Williams, J.M., A. James Gray, and M.H. Wilkerson, *Emulsion stability and rigid foams from styrene or divinylbenzene water-in-oil emulsions.* Langmuir, 1990. **6**(2): p. 437-444.
103. Manley, S.S., et al., *New insights into the relationship between internal phase level of emulsion templates and gas-liquid permeability of interconnected macroporous polymers.* Soft Matter, 2009. **5**(23): p. 4780-4787.
104. Bhumgara, Z., *Polyhipe foam materials as filtration media.* Filtration and Separation, 1995. **32**(3): p. 245-251.
105. Ruckenstein, E., *Emulsion pathways to composite polymeric membranes for separation processes.* Colloid Polym. Sci., 1989. **267**(9): p. 792-797.
106. Viswanathan, P., et al., *Cell instructive microporous scaffolds through interface engineering.* J Am Chem Soc, 2012. **134**(49): p. 20103-20109.
107. Ning, Y., et al., *Hierarchical porous polymeric microspheres as efficient adsorbents and catalyst scaffolds.* Chem Comm., 2013. **49**(78): p. 8761-8763.
108. Choudhury, S., D. Connolly, and B. White, *Supermacroporous polyHIPE and cryogel monolithic materials as stationary phases in separation science: a review.* Anal. Methods, 2015. **7**(17): p. 6967-6982.
109. Mert, E.H., M.A. Kaya, and H. Yıldırım, *Preparation and Characterization of Polyester–Glycidyl Methacrylate PolyHIPE Monoliths to Use in Heavy Metal Removal.* Des. Monomers Polym., 2012. **15**(2): p. 113-126.
110. Tunc, Y., et al., *Acrylic-based high internal phase emulsion polymeric monolith for capillary electrochromatography.* J Chromatogr A, 2010. **1217**(10): p. 1654-1659.

111. Moad, G., E. Rizzardo, and S.H. Thang, *Living Radical Polymerization by the RAFT Process—A First Update.* Aust. J. Chem., 2006. **59**(10): p. 669.
112. Moad, G., E. Rizzardo, and S.H. Thang, *Living Radical Polymerization by the RAFT Process - A Second Update.* Aust. J. Chem., 2009. **62**(11): p. 1402-1472.
113. Moad, G., E. Rizzardo, and S.H. Thang, *Living Radical Polymerization by the RAFT Process - A Third Update.* Aust. J. Chem., 2012. **65**(8): p. 985-1076.
114. Chiefari, J., et al., *Living free-radical polymerization by reversible addition-fragmentation chain transfer: The RAFT process.* Macromolecules, 1998. **31**(16): p. 5559-5562.
115. Moad, G., *The Emergence of RAFT Polymerization.* Aust. J. Chem., 2006. **59**(10): p. 661.
116. Rizzardo, E., et al., *RAFT Polymerization: Adding to the Picture.* Macromol. Symp., 2007. **248**(1): p. 104-116.
117. Keddie, D.J., et al., *Switchable Reversible Addition–Fragmentation Chain Transfer (RAFT) Polymerization in Aqueous Solution,N,N-Dimethylacrylamide.* Macromolecules, 2011. **44**(17): p. 6738-6745.
118. Moad, G. and C. Barner-Kowollik, *The Mechanism and Kinetics of the RAFT Process: Overview, Rates, Stabilities, Side Reactions, Product Spectrum and Outstanding Challenges*, in *Handbook of RAFT Polymerization*. 2008, Wiley-VCH Verlag GmbH & Co. KGaA. p. 51-104.
119. Keddie, D.J., et al., *RAFT Agent Design and Synthesis.* Macromolecules, 2012. **45**(13): p. 5321-5342.
120. Moad, G., et al., *Functional polymers for optoelectronic applications by RAFT polymerization.* Poly. Chem., 2011. **2**(3): p. 492-519.

121. Zhang, W., et al., *RAFT-mediated one-pot aqueous emulsion polymerization of methyl methacrylate in presence of poly(methacrylic acid-co-poly(ethylene oxide) methacrylate) trithiocarbonate macromolecular chain transfer agent.* Polymer, 2013. **54**(8): p. 2011-2019.

122. Zehm, D., L.P.D. Ratcliffe, and S.P. Armes, *Synthesis of Diblock Copolymer Nanoparticles via RAFT Alcoholic Dispersion Polymerization: Effect of Block Copolymer Composition, Molecular Weight, Copolymer Concentration, and Solvent Type on the Final Particle Morphology.* Macromolecules, 2013. **46**(1): p. 128-139.

123. Utama, R.H., M.H. Stenzel, and P.B. Zetterlund, *Inverse Miniemulsion Periphery RAFT Polymerization: A Convenient Route to Hollow Polymeric Nanoparticles with an Aqueous Core.* Macromolecules, 2013. **46**(6): p. 2118-2127.

124. Steinhauer, W., et al., *Block and Gradient Copolymers of 2-Hydroxyethyl Acrylate and 2-Methoxyethyl Acrylate via RAFT: Polymerization Kinetics, Thermoresponsive Properties, and Micellization.* Macromolecules, 2013. **46**(4): p. 1447-1460.

125. Shi, X., M. Miao, and Z. An, *Core cross-linked star (CCS) polymers with tunable polarity: synthesis by RAFT dispersion polymerization, self-assembly and emulsification.* Poly. Chem., 2013. **4**(6): p. 1950-1959.

126. Raffa, P., et al., *Polymeric Surfactants: Synthesis, Properties, and Links to Applications.* Chem Rev, 2015. **115**(16): p. 8504-8563.

127. George, S., et al., *Amphiphilic Block Copolymers as Stabilizers in Emulsion Polymerization: Effects of the Stabilizing Block Molecular Weight Dispersity on Stabilization Performance.* Macromolecules, 2015. **48**(24): p. 8913-8920.

128. Rizzardo, E., et al., *Synthesis of defined polymers by reversible addition-fragmentation chain transfer: The RAFT process*. 2000. p. 278-296.
129. Moad, G., et al. *Advances in raft polymerization: Improved nanostrucured materials*. 2008. New Orleans, LA.
130. Boyer, C., M.H. Stenzel, and T.P. Davis, *Building nanostructures using RAFT polymerization.* J. Polym. Sci., Part A: Polym. Chem., 2011. **49**(3): p. 551-595.
131. Sun, J.-T., C.-Y. Hong, and C.-Y. Pan, *Recent advances in RAFT dispersion polymerization for preparation of block copolymer aggregates.* Poly. Chem., 2013. **4**(4): p. 873-881.
132. Keddie, D.J., *A guide to the synthesis of block copolymers using reversible-addition fragmentation chain transfer (RAFT) polymerization.* Chem. Soc. Rev., 2014. **43**(2): p. 496-505.
133. Guerrero-Sanchez, C., et al., *Quasi-block copolymer libraries on demand via sequential RAFT polymerization in an automated parallel synthesizer.* Poly. Chem., 2013. **4**(6): p. 1857-1862.
134. Haven, J.J., et al., *Rapid and systematic access to quasi-diblock copolymer libraries covering a comprehensive composition range by sequential RAFT polymerization in an Automated synthesizer.* Macromol Rapid Commun, 2014. **35**(4): p. 492-497.
135. Haven, J.J., et al., *One pot synthesis of higher order quasi-block copolymer libraries via sequential RAFT polymerization in an automated synthesizer.* Poly. Chem., 2014. **5**(18): p. 5236-5246.

2. Preparation of inverse polymerized high internal phase emulsions using an amphiphilic macro-RAFT agent as sole stabilizer[1]

2.1 Introduction

High internal phase emulsions (HIPEs) are concentrated mixtures of droplets dispersed in another liquid, where the minimum droplet volume fraction is 74 vol%. HIPEs are commonly stabilized by commercially available, non-ionic small molecular surfactants, where these amphiphiles decrease the interfacial tension between the two phases (typically an oil phase and aqueous phase), allowing for emulsification [1, 2]. To prepare a stable HIPE, the surfactant must rapidly adsorb at the interface and lower the interfacial tension between the phases to form a rigid interfacial film [3]. Commercially available emulsifiers that can stabilize particular HIPEs [4] include Triton X-405 [5], Span 80 (Sorbitan monooleate) [6] or a mixture of nonionic, anionic, and cationic surfactants: Span 20 (Sorbitan monolaureate), DDBSS (Dodecyl benzenesulfonic acid sodium salt), and CTAB (Cetyltrimethylammonium bromide) [7, 8]. Amongst these, Span 80 is the most commonly used emulsifier for water-in-oil (w/o) HIPE stabilization [4]. As alternative to surfactants of low molar mass HIPEs can also be stabilized by amphiphilic block copolymers with a hydrophilic and hydrophobic segment, otherwise known as polymeric surfactants [9], as well as solid particles the latter referred to as Pickering emulsifiers [10-13].

Polymeric surfactants are an attractive alternative to traditional surfactants as they offer a wide variety in chemical composition and molecular

[1] A shorter version of this section has been previously published in peer reviewed journal: Polymer Chemistry. 2016 **7**(9): p. 1803-1812.

architecture [14]. However, commercially available polymeric surfactants that have been used in HIPE stabilization are limited to polyethylene oxide (PEO)-based copolymers, including Hypermers®, Pluronics® and Synperonics® [15, 16]. Although widely used to stabilize HIPEs, the stabilization of a particular system requires careful selection of surfactant or mixtures of emulsifiers in order to obtain the required hydrophobic-hydrophilic balance (HLB) to warrant HIPE stability.

When the continuous phase is solidified through polymerization, a cellular monolithic structure commonly with interconnected voids and hence open cellular network, is produced, which is referred to as a poly(HIPE) [6, 17-21]. The cell walls of the porous poly(HIPE) are functionalized by the surfactants used, either through physi- or chemisorption. The ability to tailor the functionalization of the relatively large inner total surface area of interconnected voids by use of specific emulsifiers allows for poly(HIPE) design of interest for a range of applications, one being separation science. Availability of block copolymers with a specific HLB value and chemical functionality has become straightforward with the development of reversible-deactivation radical polymerization techniques. Among them, the reversible addition–fragmentation chain transfer (RAFT) process is particularly attractive due to its compatibility with a vast array of monomers and mild reaction conditions [22, 23]. Through the use of RAFT it is now possible to synthesize a wide variety of macromolecules using non-specialized equipment, allowing for the synthesis of well-defined (co)polymers with narrow molecular weight distributions and controlled architecture [24, 25]. The RAFT process allows the synthesis of amphiphilic block polymers required for the fabrication of HIPEs, with the most common method being sequential polymerization of two monomers of

opposing lyophilicity (e.g. a hydrophilic monomer and then a hydrophobic monomer) [26, 27].

Currently, the most explored methods to functionalize polyHIPEs include the incorporation of a co-monomer with the desired functionality, or via a post-polymerization functionalization approach [28]. Although functionalization via post-polymerization allows for greater control over the morphology and void diameter of the polyHIPE, this process includes an additional step. Battaglia *et al.* have recently introduced a slightly different method in which commercially available amphiphilic block copolymers (polystyrene-*b*- poly(ethylene oxide) (PS−PEO), poly(1,4-butadiene)-*b*-poly-(ethylene oxide) (PBD−PEO), poly(1,4-butadiene)-*b*-poly-(acrylic acid) (PBD−PAA), and polystyrene-*b*-poly(acrylic acid) (PS−PAA)) were employed as the macromolecular surfactants for water-in-oil emulsions to produce polystyrene/divinylbenzene foams [29]. The presence of the hydrophilic block of the block copolymer on the void surfaces of styrene-divinylbenzene polyHIPEs was demonstrated.

Following on from this work, Gao *et al.* introduced a well-defined amphipathic macro-RAFT agent (denoted poly($Styrene_m$-b-AA_n)) that was able to stabilize a w/o HIPE and prepare Sty-*co*-DVB polyHIPEs possessing closed voids [30]. In that work the morphology of the obtained polyHIPEs were tailored by means of controlling emulsion parameters such as the initiator and aqueous phase volume fraction, however varying the composition of the diblock copolymer was not used to explore possible polyHIPE morphologies. This concept was explored by Debuigne *et al.* by using a series of well-defined amphiphilic poly(ethylene oxide)-*b*-poly(styrene) (PEO-b-PSt) as polymeric surfactants to stabilize water-in-oil (w/o) HIPEs [31]. They identified important parameters such as the length

of hydrophilic block for the preparation of Sty-*co*-DVB polyHIPEs where the surface is coated by a polymeric surfactant.

In this chapter, the preparation of an inverse, oil-in-water (o/w) HIPE, (comprising 80 vol% dispersed phase) are explored. The system is stabilized by an amphiphilic macro-RAFT agent (as a quasi (block-like) copolymer poly(butyl acrylate)-*qb*-poly(acrylic acid)). The effect of amphiphilic macro-RAFT agent concentration, pH, initiators (both water soluble and oil soluble, in addition to redox initiation), hexadecane (as a hydrophobic organic modifier to prevent Ostwald ripening) and the polymerization temperature on the morphology of the resulting materials was investigated. Furthermore, the composition of the polymeric stabilizer (the ratio of hydrophilic to hydrophobic units) was varied with an aim to prepare highly interconnected, hydrophilic polyHIPEs. Ultimately, these materials have potential applications for use as a stationary phase in flow through applications e.g. for extraction or as the stationary phase in separation science.

2.2 Experimental Section

2.2.1 Materials

Acrylic acid (AA, Merck, ≥99%) was purified by distillation under reduced pressure. *n*-Butyl acrylate (BA, Sigma-Aldrich, 99%) was passed through a column of Al_2O_3 to remove the inhibitor. The RAFT agent, 2-[[(butylsulfanyl)-carbonothioyl]sulfanyl] propanoic acid (PABTC), was synthesized as described in Ref. [32].

Acrylamide (AM, Sigma-Aldrich, ≥98%), N,N'-methylenebisacrylamide (MBAM, Sigma-Aldrich, ≥99.5%)), methanol (Fluka), basic alumina (Al_2O_3, Brockman activity I, 60-325 mesh), hexadecane (Sigma-Aldrich), N,N,N',N'- tetramethylethylendiamine (TEMED, Sigma-Aldrich, 99%), sodium hydroxide (Sigma-Aldrich, ≥98.0%) and ammonium persulfate (APS, Ajax Chemicals, ≥98.0%), were all used as received. Toluene was obtained from Chem-Supply (Gillman, SA, AUS). 2, 2′-azobis(isobutyronitrile) (AIBN, MP Biomedicals, Eschwege, Germany) and potassium persulfate (KPS, M&B, 98%) were recrystallized from methanol and water, respectively.

2.2.2 Synthesis of amphiphilic polymeric surfactant by RAFT polymerization

A series of amphiphilic macro-RAFT agents consisting of AA and BA were synthesised as reported in the literature [33]. The Z group of the RAFT agent (PABTC) is an *n*-butyl group and the R group is 2-propionic acid, as shown in **Figure 2.1**. AA was chosen for its high solubility in basic water, aiding dissolution of the macro-RAFT agent in the aqueous continuous phase.

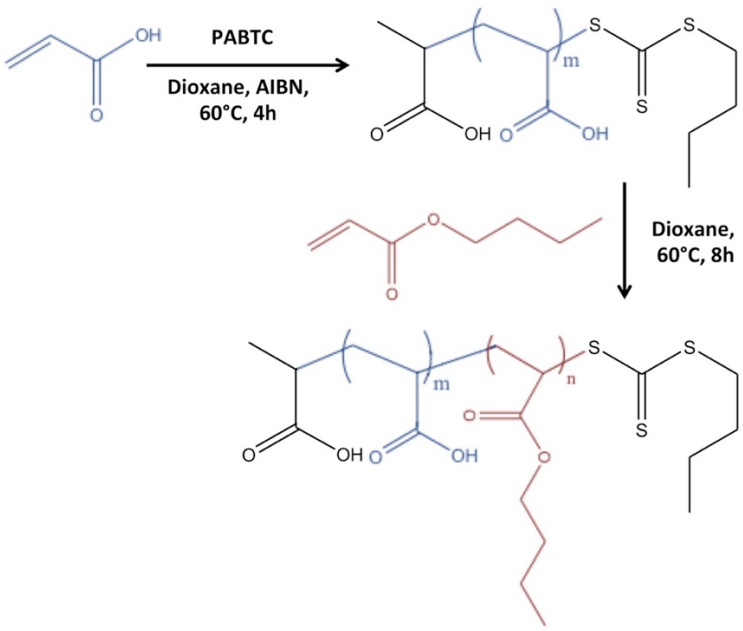

Figure 2.1. Schematic representation of the RAFT polymerization approach towards (quasi)-copolymerization of Acrylic acid (AA) and Butyl acrylate (BA) using 2-[[(butylsulfanyl)-carbonothioyl]sulfanyl] propanoic acid (PABTC) at 60 °C.

A typical polymerization protocol (one-pot, two-step polymerization) used in this work is summarized: In a first step, 1 g (4.2×10^{-3} mol) of PABTC and 0.068 g (4.0×10^{-4} mol) of AIBN were introduced into a round-bottom flask which was then sealed with a rubber septum, and purged with argon for 10 min. Then in a second step 1.51 g (2.1×10^{-2} mol) of AA was dissolved in 30 mL of dioxane and the solution was added to the round-bottom flask. This was purged with argon for 10 min. The reaction was allowed to proceed at 60 °C for 4 h under constant stirring. At this time, the reaction was stopped by removing the flask from the oil bath and a small aliquot of the solution was taken for electrospray ionization mass spectroscopy (ESI-MS) studies to determine the molecular weight of the AA single block.

For the polymerization of the hydrophobic block, BA was added to the round bottom flask at a molar ratio (relative to the initial chain transfer agent concentration) equal to the desired number of monomer units per macro-RAFT agent. The mixture was purged with argon for 10 min and further polymerization for 8 h at 60°C was performed. At this time, a small aliquot of the solution was removed for size exclusion chromatography (SEC) and ^{1}H NMR analysis, the results of which are summarized in **Table 2.1**. Dioxane was removed through rotary evaporation under reduced pressure. The polymer was then stored at 4 °C until use.

Table 2.1. Macro-RAFT agents synthesized in this study

$(AA)_x$-*qb*-$(BA)_y$	X (feed)	Y (feed)	BA/RAFT[a] (NMR)	$M_{n,SEC}$ [b] (g mol^{-1})	Đ
Qb-1	5	20	19.5	3100	1.05
Qb-2	20	5	-	2200	1.15
Qb-3	5	10	12.8	1900	1.07
Qb-4	5	5	5.2	750	1.19
Qb-5	10	20	20.5	3700	1.05

[a]Number of units of BA were determined by ^{1}H NMR using the signal of RAFT end group around 3.4 ppm respect to signal of methylene group of BA around 4.1 ppm. [b]Molecular weight and polydispersity determined by SEC analysis (THF used as eluent). Calculated according to PS standards.

2.2.3 Synthesis of hydrophilic 'inverse' polyHIPEs

The prepared amphiphilic macro-RAFT agents were used as stabilizer for the preparation of acrylamide-based polyHIPEs. In a typical procedure, the macro-RAFT agent was dissolved in 4 mL of water containing NaOH, acrylamide (AM, 1.420 g, 1.99×10^{-2} mol), the crosslinker N,N'-methylenebisacrylamide (MBAM, 0.309g, 2.00×10^{-3} mol) and the radical initiator KPS (0.04 g, 1.47×10^{-4} mol). In order to provide a suitable pH

environment to ensure the solubility of the macro-RAFT agent, differing amount of NaOH were required depending on the intended concentration of the macro-RAFT agent used. Using a syringe pump, the dispersed phase (toluene, 16 mL) was then added drop-wise at a rate of 0.8 ml per min with constant stirring (magnetic stirrer) at 1000 rpm. The temperature of the emulsion has already been found to influence droplet coalescence and the size of primary voids [34]. Because of this, the flask containing the continuous phase was kept at 30 °C by using a water bath for all emulsions during their preparation.

The emulsion was stirred for an additional 20 min after complete addition of the internal toluene phase. The emulsion was transferred to a glass vial and then cured at 60 °C in a water bath for 24 h. A small aliquot of all emulsions were kept in closed vials in the dark at room temperature, in order to determine emulsion stability. In order to study the droplet size of the emulsion, small samples of the HIPEs were withdrawn with a Pasteur pipette, then deposited directly on a clean microscope glass slide and analyzed. The resultant polyHIPE was purified via Soxhlet extraction with acetone for 72 hours as well as 72 hours with water. The experimental conditions used for the preparation of the different polyHIPEs can be found in **Table 2.2**.

2.2.4 Characterization

NMR analyses were performed on either a 400 MHz or 600 MHz Bruker Ultra Shield Avance Spectrometer. For all NMR analyses deuterated solvents were used as stated. Size exclusion chromatography (SEC) was performed with a Wisco-tech instrument using a refractive index detector (RID) and two chromatography columns (two PSS S linear 3µm, Polymer

Standard Services GmbH, PSS), THF (HPLC grade) was used as an eluent at a flow rate of 0.5 mL/min. The column oven was kept at 40 °C. The calculated molecular weights were based on calibration with respect to polystyrene (PS) standards of narrow dispersity with a molecular weight range of 160–154000 g mol^{-1} (PSS-Polymer Laboratories). The injection volume was 0.1 mL. Electrospray Mass Spectrometer Analysis was carried out using a ThermoFinnegan LTQ Orbitrap detector with Finnigan LCQ Data Processing and Instrument Control Software.

Emulsion droplets were observed using an optical microscope Nikon (model Eclipse E200), equipped with a camera (Tucsen, model IS500). Images of the emulsions were analyzed by ImageJ (NIH image) and the mean droplet size (n=100) and droplet size distribution were evaluated by triplicate. PolyHIPEs were characterized by field emission gun scanning electron microscopy (FE-SEM) studies using a Hitachi SU-70 FESEM in the Central Science Laboratory, University of Tasmania. All samples were platinum coated for 15 s in an argon atmosphere (Emitech 550, Emitech Ltd., UK), except where samples scanning electron microscopy coupled with energy dispersive X-ray (SEM-EDX) analysis were prepared and the materials were sputter-coated with carbon (Ladd 40000 carbon evaporator).

The calculation of the average void and window diameter (if windows were present) was performed on sets of at least 100 voids and 100 windows, respectively, using the image analysis software ImageJ (NIH image). A statistical correction was employed to obtain more accurate value, as each value was multiplied by $2/(3^{1/2})$ as described by Carnachan et al.[34].

The sulfur content of the polyHIPEs was determined with a Thermo Finnigan EA 1112 Series Flash Elemental Analyser. FTIR spectra were recorded by a Bruker Vertex 70 infrared spectrometer equipped with an ATR probe. Raman spectra of samples were recorded in the frequency range of 350 to 5000 cm^{-1} using a Renishaw inVia Raman microscope with Streamline. Solid samples were pressed gently using a spatula before being placed on the sample holder. A CCD line detector in the exit focal plane of the monochromator was used for recording the spectra. The laser source was a Nd:YAG laser. The Brunauer–Emmett–Teller (BET) surface area and microporosity were assessed using a Tristar II analyzer for the nitrogen adsorption/desorption isotherm at 77 K (Particle and Surface Science, Gosford, AUS). A Metertech SP-8001 UV/Vis spectrophotometer was used to evaluate the concentration of macro-RAFT agent removed from the polyHIPEs after the soxhlet extraction with acetone.

Table 2.2. Conditions used for the preparation of hydrophilic polyHIPE

Sample code	macro-RAFT agent	%wt [1]	Initiator (temperature)	pH [2]	Oil modifier (Hexadecane (HD))	HIPE stability (hours)	<D> (µm) Optical microscopy		(SEM) (µm)	
							Fresh	After 24h	<D> [3]	<d> [3]
A1	Qb-1	3.5	KPS (60 °C)	8.3	-	>12	63.2	68.0	12.9	(-)
A2	Qb-1	7	KPS (60 °C)	7.4	-	>12	78.1	71.8	22.2	2.2
A3	Qb-1	10.5	KPS (60 °C)	8.2	-	>12	86.9	49.7	42.9	(-)
A4	Qb-1	14	KPS (60 °C)	8.6	-	>12	68.4	45.7	11.0	(-)
A5	Qb-1	17.5	KPS (60 °C)	7.7	-	>12	59.7	40.2	10.1	(-)
A6	Qb-1	7	AIBN (60 °C)	7.4	-	>12	57.5	49.9	33.8	(-)
A7	Qb-1	7	KPS/ TEMED (RT)	7.4	-	>12	75.0 [4]	71.3	16.2	1.0
A8	Qb-1	7	KPS (60 °C)	7.4	5% wt [1]	>24	49.2	54.4	18.2	(-)
A9	Qb-1	7	KPS/ TEMED (RT)	7.4	5% wt [1]	>24	58.3 [4]	51.3	12.3	0.8
A10	Qb-1	7	KPS/ TEMED (RT)	7.4	20% wt [1]	>24	49.8 [4]	51.5	12.6	3
B1	Qb-3	4.1[5]	KPS/ TEMED (RT)	7.7	5% wt [1]	>48	32.3 [4]	26.8	5.3	0.8
B2	Qb-3	7	KPS/ TEMED (RT)	7.3	5% wt [1]	>48	28.6 [4]	31.5	8.2	1.3
C1	Qb-4	1.5[5]	KPS/ TEMED (RT)	7.1	5% wt [1]	>48	16.8 [4]	20.5	4.3	0.4
D1	Qb-5	7.8[5]	KPS/ TEMED (RT)	6.5	5% wt [1]	< 10 min	-	-	-	-

[1] All amounts are based on the weight percentage (w.r.t. the continuous phase). [2] Differing amounts of NaOH were added depending on the intended concentration of the macro-RAFT agent (at a basic pH, carboxyl groups are deprotonated and poly(acrylic acid) is soluble in water). [3] A void describes the pores of the polyHIPE and <D> is average size of voids. Window refers to the interconnecting pores between two adjacent droplets and <d> is average size of windows. [4] Sample stability test was performed before adding TEMED. [5] These amounts are equivalent to the same molar ratio used for sample A3, converted by using Mn of the macro-RAFT agent obtained by size exclusion chromatography.

2.3 Results and Discussion

2.3.1 Synthesis of amphiphilic quasiblock macro-RAFT agent

RAFT is a simple and effective polymerization technique, which yields well-controlled polymers exhibiting an almost infinite range of functionalities [35, 36]. The macro-RAFT agent can be modified through alterations to the length of both blocks. The AA block is pH-sensitive; the BA block is hydrophobic and hence the polymer is amphiphilic in nature. Alterations in the length of each block provide additional control over the behaviour of the macro-RAFT agent. The high propagation rate coefficient of both BA and AA together with their high efficiency in one-pot RAFT polymerization means that specific amphiphilic block co-polymers to be used as stabilizers can be prepared in a simple fashion.

This one-pot polymerization technique has been utilized to achieve the synthesis of quasi (block-like) copolymers using sequential monomer addition [37, 38]. This approach yields quasi-block copolymers (Qb) when the conversion of monomer in the first step (e.g. acrylic acid) is lower than 100% prior to a second monomer being incorporated [39]. The NMR spectrum of the macro-RAFT-AA_5 revealed the presence of unreacted AA after the first polymerization step, suggesting the formation of quasi-copolymers after the polymerization reaction of the second block of BA, during which time residual AA monomer can be consumed (See **Table 2.1**).

The molecular weight of the macro-RAFT-AA_5 was estimated by electrospray ionization mass spectrometry (ESI-MS). **Figure 2.2** shows a typical mass spectrum for the PABTC-mediated polymerization of acrylic acid targeting a degree of polymerization of 5 (RAFT-AA_5). The spectrum

indicates a distribution of AA oligomers containing a different number of repeat units of AA (from 2 up to 8), which were chain extended in the second step polymerization of BA. For every macro-RAFT-AA_5 polymer analyzed the raw ESI-MS spectrum was qualitatively similar to that in **Figure 2.2.**

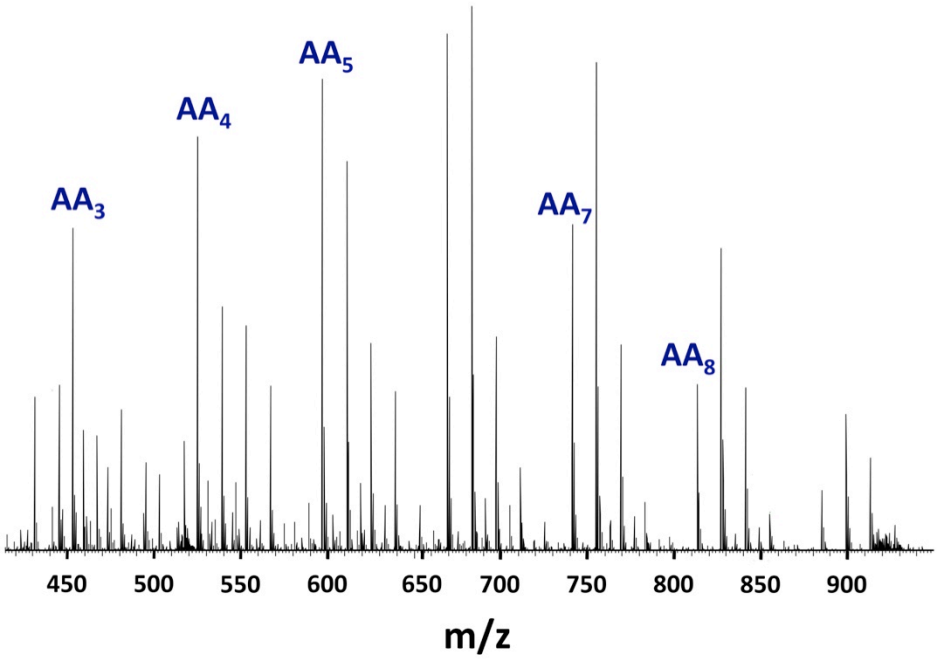

Figure 2.2. Mass spectrum of RAFT-AA_5 obtained by ESI-MS.

The number of BA units in each quasi-copolymer was estimated by comparing the ^{1}H NMR integral of the S-CH_2- group of PABTC at 3.4 ppm and the –O-CH_2- groups of the n-butyl group of each BA repeat unit at ~4.1 ppm (see **Figure 2.3A**). As reported in **Table 2.1**, there was a good agreement between the targeted units of the BA and the actual number of units of BA in the prepared quasi-copolymers. This indicates the controlled character of the polymerization process when using PABTC as RAFT agent for the polymerization of BA. SEC analyses of the three different macro-

RAFT agents showed copolymers were prepared under RAFT control ($Đ$ < 1.2) as well as the elution at longer retention times of copolymers containing a lower amount of BA units (see **Figure 2.3B**).

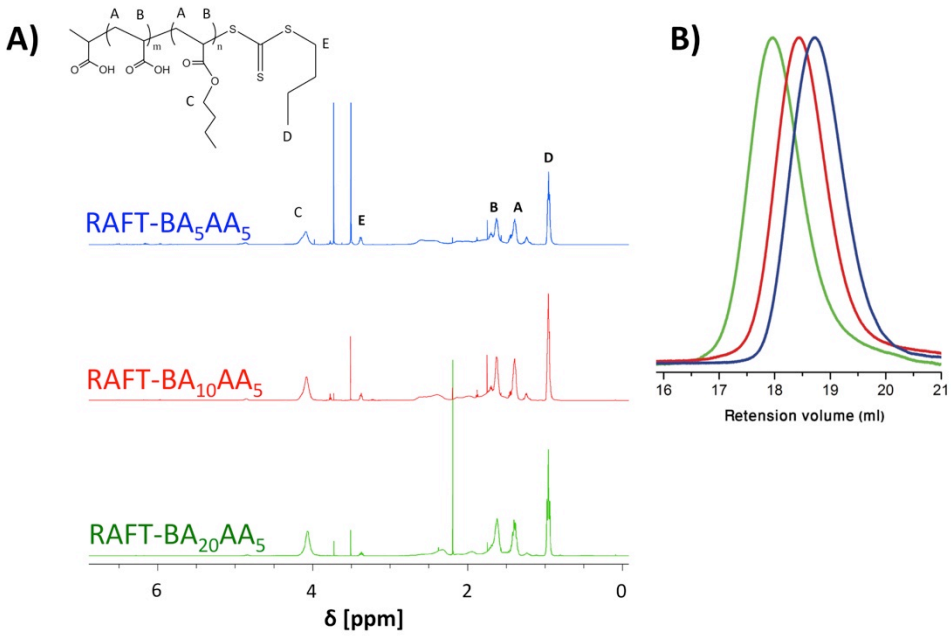

Figure 2.3. ^{1}H-NMR spectra ($CDCl_3$, 600 MHz) (A) and SEC (B) of RAFT-BA_{20}-AA_5 (green), RAFT-BA_{10}-AA_5 (red), RAFT-BA_5-AA_5 (blue) quasi-block copolymers.

2.3.2 Stability of oil-in-water HIPEs using quasi-block copolymers as surfactants

At basic pH, the poly(AA-*qb*-BA) quasiblock copolymers prepared here are anionic polyelectrolytes and can exhibit properties similar to an anionic surfactant, while still bearing the reactive trithiocarbonate terminal group. In order to establish the possibility of stabilizing HIPEs with these polymers, macro-RAFT agent-Qb1 (see **Table 2.2**) was chosen as a starting point to

examine its potential for the stabilization of toluene-in-water emulsions, with Acrylamide (AM), N,N'-methylenebisacrylamide (MBAM) and NaOH present in the water phase. 3.5% wt of the macro-RAFT agent with respect to the aqueous phase resulted in the successful stabilization of HIPEs with oil volume fractions between 60 and 90%. The emulsion droplets were spherical but polydisperse (See **Figure 2.4**).

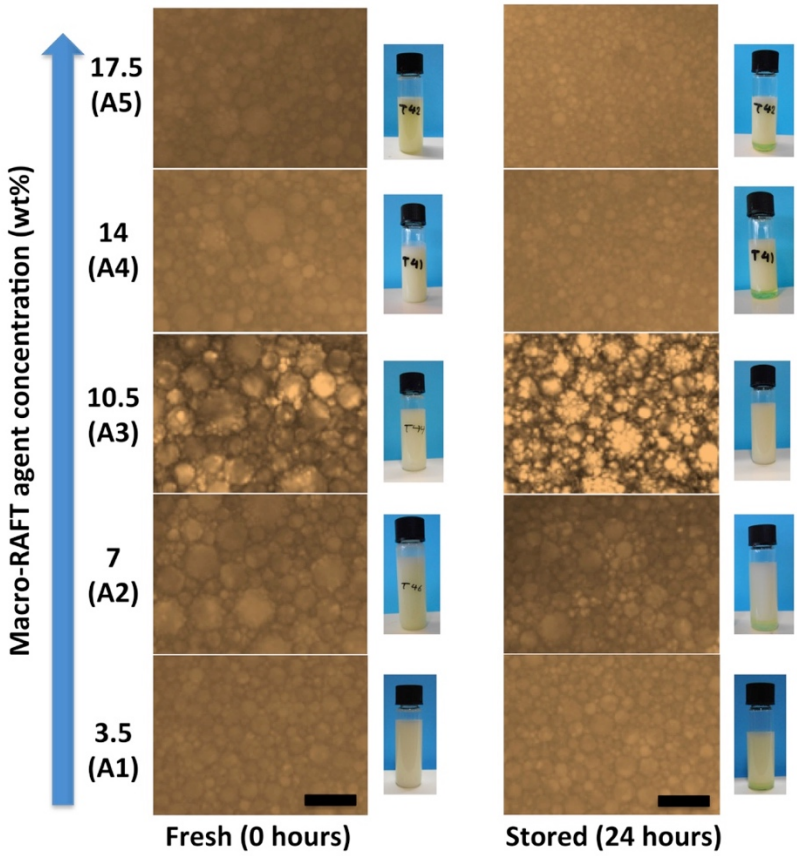

Figure 2.4. Optical microscopy and photographs of HIPEs stabilized by different amount of macro-RAFT agent-Qb1; after preparation (0 hours, left column) and after 24 hours (right column). The scale bar in all cases is 40 μm.

The drop test method was used to determine that the prepared HIPE was an inverse (o/w type) system [40, 41] (see **Figure 2.5**).

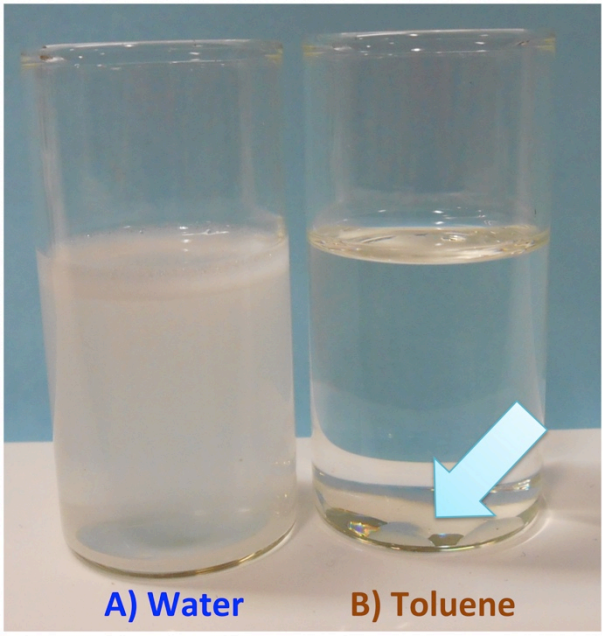

Figure 2.5. The emulsion type was determined by the drop test method. One drop of the formed HIPE with macro-RAFT agent-Qb1 was placed into (A) water and (B) toluene. The emulsion droplet was seen to disperse in the water but remained as a droplet in toluene.

The Hydrophile-Lipophile Balance (HLB) is obtained using the Griffin's method (eq 2.1), from the molecular weight ratio of the hydrophilic block (M_h) and the total molecular weight (M):

$$HLB = 20 \times M_h/M \qquad (2.1)$$

The HLB values for all macro-RAFT agents are summarized in **Table 2.3**.

Table 2.3. HLB values of macro-RAFT agents synthesized in this study

$(AA)_x$-*qb*-$(BA)_y$	X (feed)	Y (feed)	HLB	
			[a] Theoretical	[b] Obtained
Qb-1	5	20	2.7	2.7
Qb-2	20	5	13.0	-
Qb-3	5	10	4.6	3.9
Qb-4	5	5	6.9	6.8
Qb-5	10	20	4.5	4.4

[a] Theoretical HLB number is determined by the Griffin's rule: HLB = 20×Mh hydrophilic part/Mw (hydrophilic part + hydrophobic part), where Mh is the molecular weight of the hydrophilic block and Mw is the molecular weight of the surfactant. It is calculated based on the feed units, assuming complete conversion of polymerization. [b] Obtained HLB number is calculated based on the number of BA units calculated by ^{1}HNMR. In the case of inverse HIPE (oil in water), the HLB value is normally in the range of 10-16.

Additionally, the macro-RAFT agent-Qb2 was designed for use based on its HLB value, which is suitable for the stabilization of o/w emulsions [42]. However, no amount of this polymer and/or varying the internal phase volume resulted in sufficiently stable emulsions for curing. Similarly, an $(AA)_5$ macro-RAFT agent (no BA units) was unable to stabilize any emulsion under these conditions.

Optical microscopy was used to examine the synthesized HIPEs immediately after preparation as well as 24 hours post-synthesis, in order to examine emulsion stability. Optical micrographs and photos of the resultant emulsions under various conditions of macro-RAFT loading (in this instance Qb1) are shown in **Figure 2.4**. The mean emulsion droplet diameter slightly increased with increasing amounts of macro-RAFT agent, reaching a maximum of ~87 μm when the macro-RAFT agent concentration was ~ 10.5% wt (w.r.t. the continuous phase). At higher levels (> 14% wt) the mean droplet diameter decreased to ~60 μm. Further increases to the

amount of macro-RAFT did not result in any further reduction in the droplet size.

Given the solubility of pAA in water is reduced at low pH, it was expected that the HIPE would be relatively unstable under acidic conditions. This was demonstrated by the addition of a few drops of concentrated HCl to a prepared emulsion (HIPE formulation A2), whereby phase separation immediately occurred (see **Figure 2.6**).

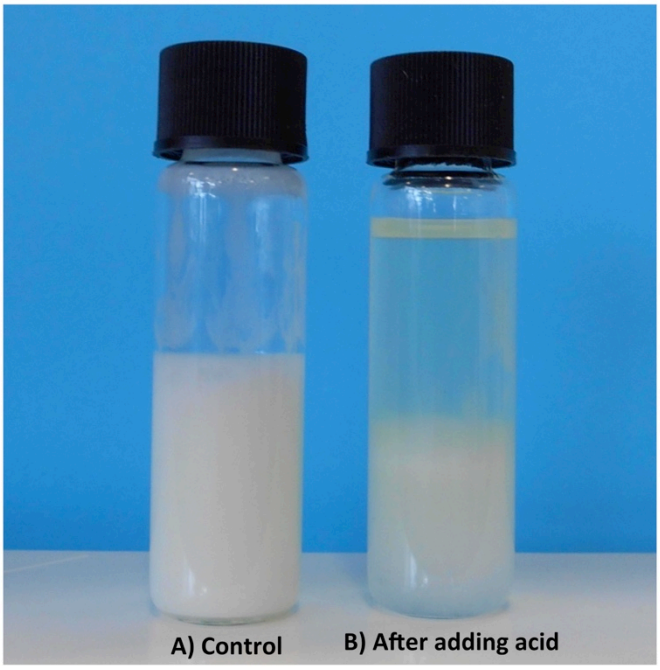

Figure 2.6. Triggered demulsification by addition of acid (emulsion formed with macro-RAFT agent-Qb1): A) Control HIPE, B) After addition of acid.

Additionally HIPE stability was investigated under basic conditions (pH > 9) using HIPE formulation A2. In order to do this, we added further NaOH to

the aqueous phase of HIPE A2 formulation (the pH of this solution was 12.5) prior to mixing and emulsification with toluene. After 1 hour, the emulsion had separated into three phases; a clear liquid as top layer, a middle layer similar to the freshly prepared emulsion, and a yellow oil at the bottom of the vial (**Figure 2.7**).

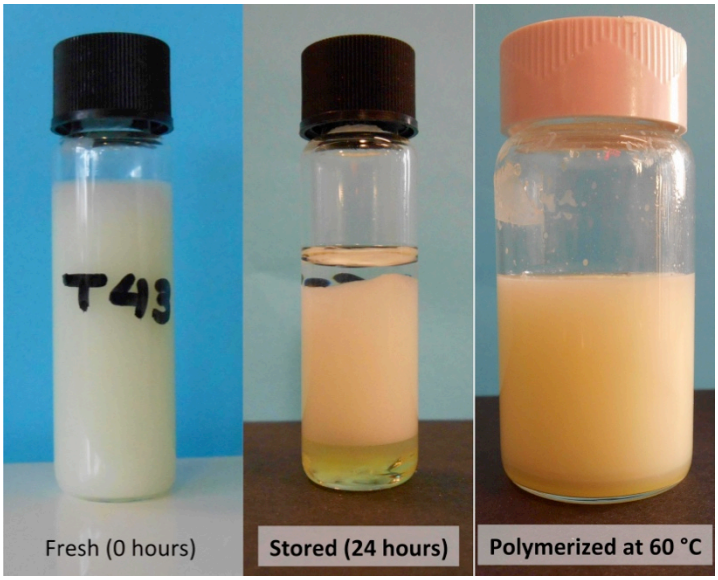

Figure 2.7. Effect of basic conditions on the HIPE stability within 24 h, HIPE formulation A2 (emulsion formed with macro-RAFT agent-Qb1). For the polyHIPE obtained by this formulation (KPS, 60 °C, 24 hours) a layer of tough yellow polymer was found at the bottom of the vial.

The oily yellow layer was transformed into a tough polymeric mass after polymerization of the HIPE (60 °C for 24 hours), suggesting that the macro-RAFT agent is not an efficient emulsifier at high pH (**Figure 2.7**). This result may be attributed to the increased ionic strength of the system at a more basic pH, reducing the stability of the inverse HIPE.

For further study, the macro-RAFT agent-Qb1 was investigated by NMR under basic conditions and at different temperatures, by measuring the NMR spectra of the copolymer as a function of time potential changes in NMR spectra were recorded. As shown in **Figure 2.8** no major changes in NMR spectra occurred upon increasing temperature up to 60 °C. Hence, sodium hydroxide was added to the aqueous phase for all samples in order to ensure the pH was between 7 and 8.

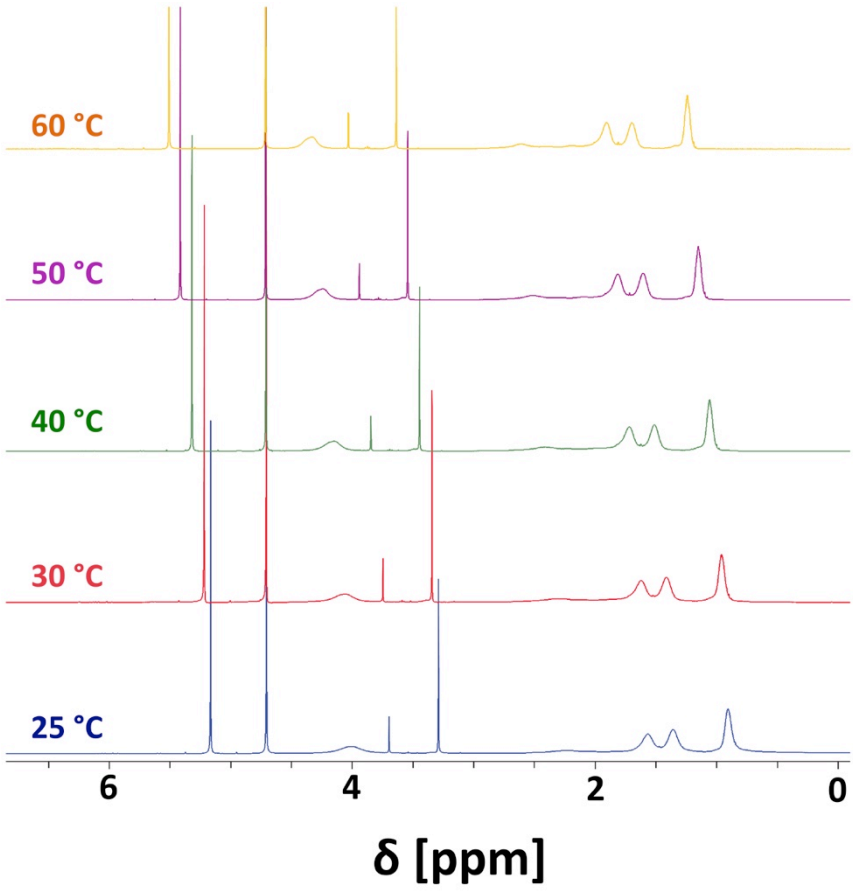

Figure 2.8. ^{1}H-NMR spectra (D_2O, 400 MHz) of RAFT-BA_{20}-AA_5 (0.2 g in 1 ml D_2O in presence of 0.01g of NaOH and 0.01 g Trioxane (as internal standard)) at 25, 30, 40, 50 and 60 °C.

2.3.3 Synthesis of hydrophilic polyHIPEs

The o/w emulsions discussed in the previous section were polymerized in order to obtain porous polyHIPEs. A homogeneous and stable yellow polyHIPE A1 was obtained that retained the shape and volume of the mold (no apparent shrinkage was observed). The polymerized samples could be handled without breakage (**Figure 2.9**).

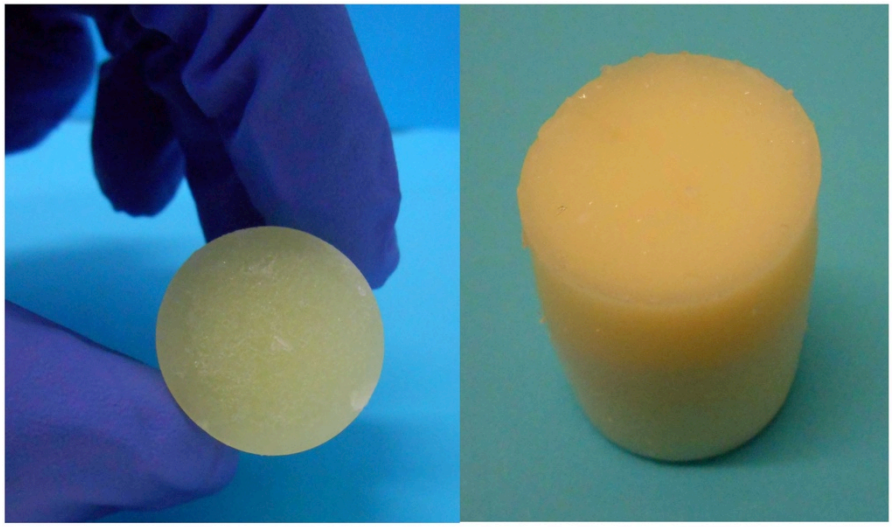

Figure 2.9. A yellow solid macroporous polyHIPE obtained by polymerized formulation of HIPE A1 (KPS, 60 °C, 24 hours, after preparation).

Increasing the macro-RAFT agent-Qb1 concentration from 3.5% wt to 17% wt had a significant effect on the morphology of the resulting polyHIPEs (e.g. on the void size) as can be seen from the SEM images (**Figure 2.10**).

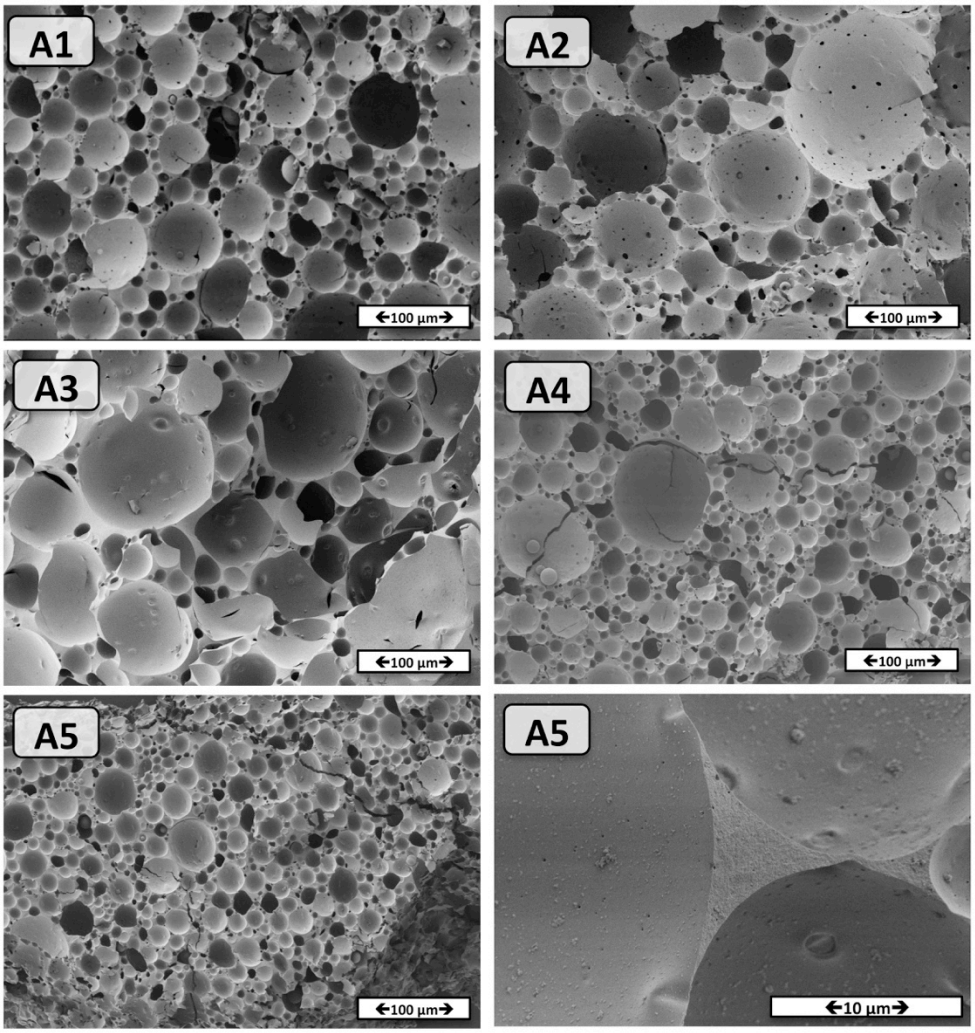

Figure 2.10. Scanning electron micrographs of emulsion templated macroporous polymer made by polymerization of HIPEs stabilized solely by different amount of macro-RAFT agent-Qb1 (w.r.t. the continuous phase) at 60 °C in presence of KPS as initiator.

The prepared polyHIPEs retained their yellow colour after washing the samples with acetone using a Soxhlet apparatus and subsequent washing with water (**Figure 2.9**), providing a visual cue regarding the incorporation of the macro-RAFT agent. Elemental analysis confirmed the presence of

sulfur amount within the polyHIPEs (e.g. the sulfur content within polyHIPE A3 was 0.41%). Further evidence for the presence of the macro-RAFT agent on the surface of the polyHIPE was obtained from Energy Dispersive X-ray analysis (EDX), clearly indicating that sulfur was present at the surface of the polyHIPE A3 (**Figure 2.11**).

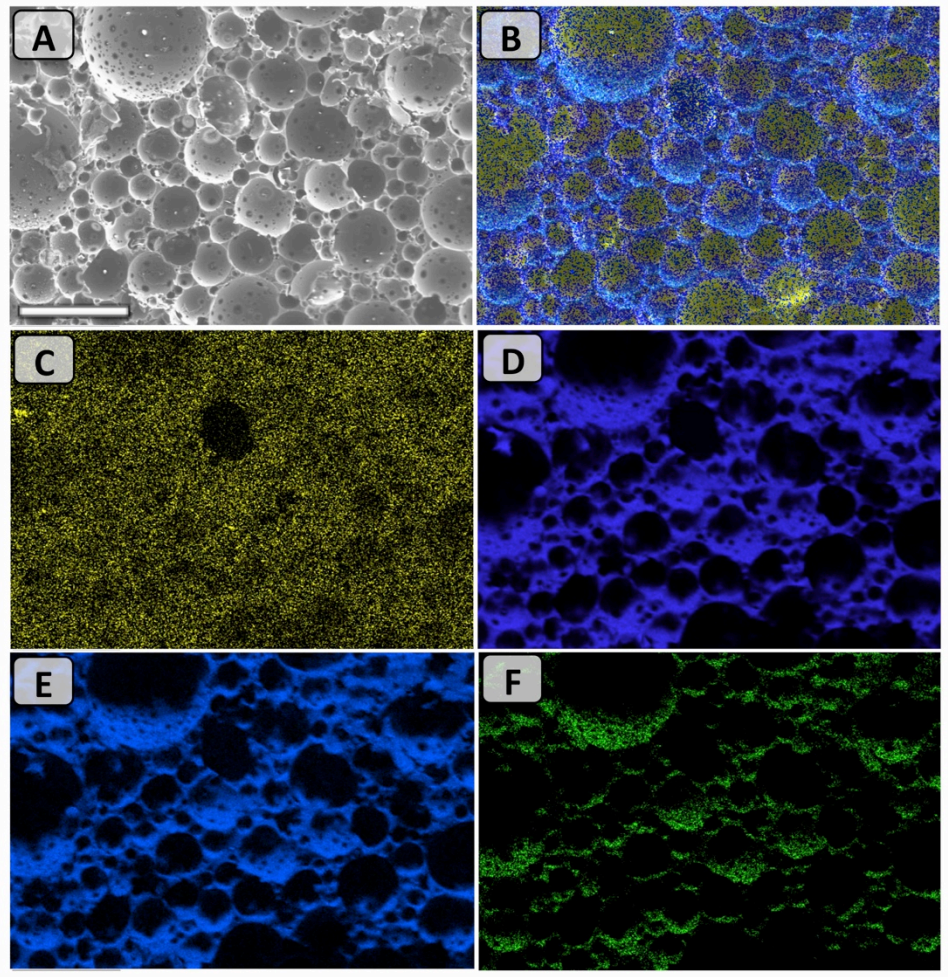

Figure 2.11. EDX mapping analysis on polyHIPE A3; (A) SEM image and (B) Overall mapping elements on the same spot: corresponding to sulfur (C), carbon (D), oxygen (E), and nitrogen (F) mapping. Scale bar is 50 μm.

As KPS was used as initiator, the sulfur content is likely due in part to the presence of initiator-derived endgroups. To determine the amount of the RAFT-agent "trapped" inside the polyHIPE, the washes from the polyHIPE during purification were analyzed. The solvent washings (acetone) were yellow, suggesting the removal of some diblock-copolymer from the material, and these washings were analyzed by using UV-Vis spectroscopy [43]. It was determined that, in the case of polyHIPE A3, the amount of removed macro-RAFT agent- Qb1 is ~ 29-31% wt.

To further investigate the inclusion of the macro-RAFT agent within the polyHIPE structure, FTIR analyses were performed on the resultant material, in comparison to a sample of AM-MBAM polymerized in bulk (KPS as initiator) subjected to the same washing protocol. The FTIR spectrum of PolyHIPE A3 shows the presence of an extra band at 1710 cm^{-1} respect to bulk polymer, which is present in the FTIR spectrum of the macro-RAFT agent (**Figure 2.12**). This signal corresponds to the carbonyl stretch of the carboxylic acid group of the AA block, and is a good evidence of the incorporation of the macro-RAFT agent into the polymer structure.

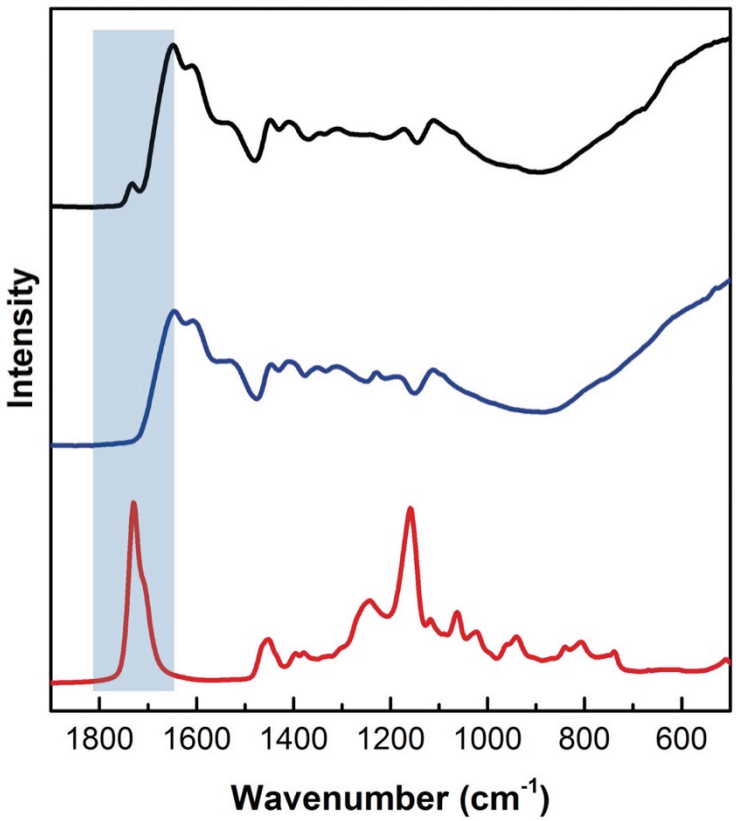

Figure 2.12. ATR-IR of macro-RAFT agent-Qb1 (red line), bulk polymer (blue line) and polyHIPE A3 (black line). The peak around 1650-1800 cm^{-1} is highlighted.

Further spectroscopic analysis of prepared polyHIPES was performed via Raman spectroscopy at randomly selected regions across the polyHIPE surface. Peaks in the Raman spectrum of the macro-RAFT agent used to prepare polyHIPE A3 correlate with peaks observed in the spectrum obtained from subtracting the bulk poly(AM-co-MBAM) polymer from A3 (see **Figure 2.13A**). In addition, the polyHIPE surface was mapped for the presence of the C=S peak at 1107 cm^{-1} (**Figure 2. 13B**). The map confirmed the presence of the C=S groups in the same physical location as the walls of the polyHIPE voids, which are solely due to the trithiocarbonate end group of the RAFT agent.

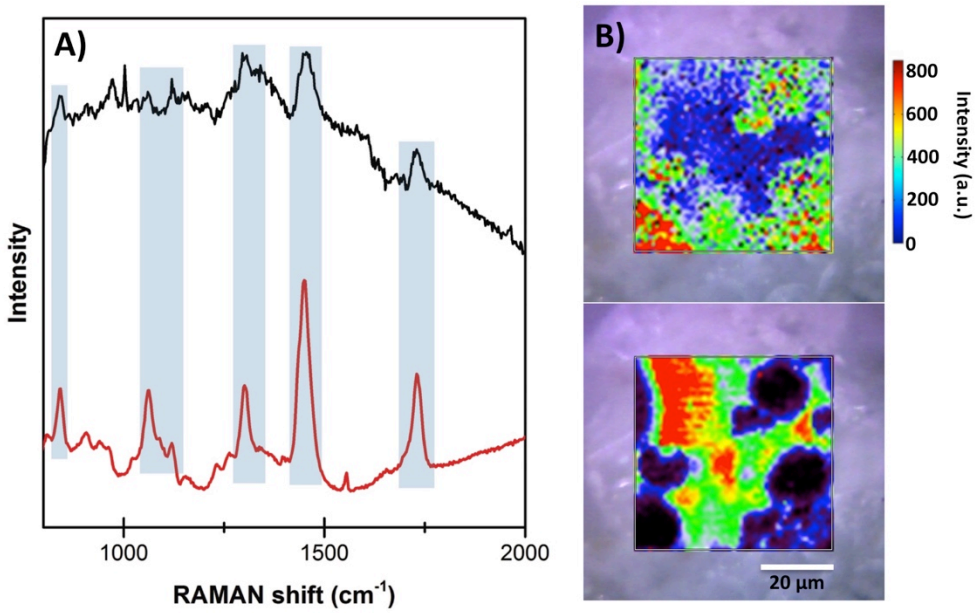

Figure 2.13. (A) Raman spectra of macro-RAFT agent-Qb1 (Red line), difference between polyHIPE A3 and bulk polymer (Black line)**.** (B) Raman mapping (upper) is based on the C=S peak at 1107 cm^{-1} of macro-RAFT agent-Qb1 on the surface of polyHIPE A3 by normalizing the peak intensity. Raman mapping (bottom) based on signal to baseline from 1383 to 1493 cm^{-1} at the same area (Dark blue regions in the lower image are void locations within the polyHIPE.)

2.3.4 Effect of initiator

Oil-soluble (AIBN) and water-soluble (APS) thermal initiators, as well as a redox initiation system (TEMED/ KPS) were also investigated for the preparation of polyHIPEs and their influence on the resultant morphology of the material. In all cases the macro-RAFT agent-Qb1 concentration was kept constant at 7% wt (w.r.t. the continuous phase). Stable emulsions were not obtained when APS was employed as the water-soluble initiator. Upon further investigation it was found that when APS was added to a pre-formed

emulsion, phase separation immediately occurred (**Figure 2.14**). This may have been due to changes of the pH of the HIPE.

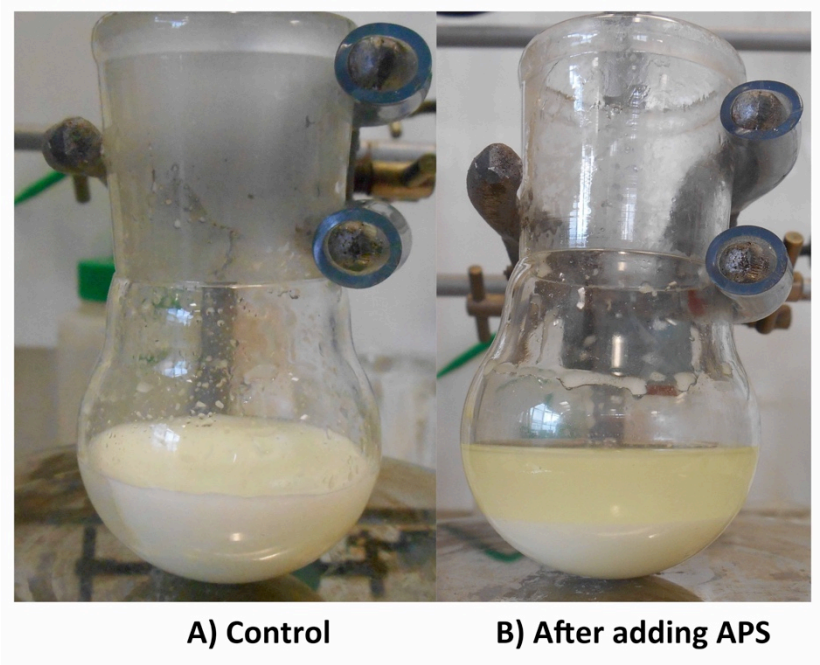

Figure 2.14. Phase separation after addition of APS to the HIPE formulation A2 A) Control HIPE, B) After addition of APS (Image was taken at an interval of 2 min).

When AIBN (dissolved in the toluene phase) was used, a predominately closed-structure polyHIPE was obtained (**Figure 2.15** (sample A6)). It has been shown previously that the locus of initiation has a significant effect on porosity of the resultant polyHIPE [44]. In this case, more extensive droplet coalescence can occur as the polymerization is not "localized" at the oil–water interface when the initiator is in the organic phase. Variation in the structure of a polymerized emulsion by changing initiators was also reported by Wu *et al.* for the preparation of poly(sty-co-DVB) by polymerization of medium internal phase emulsion templates [45]. They observed that

changing the initiator from water-soluble (KPS) to oil soluble (AIBN) resulted in materials with a more open structure; here we demonstrate the opposite trend in an inverse (o/w) system.

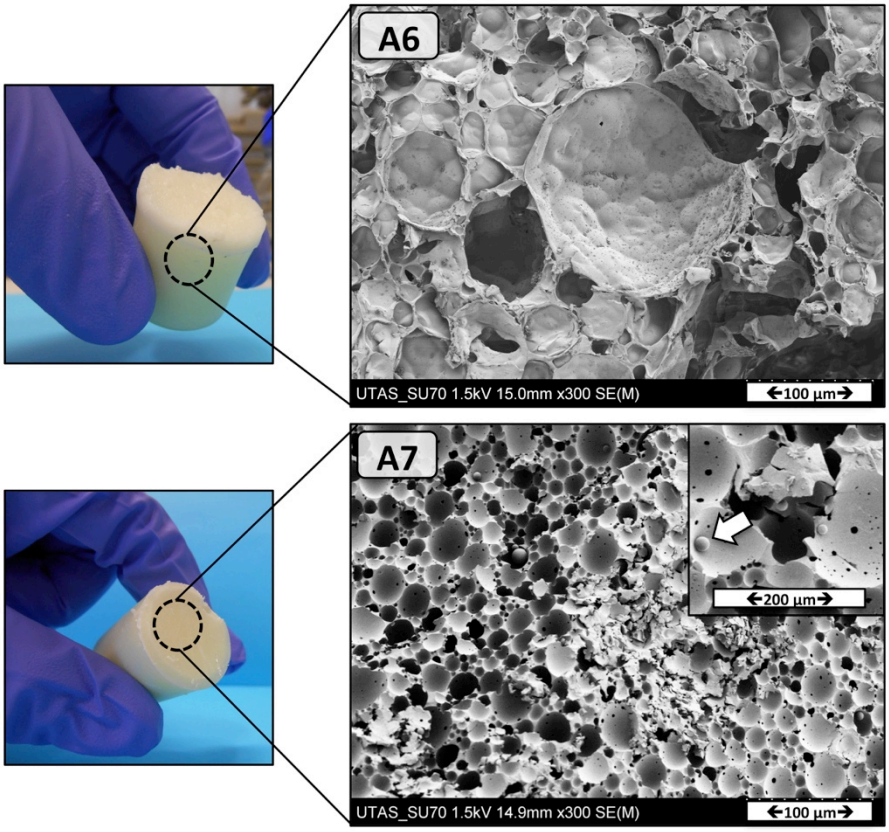

Figure 2.15. SEM of polyHIPEs stabilized by 7% wt of macro-RAFT agent-Qb1, polymerized at 60 °C (A6- in presence of AIBN as initiator) and (A7- in presence of TEMED (a reducing agent) with KPS) at room temperature.

In order to reduce droplet coalescence and Ostwald ripening, room-temperature polymerization using a KPS/TEMED redox couple as initiator was performed. SEM analysis of the resulting polymer (sample A7) is shown in **Figure 2.15**, showing heterogeneity in the structure as well as the

formation of micron-sized particles within some voids. This could be explained considering the partition of monomer toward the oil phase and the formation of water in oil droplets within the HIPE [46]. It is believed that, as the polymerization begins at room temperature, the effect of destabilizing mechanisms such as coagulation and Ostwald ripening decreases, causing a more homogeneous structure within the obtained polyHIPE [47].

2.3.5 Effect of hexadecane as an organic modifier

The preparation of a hydrophilic polyHIPE from an inverse HIPE typically requires careful emulsion stabilization and polymerization due to the possibility of Ostwald ripening [48]. Ostwald ripening in emulsions is a process of gradual growth of the larger droplets at the expense of smaller ones due to mass transport of soluble dispersed phase (oil) through the continuous phase (water) leading to emulsions containing droplets with different sizes [49]. In the case of o/w emulsions, the addition of a particularly hydrophobic oil such as hexadecane (HD) is known to help arrest ripening, due to reduced transport through the continuous phase [50]. In this work, HD was added the oil phase of our emulsions (5% wt w.r.t. continuous phase) followed by polymerization either with KPS (at 60 °C, sample A8) or KPS/TEMED (at room temperature, sample A9). When KPS was used as initiator, optical microscopy (**Figure 2.16**) and SEM analysis (**Figure 2.17**) demonstrated that the addition of HD resulted in emulsions with smaller droplet sizes that were stable over a longer period of time, resulting in a more regular porous structure (in comparison to **Figure 2.10**).

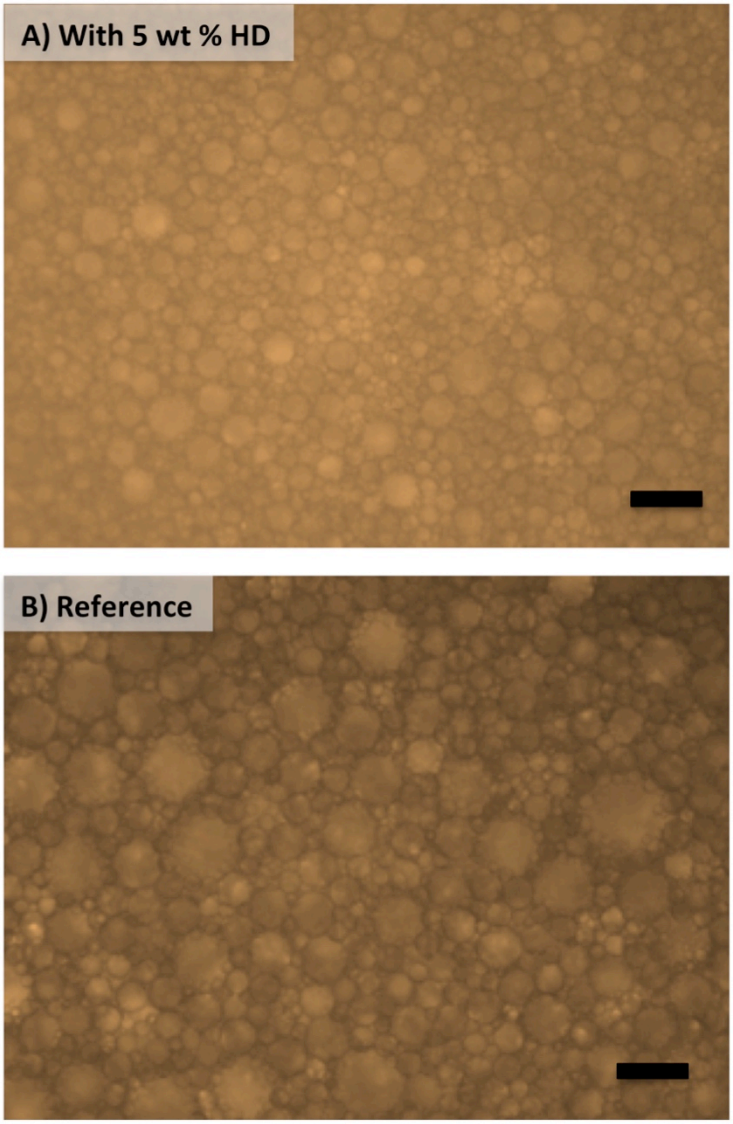

Figure 2.16. Optical microscopy of HIPEs stabilized by macro-RAFT agent-Qb1 7 wt%. A) in the presence of 5 wt% hexadecane (HD) B) Without adding hexadecane (HD). Scale bar is 50 μm.

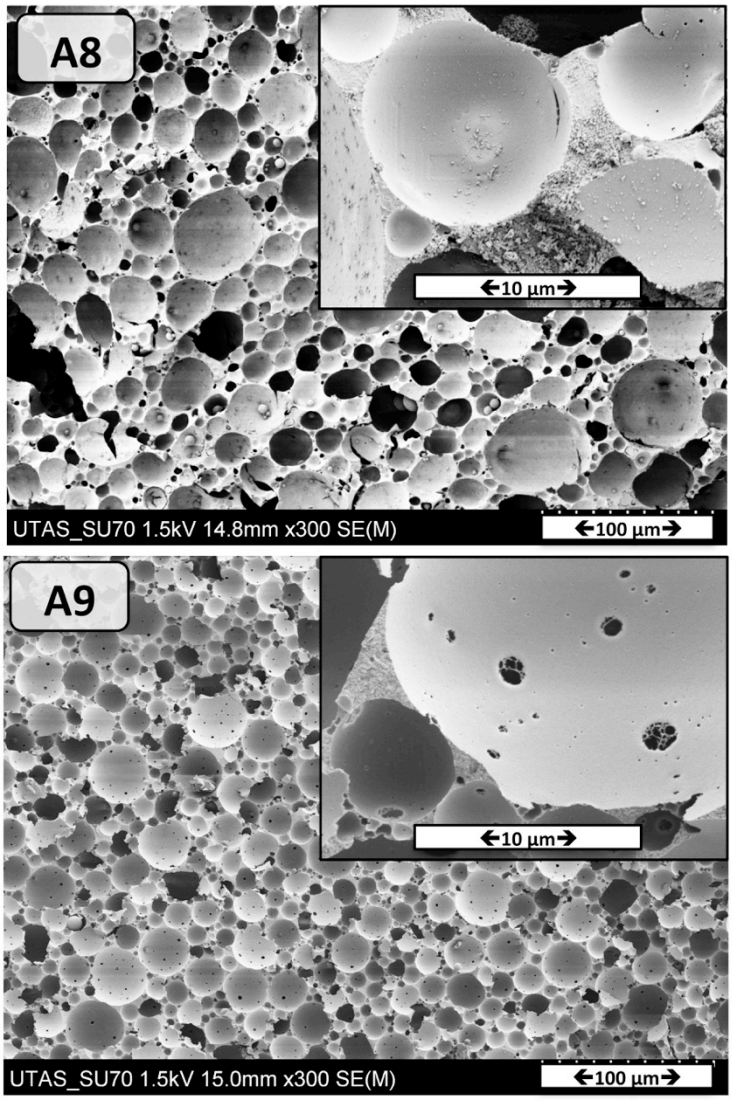

Figure 2.17. SEM of PolyHIPEs stabilized by 7% wt of macro-RAFT agent-Qb1, polymerized in presence of 5% wt hexadecane as oil modifier (A8) polymerized at 60 °C with KPS (A9) polymerized at room temperature (TEMED/ KPS).

When KPS/TEMED was used (A9), smaller voids were formed compared to A8, in addition to evidence of interconnectivity (windows) on the voids, which was not observed in polyHIPE A8. These two differences may result

from the polymerization temperature and the effect of that on the interfacial tension between oil droplet and aqueous phase. Increasing the HD loading to 20 wt % (polyHIPE A10, **Figure 2.18**) resulted in a polyHIPE with significant heterogeneity.

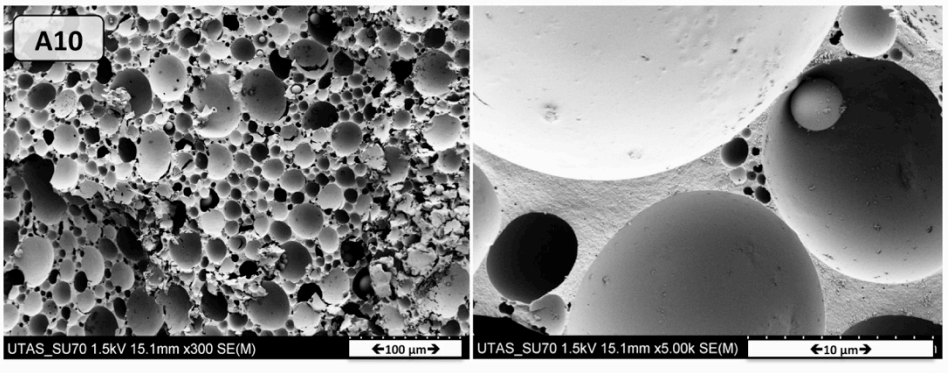

Figure 2.18. SEM of polyHIPE stabilized by 7 wt% of macro-RAFT agent-Qb1 in the presence of 20 wt % of hexadecane in the oil phase polymerized at room temperature (TEMED/KPS).

2.3.6 Tuning the polyHIPE structure by means of the macro-RAFT agent composition

Finally, the effect of the diblock copolymer composition on the stability and nature of the resultant emulsion was considered. To establish the role of the hydrophobic BA block, macro-RAFT agents Qb3 and Qb4 were used (both consisting of 5 AA repeat units with differing BA lengths). The procedure for the preparation of HIPE A9 was chosen and all other variables were kept constant (the same mole equivalent of the diblocks were used in each case). HIPEs were successfully prepared (denoted HIPE B1 (using macro-RAFT agent-Qb3) and HIPE C1 (using macro-RAFT agent-Qb4)), with both showing increased stability in comparison to HIPE A9 of 48 hours storage

without phase separation (See **Table 2.2**). SEM images of the obtained polyHIPEs after polymerization are shown in **Figure 2.19.** In comparison to polyHIPE A9, both polyHIPEs B1 and B2 possess open porous networks with an increased number of windows. This increased level of interconnectivity was also demonstrated with an increase in BET specific surface area (2.17 m^2 g^{-1} for B1, as opposed to 1.17 m^2 g^{-1} for A9). These results suggest that macro-RAFT agents with a shorter hydrophobic block favour the formation of open network, interconnected inverse polyHIPEs in comparison to macro-RAFT agents with a longer hydrophobic block. It is believed that macro-RAFT agents with longer hydrophobic blocks are less labile during the HIPE preparation and stabilization, providing greater stabilization of the obtained polyHIPE, as reported previously [29].

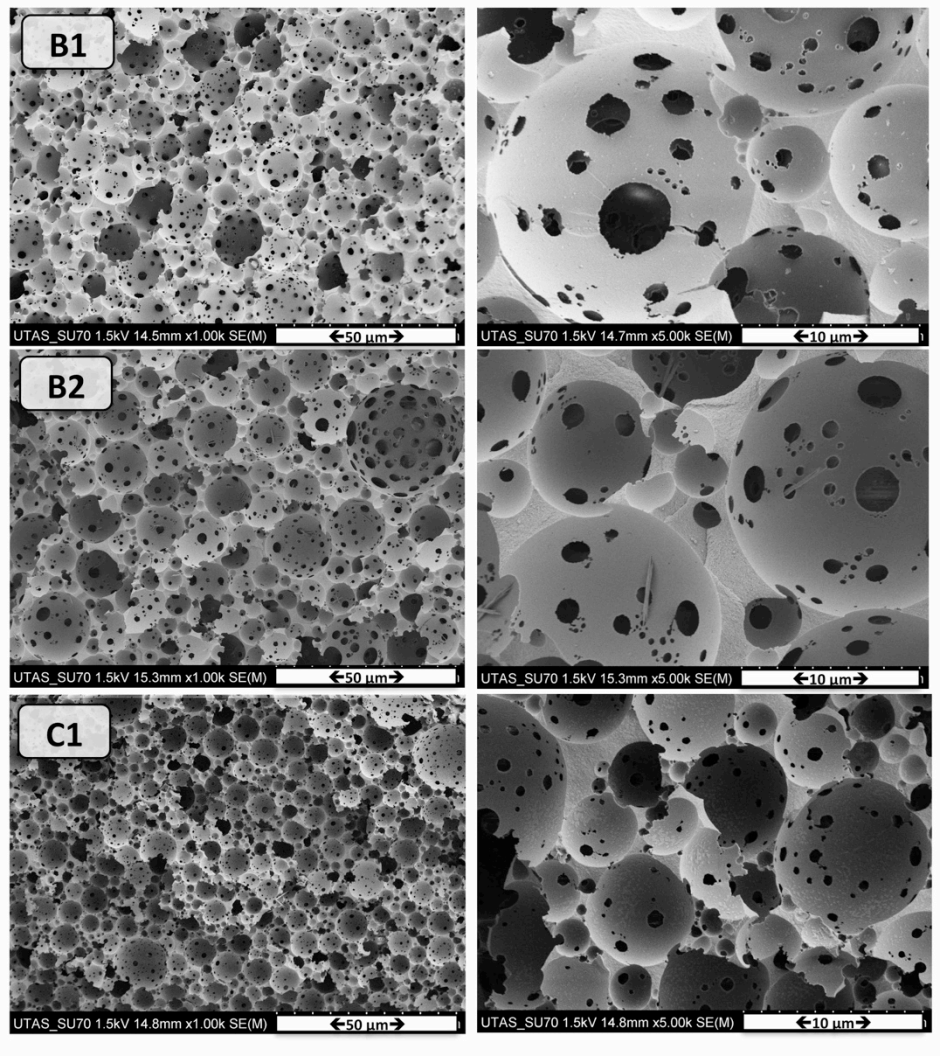

Figure 2.19. SEM of PolyHIPE stabilized by B1) macro-RAFT agent-Qb3 4.1% wt, B2) macro-RAFT agent-Qb3 7% wt C1) macro-RAFT agent-Qb4 1.5% wt, in presence of 5% wt of hexadecane in oil phase and polymerized at room temperature (TEMED/KPS).

The macro-RAFT agent-Qb5 was synthesized to investigate the influence of increasing the number of hydrophilic units (from 5 to 10 in comparison to Qb1) on the stability of the resultant HIPE, while keeping the hydrophobic block length constant. In this instance phase separation of the HIPE

occurred in less than 10 minutes. Rapid room temperature polymerization of this system (using the TEMED/KPS redox couple) resulted in a heterogeneous polyHIPE (D1, **Figure 2.20**) with extremely large voids. In conjunction with the influence of changing the BA block length, the resultant structure and connectivity of the formed polyHIPE is strongly dependent on the nature and composition of the diblock copolymer used as stabilizer.

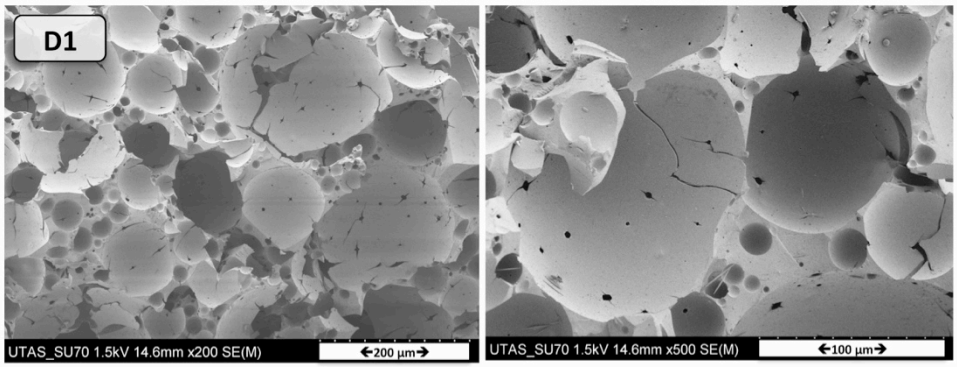

Figure 2.20. SEM of PolyHIPE stabilized by macro-RAFT agent-Qb5 7.8% wt, in presence of 5% wt of hexadecane in oil phase and polymerized at room temperature (TEMED/KPS). The amount of macro-RAFT agent for polyHIPEs B1, C1, and D1 are the same based on mole equivalent.

2.4 Concluding remarks

In this chapter, a strategy to produce functional polyHIPEs by introducing macro-RAFT agent as a surfactant was established. The results indicate that poly($(AA)_x$-*qb*-$(BA)_y$) can stabilize high internal phase o/w emulsions. By the polymerization of the continuous phase of these systems, highly porous emulsion templated materials were prepared. EDX with SEM revealed the presence of sulfur on the surface. FT-IR spectra for the polyHIPEs showed

new carboxyl groups within the polyHIPE which come from the macro-RAFT agent. Raman mapping showed a significant proportion of the C=S functionality on the void structure of the polyHIPE. This is consistent with the presence of the RAFT moiety on the surface. The successful preparation highlights the ability to stabilize the oil-in-water system with a well-chosen amphiphilic macro-RAFT agent.

It is believed that the RAFT functionality on the surface of the polyHIPE materials could provide a powerful substrate for subsequent surface chemistry reactions. The long-term aim is to decorate these materials with different functional groups. Future work will focus on the extension of this approach to a wider range of materials, and on achieving fine control over porous structure by tuning the hydrophilic and hydrophobic units.

2.5 References

1. Zhang, H. and A.I. Cooper, *Synthesis and applications of emulsion-templated porous materials.* Soft Matter, 2005. **1**(2): p. 107-113.
2. Aveyard, R., B.P. Binks, and J.H. Clint, *Emulsions stabilised solely by colloidal particles.* Advances in Colloid and Interface Science, 2003. **100-102**: p. 503-546.
3. Ford, R.E. and C.G. Furmidge, *Studies at Phase Interfaces .2. Stabilization of Water-in-Oil Emulsions Using Oil-Soluble Emulsifiers.* J. Colloid Interface Sci., 1966. **22**(4): p. 331-341.
4. Silverstein, M.S., *PolyHIPEs: Recent advances in emulsion-templated porous polymers.* Prog. Polym. Sci., 2014. **39**(1): p. 199-234.
5. Krajnc, P., D. Štefanec, and I. Pulko, *Acrylic Acid "Reversed" PolyHIPEs.* Macromol Rapid Commun, 2005. **26**(16): p. 1289-1293.

6. Williams, J.M., *High internal phase water-in-oil emulsions: influence of surfactants and cosurfactants on emulsion stability and foam quality.* Langmuir., 1991. **7**(7): p. 1370-1377.
7. Barbetta, A. and N.R. Cameron, *Morphology and surface area of emulsion-derived (PolyHIPE) solid foams prepared with oil-phase soluble porogenic solvents: Span 80 as surfactant.* Macromolecules, 2004. **37**(9): p. 3188-3201.
8. Zhang, S., J. Chen, and V.T. Perchyonok, *Stability of high internal phase emulsions with sole cationic surfactant and its tailoring morphology of porous polymers based on the emulsions.* Polymer, 2009. **50**(7): p. 1723-1731.
9. Pons, R., *Polymeric Surfactants as Emulsion Stabilizers*, in *Amphiphilic Block Copolymers*, P.A. Lindman, Editor. 2000, Elsevier Science B.V.: Amsterdam. p. 409-422.
10. Pickering, S.U., *CXCVI.-Emulsions.* Journal of the Chemical Society, Transactions, 1907. **91**: p. 2001-2021.
11. Colver, P.J. and S.A.F. Bon, *Cellular Polymer Monoliths Made via Pickering High Internal Phase Emulsions.* Chemistry of Materials, 2007. **19**(7): p. 1537-1539.
12. Haibach, K., et al., *Tailoring mechanical properties of highly porous polymer foams: Silica particle reinforced polymer foams via emulsion templating.* Polymer, 2006. **47**(13): p. 4513-4519.
13. Amalvy, J.I., et al., *Use of sterically-stabilised polystyrene latex particles as a pH-responsive particulate emulsifier to prepare surfactant-free oil-in-water emulsions.* Chemical Communications, 2003(15): p. 1826-1827.
14. Heinen, J.M., et al., *Phase behavior of amphiphilic diblock co-oligomers with nonionic and ionic hydrophilic groups.* J Phys Chem B, 2013. **117**(10): p. 3005-18.

15. Tadros, T., *Polymeric surfactants in disperse systems.* Adv Colloid Interface Sci, 2009. **147-148**: p. 281-299.
16. Tadros, T.F., *Surfactants in Foams*, in *Applied Surfactants*. 2005, Wiley-VCH Verlag GmbH & Co. KGaA. p. 259-284.
17. Bartle, H. and W. v. Bonin, *Über die Polymerisation in umgekehrter Emulsion [On the polymerisation in reversed emulsions].* Makromol. Chem., 1962. **57**: p. 74-95.
18. Bartle, H. and W. v. Bonin, *Über die polymerisation in umgekehrter emulsion: II [On the polymerisation in reversed emulsions].* Makromol. Chem., 1963. **66**: p. 151-156.
19. Lissant, K.J. and K.G. Mayhan, *A study of medium and high internal phase ratio water/polymer emulsions.* J. Colloid Interface Sci., 1973. **42**(1): p. 201-208.
20. Barby, D. and Z. Haq, *Low density porous cross-linked polymeric materials and their preparation.* EP0060138, 1982.
21. Barbetta, A. and N.R. Cameron, *Morphology and Surface Area of Emulsion-Derived (PolyHIPE) Solid Foams Prepared with Oil-Phase Soluble Porogenic Solvents: Three-Component Surfactant System.* Macromolecules, 2004. **37**(9): p. 3202-3213.
22. Keddie, D.J., *A guide to the synthesis of block copolymers using reversible-addition fragmentation chain transfer (RAFT) polymerization.* Chem. Soc. Rev., 2014. **43**(2): p. 496-505.
23. Zard, S.Z., *The Radical Chemistry of Thiocarbonylthio Compounds: An Overview*, in *Handbook of RAFT Polymerization*. 2008, Wiley-VCH Verlag GmbH & Co. KGaA. p. 151-187.
24. Gregory, A. and M.H. Stenzel, *Complex polymer architectures via RAFT polymerization: From fundamental process to extending the scope using click chemistry and nature's building blocks.* Progress in Polymer Science, 2012. **37**(1): p. 38-105.

25. Zhao, W., et al., *Optimization of the RAFT polymerization conditions for the in situ formation of nano-objects via dispersion polymerization in alcoholic medium.* Polymer Chemistry, 2014. **5**(24): p. 6990-7003.
26. Sun, J.-T., C.-Y. Hong, and C.-Y. Pan, *Recent advances in RAFT dispersion polymerization for preparation of block copolymer aggregates.* Poly. Chem., 2013. **4**(4): p. 873-881.
27. Moad, G., E. Rizzardo, and S.H. Thang, *Living Radical Polymerization by the RAFT Process - A Third Update.* Aust. J. Chem., 2012. **65**(8): p. 985-1076.
28. Kircher, L., P. Theato, and N.R. Cameron, *Functionalization of Porous Polymers from High-Internal-Phase Emulsions and Their Applications*, in *Functional Polymers by Post-Polymerization Modification*. 2012, Wiley-VCH Verlag GmbH & Co. KGaA. p. 333-352.
29. Viswanathan, P., et al., *3D Surface Functionalization of Emulsion-Templated Polymeric Foams.* Macromolecules, 2014. **47**(20): p. 7091-7098.
30. Luo, Y., A.-N. Wang, and X. Gao, *One-pot interfacial polymerization to prepare PolyHIPEs with functional surface.* Colloid and Polymer Science, 2015. **293**(6): p. 1767-1779.
31. Mathieu, K., C. Jerome, and A. Debuigne, *Influence of the Macromolecular Surfactant Features and Reactivity on Morphology and Surface Properties of Emulsion-Templated Porous Polymers.* Macromolecules, 2015. **48**(18): p. 6489-6498.
32. Ferguson, C.J., et al., *Ab Initio Emulsion Polymerization by RAFT-Controlled Self-Assembly.* Macromolecules, 2005. **38**(6): p. 2191-2204.

33. Siauw, M., B.S. Hawkett, and S. Perrier, *Short chain amphiphilic diblock co-oligomers via RAFT polymerization.* Journal of Polymer Science Part A: Polymer Chemistry, 2012. **50**(1): p. 187-198.
34. Carnachan, R.J., et al., *Tailoring the morphology of emulsion-templated porous polymers.* Soft Matter, 2006. **2**(7): p. 608-616.
35. Chiefari, J., et al., *Living free-radical polymerization by reversible addition-fragmentation chain transfer: The RAFT process.* Macromolecules, 1998. **31**(16): p. 5559-5562.
36. Moad, G., E. Rizzardo, and S.H. Thang, *Living Radical Polymerization by the RAFT Process - A Second Update.* Aust. J. Chem., 2009. **62**(11): p. 1402-1472.
37. Haven, J.J., et al., *Rapid and systematic access to quasi-diblock copolymer libraries covering a comprehensive composition range by sequential RAFT polymerization in an Automated synthesizer.* Macromol Rapid Commun, 2014. **35**(4): p. 492-497.
38. Guerrero-Sanchez, C., et al., *Quasi-block copolymer libraries on demand via sequential RAFT polymerization in an automated parallel synthesizer.* Poly. Chem., 2013. **4**(6): p. 1857-1862.
39. Haven, J.J., et al., *One pot synthesis of higher order quasi-block copolymer libraries via sequential RAFT polymerization in an automated synthesizer.* Poly. Chem., 2014. **5**(18): p. 5236-5246.
40. Binks, B.P. and S.O. Lumsdon, *Influence of particle wettability on the type and stability of surfactant-free emulsions.* Langmuir., 2000. **16**(23): p. 8622-8631.
41. Zhou, S., A. Bismarck, and J.H.G. Steinke, *Interconnected macroporous glycidyl methacrylate-grafted dextran hydrogels synthesised from hydroxyapatite nanoparticle stabilised high internal phase emulsion templates.* Journal of Materials Chemistry, 2012. **22**(36): p. 18824-18829.

42. Utama, R.H., M.H. Stenzel, and P.B. Zetterlund, *Inverse Miniemulsion Periphery RAFT Polymerization: A Convenient Route to Hollow Polymeric Nanoparticles with an Aqueous Core.* Macromolecules, 2013. **46**(6): p. 2118-2127.
43. Skrabania, K., et al., *Examining the UV-vis absorption of RAFT chain transfer agents and their use for polymer analysis.* Polymer Chemistry, 2011. **2**(9): p. 2074-2083.
44. Gurevitch, I. and M.S. Silverstein, *Polymerized pickering HIPEs: Effects of synthesis parameters on porous structure.* J. Polym. Sci., Part A: Polym. Chem., 2010. **48**(7): p. 1516-1525.
45. Wu, R., A. Menner, and A. Bismarck, *Macroporous polymers made from medium internal phase emulsion templates: Effect of emulsion formulation on the pore structure of polyMIPEs.* Polymer, 2013. **54**(21): p. 5511-5517.
46. Lovelady, E., et al., *Preparation of emulsion-templated porous polymers using thiol–ene and thiol–yne chemistry.* Polymer Chemistry, 2011. **2**(3): p. 559-562.
47. Kronberg, B., K. Holmberg, and B. Lindman, *Colloidal Stability*, in *Surface Chemistry of Surfactants and Polymers*. 2014, John Wiley & Sons, Ltd. p. 335-360.
48. Kovačič, S., D. Štefanec, and P. Krajnc, *Highly Porous Open-Cellular Monoliths from 2-Hydroxyethyl Methacrylate Based High Internal Phase Emulsions (HIPEs): Preparation and Void Size Tuning.* Macromolecules, 2007. **40**(22): p. 8056-8060.
49. Tadros, T.F., *Applications of Surfactants in Emulsion Formation and Stabilisation*, in *Applied Surfactants*. 2005, Wiley-VCH Verlag GmbH & Co. KGaA. p. 115-185.
50. Davis, S.S., H.P. Round, and T.S. Purewal, *Ostwald ripening and the stability of emulsion systems: an explanation for the effect of an*

added third component. Journal of Colloid and Interface Science, 1981. **80**(2): p. 508-511.

3. PEO-based brush-type amphiphilic macro-RAFT agents and their assembled polyHIPE monolithic structures for applications in separation science

3.1 Introduction

Macroporous polymer materials with interconnected structures represent a useful class of polymers used in different fields including separation science in the last decades [1]. An increasingly exploited method for the preparation of highly porous scaffolds is based on the solidification of the continuous phase of a high internal phase emulsion (HIPE) through polymerization. A cellular monolithic structure, commonly with interconnected voids and hence an open cellular network is produced, referred to as a poly(HIPE) [2-7]. These materials have been applied extensively to different applications [8], including membrane separator for batteries [9-12], electro-chemical sensors [13], tissue engineering [14-17], supported catalysis [18], water purification [19, 20], and separation science [21-24].

All the demonstrated examples in separation science consist of polymers that are hydrophobic in nature, which limits their applications to separation of non-polar analytes in reversed phase mode [25]. Introducing polar functional groups in the developed poly(HIPE) makes possible the separation of such analytes of different polarities.

In chapter two, an amphiphilic copolymer (a "macro-RAFT agent") was used as an anionic emulsifier in an inverse HIPE approach. This method offers attractive possibilities for the development of special coatings of the

resultant hydrophilic polyHIPE after the curing step while the RAFT-end group remained at the surface [26]. The aim in this chapter is to develop a surfactant-assisted functionalization strategy for preparation of porous polymers by HIPE polymerization, whereby the obtained porous polymers have a specific application [27].

PolyHIPEs with a hydrophilic surface are able to be produced through several different methods: post-synthesis modification of hydrophobic polyHIPEs from water-in-oil (w/o) HIPEs [28-30], the synthesis of inverse HIPEs (using an oil-in-water (o/w) template) in which the monomer is placed in aqueous phase [31-34], or the synthesis of bi-continuous hydrophobic polyHIPEs wherein a hydrophilic co-monomer is placed in the aqueous phase of an internal phase in w/o HIPEs [35-38]. Viswanathan *et al.* developed a new method for direct hydrophilic functionalization of a hydrophobic polyHIPE by introducing commercially available polymeric surfactants into a w/o HIPE through physical or chemical entanglement [39]. 3D surface functionalization was obtained in which the hydrophilic part of the polymeric surfactant (such as acrylic acid groups) decorated the surface of the voids of the obtained polyHIPE. Debuigne *et al.* reported the synthesis of a hydrophilic surface modified polyHIPE using an amphiphilic macro-RAFT agent for stabilization of the HIPE template [27]. The presence of RAFT functionality at the chain end of the polymer in the oil phase (styrene and divinylbenzene) provides a possibility for preparation of the porous polymer under RAFT control.

The preparation of a hydrophilic polyHIPE from an o/w HIPE usually requires more careful emulsion stabilization than normal HIPE (w/o HIPE) [40]. The use of PEO-based “brush-like” monomers is anticipated to increase stabilization due to a larger surface area occupied per chain and the higher surface mobility of PEO chains [41, 42]. PEO has been found to

provide surfaces with anti-fouling properties as a result of its hydrophilicity, high surface water mobility and low interfacial free energy with water [43]. PEO-based macromolecules have demonstrated their unique potential as steric stabilizers for emulsion polymerization and may enhance their stability against freeze-thaw or shear force [44]. We hypothesize that the PEO-based brush-type amphiphilic macro-RAFT agents with appropriate wettability will be adsorbed at the oil–water interface, in a similar fashion as polymeric surfactant, and will provide stability against coalescence of the oil droplets, while the PEO block anchoring assists the attachment of these polymeric surfactants to the surface of the obtained polyHIPE upon polymerization (**Figure 3.1**).

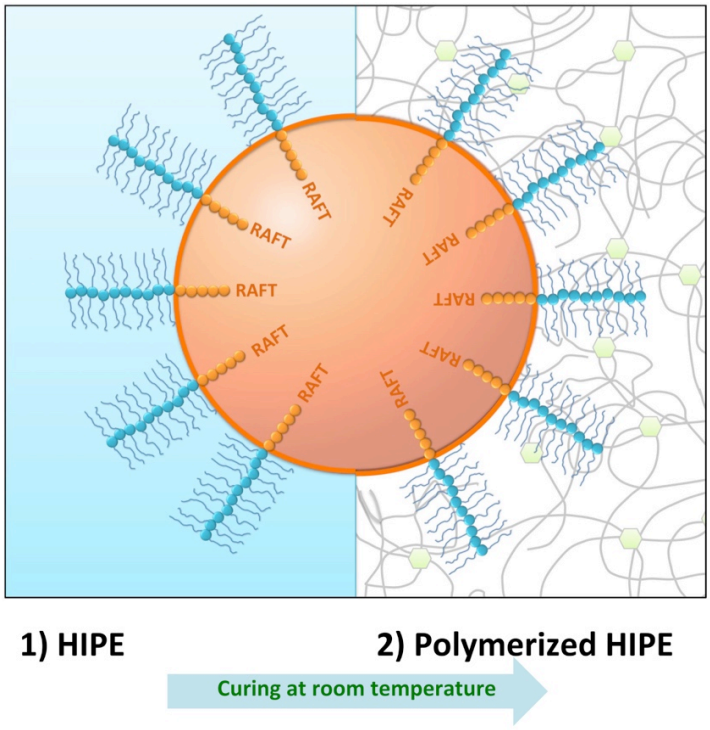

Figure 3.1. Mechanism of polyHIPE surface functionalization. 1) HIPEs stabilized by PEO-based brush-type amphiphilic macro-RAFT agents as surfactants 2) These amphiphilic species can be surface functionalized through PEO brush-type block (physical or chemical) entanglement.

As these polymers adopt the format of the mold used as the reactor, an inverse high internal phase emulsion can be introduced into capillary tubing and by *in situ* polymerization of the continuous phase, it can be covalently attached to a surface modified silica capillary. Due to the aspect ratio of the capillary, the morphology of the hydrophilic polyHIPE is likely to differ to that of the bulk material, representing a synthetic challenge to replicate ideal conditions to prepare a porous monolithic structure. These monolithic columns can potentially offer several advantages in the design of high performance columns to be used in liquid chromatography including the high porosity and consequently a low resistance to the mass transfer (low C-term in the van Deemter equation) [45]. In addition, the active chain end (the RAFT-end group) sits at the surface of the material, and its role can be readily studied with respect to potential further surface functionalization.

In this chapter, the surface chemistry of a hydrophilic polyHIPE inside a capillary format was studied by liquid chromatography. This technique was particularly informative, revealing the role and relevance of the surface chemistry of the polyHIPE with respect to the retention time of different compounds in different modes of chromatography.

3.2 Experimental Section

3.2.1 Materials

Poly (ethylene glycol) methyl ether acrylate (PEO MA, average Mn ≈ 480) was purchased from Sigma-Aldrich and used as received. Styrene (Sty, Aldrich, 99%) was passed through a column of Al_2O_3 to remove the inhibitor. The RAFT agent, 2-[[(butylsulfanyl)-carbonothioyl]sulfanyl] propanoic acid (PABTC), was synthesized as described in Ref [46].

4,4′-azobis(4-cyanovaleric acid) (V501, >98%, Aldrich) was used as received. Acrylamide (AAM, Sigma-Aldrich, ≥98%), N,N'-methylenebisacrylamide (MBAM, Sigma-Aldrich, ≥99.5%)), methanol (Fluka), basic alumina (Al_2O_3, Brockman activity I, 60-325 mesh), N,N,N',N'- tetramethylethylendiamine (TEMED, Sigma-Aldrich, 99%), were all used as received. 3-(trimethoxysilyl)propyl methacrylate (γ - MAPS) was obtained from Sigma (St. Louis, MO, USA). Toluene was obtained from Chem-Supply (Gillman, SA, AUS). Potassium persulfate (KPS, M&B, 98%) was recrystallized from water.

3.2.2 Synthesis of PEO-based amphiphilic surfactant by RAFT polymerization

A series of amphiphilic quasi-block macro-RAFT agents (Qb) consisting of PEO MA and Sty were synthesized as reported in the literature.[47] The PEO-based (PEO MA, average $M_n \approx 480$) was selected as it provides a hydrophilic group to assist the solubility of the macro-RAFT agent in the aqueous continuous phase. A typical polymerization protocol that was adopted is summarized: In first step, 1 g (4.20×10^{-3} mol) of PABTC and 0.12 g (4.20×10^{-4} mol) of V501 were introduced to a round-bottom flask and which was then sealed with a rubber septum, and solids were purged with ultra pure argon for 10 min. In a second step, 10.08 g (2.10×10^{-2} mol) of PEO MA was then dissolved in 100 mL of dioxane before addition to the round-bottom flask to obtain a solution. This was purged with ultra pure argon for 10 min. The reaction was allowed to proceed at 70 °C for 6 h under constant stirring. After quenching the reaction in an ice bath, a small aliquot of the solution was removed for ^{1}H NMR analysis to determine the conversion of the PEO MA single block. Styrene and V501 were then added to the round bottom flask at a molar ratio (relative to the initial chain transfer agent concentration) equal to the desired number of monomer

repeat units per macro-RAFT agent. The mixture was purged with ultra pure Argon for 10 min and further polymerization for 12 h at 70°C was performed. After which a small aliquot of the solution was removed for SEC and ^{1}H NMR analysis. The degree of polymerization of the macro-RAFT agent was determined by ^{1}H NMR spectroscopy. **Figure 3.2** shows the NMR spectrum of RAFT- PEO MA-b-Sty.

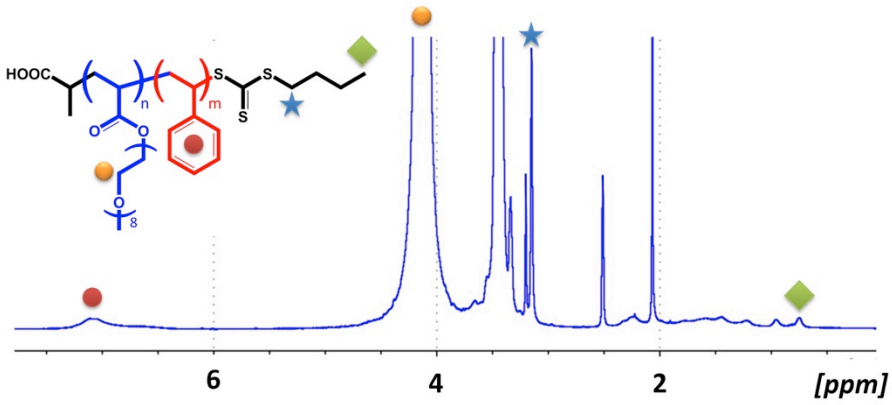

Figure 3.2. ^{1}HNMR spectrum of macro-RAFT agent Qb-2 (DMSO-d6).

Dioxane was then removed through rotary evaporation under reduced pressure and all polymers were purified by dialysis. Dialysis was performed by placing the polymer into dialysis tubing (MWCO 2000) and then submerging the polymer and tubing in deionised water (DI) with agitation (see **Figure 3.3**). Water was removed via freeze-drying of the macro-RAFT agents at -30 °C under reduced pressure for at least 100 hours. The polymer was then stored at 4 °C until use. **Table 3.1** shows the characteristic data for the PEO MA homopolymers and P(PEO MA)-qb-P(Sty) diblock copolymers synthesized in this study.

Table 3.1. Macro-RAFT agents synthesized in this study

$(PEOMA)_X$-qb-$(Sty)_Y$	X (feed) (PEOMA)[a]	Y (feed) (Sty)[a]	Sty/RAFT (NMR)[b]	Conversion		$M_{n\ th}$ (g mol^{-1})[c]	Mn, SEC (g mol^{-1})[d]	Đ
				First Step	Second Step			
Qb-1	5	5	2.1	98.2	54.6	2879.5	2600	1.18
Qb-2	10	10	3.4	98.1	49.4	5461.6	3600	1.18
Qb-3	20	20	4.6	88.9	28.6	9368.5	5000	1.20
Qb-4	50	50	8.4	37.2	24.0	10416.1	7800	1.46

[a]The feed units obtained a theoretical hydrophilic-lipophilic balance (HLB) value for all macro-RAFT agent around 16, determined by the Griffin's rule: HLB = 20×M_h hydrophilic part/M_w (hydrophilic part + hydrophobic part), where M_h is the molecular weight of the hydrophilic block and M_w is the molecular weight of the surfactant. [b]Determined by ^{1}HNMR in DMSO-d6. [c] $Mn,th=\frac{[monomer]0\times M\ monomer}{[RAFT]0}\times conversion + Mn, macro\_RAFT$. [d]Determined by SEC in THF (calibration Sty).

Figure 3.3. Typical procedure for purification of macro-RAFT agent by using dialysis tubing (MWCO 2000).

The SEC analyses of four different macro-RAFT agents are illustrated in **Figure 3.4**.

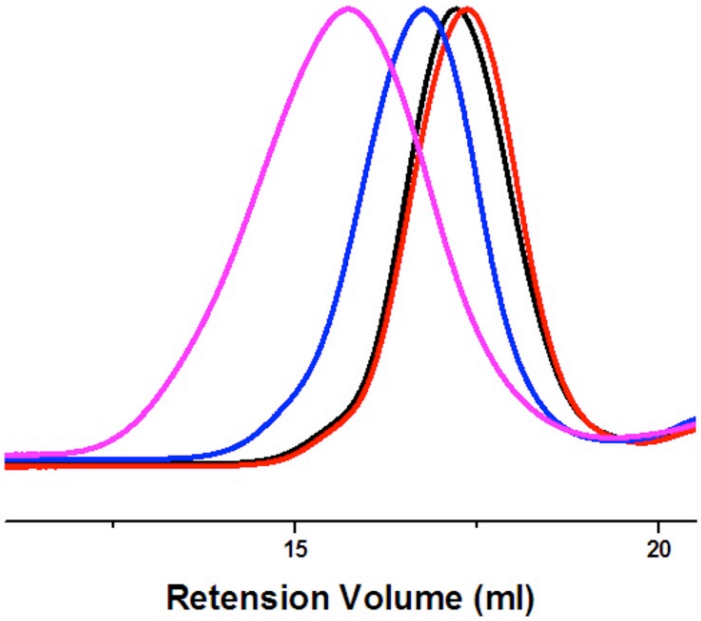

Figure 3.4. A) SEC chromatograms of macro-RAFT agents, from right to left: Qb-1 (red), Qb-2 (black), Qb-3 (blue) and Qb-4 (pink).

3.2.3 Synthesis of hydrophilic 'inverse' polyHIPEs

The macro-RAFT agent was dissolved in 4 ml water without any adjustment of pH. Toluene (16 ml) was added drop-wise to an aqueous solution of macro-RAFT agent with a desired concentration; at a rate of 0.8 mL min^{-1} with constant stirring (magnetic stirrer) at 1000 rpm. The emulsion was stirred for an additional 20 min after complete addition of the internal toluene phase. The drop test method was used to determine the type emulsion prepared and optical microscopy was used to examine emulsion stability.

The macro RAFT agents prepared were used as stabilizers of o/w emulsions. A range of different monomers and crosslinkers were tested attempting to obtain macroporous polyHIPEs. The successful combination of the monomer-crosslinker was selected based on the solubility in water and possibility for polymerization at room temperature (**Figures 3.5 and 3.6**).

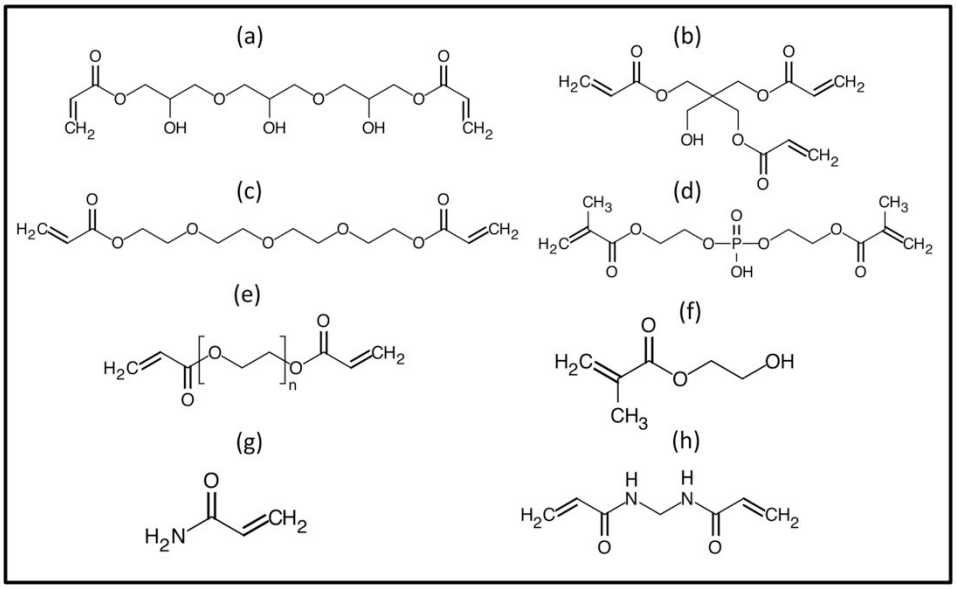

Figure 3.5. Monomers and cross-linkers used in aqueous phase

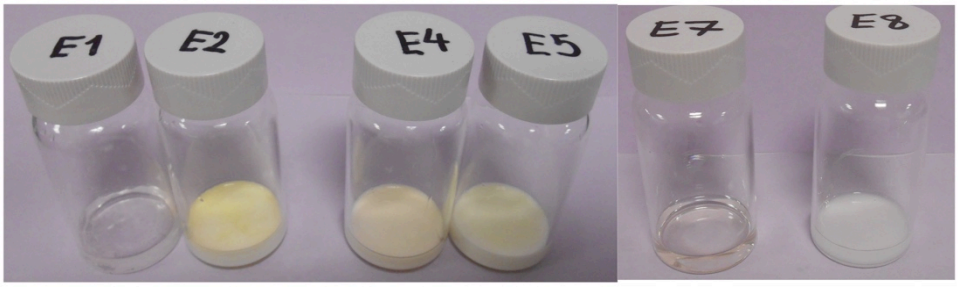

Figure 3.6. Typical polymerization of monomers in water in presence of redox initiation system (TEMED/ KPS). From the left to right: Glycerol 1,3-diglycerolate diacrylate, Pentaerythritol triacrylate, Tetra(ethylene glycol)

diacrylate, Bis[2-(methacryloyloxy)ethyl] phosphate, Poly (ethylene glycol) diacrylate, 2-Hydroxyethyl methacrylate and acrylamide.

A successful monomer and crosslinker couple; acrylamide (AM, 1.420 g, 1.99×10^{-2} mol) and the crosslinker N,N'-Methylenebisacrylamide (MBAM, 0.309g, 2.00×10^{-3} mol) were dissolved in 4 ml of water containing macro-RAFT agents. The initiator KPS (0.04 g, 1.47×10^{-4}) was also dissolved in the above aqueous solution. The continuous phase toluene (16 mL) was then added drop-wise at a rate of 0.8 ml per min with constant stirring at 1000 rpm. The emulsion was stirred for an additional 20 min after complete addition of the internal toluene phase. The emulsion was transferred to a mold (a glass container) and appropriate amounts of TEMED were added to emulsion after formation, which already contained KPS and cured at room temperature. The resulting polyHIPE was purified via Soxhlet extraction with methanol for 48 h as well as 48 h with water. The purified monolith was dried under vacuum oven for at least 72 h to constant weight under vacuum at 30 °C. The experimental conditions used for the preparation of the different polyHIPEs can be found in **Table 3.2.**

Table 3.2. Conditions used for the preparation of hydrophilic polyHIPE

Sample code	macro-RAFT agent	%wt [1]	Monomers in aqueous phase	HIPE Stability	Attachment to the capillary format column [3]	<D> (µm) Optical microscopy[4]		(SEM) (µm)	
						Fresh	After 12h	<D> [5]	<d> [5]
A1	Qb-1	10	-	>12	-	65.6	57.9	-	-
A2	Qb-2	10	-	>15 days [2]	-	41.2	40.6	-	-
A3	Qb-3	10	-	>12	-	17.2	92.8	-	-
A4	Qb-4	10	-	>1	-	-	-	-	-
A5	Qb-2	10	**AAM-MBAM**	>72	Yes	41.5	39.9	8.0	1.3
A6	Qb-2	20	**AAM-MBAM**	>72	No	38.5	33.1	9.5	2.0
A7	Qb-2	50	**AAM-MBAM**	>72	No	-	-	-	2.9
A8	Qb-2	10	**AAM-MBAM- 20% wt more monomers** [6]	>24	Yes	39.5	35.3	9.4	1.6
B1	End group removed Qb-2	10	**AAM-MBAM- 20% wt more monomers** [6]	>24	No	51.8	47.3	9.4	1.0

[1] All amounts are based on the weight percentage (w.r.t. the continuous phase). [2] The HIPE was stable for more than 15 days after preparation. [3] The surface of capillary was modified with 3-(trimethoxysilyl)propyl methacrylate (γ -MAPS). [4] A void describes the pores of the PolyHIPE and <D> is average size of voids. Window refers to the interconnecting pores between two adjacent droplets and <d> is average size of windows. [5] Sample stability test was performed before adding TEMED. [6] The amount of the monomers is increased by 20 %wt respect to HIPE A5.

3.2.4 In situ preparation of hydrophilic polyHIPE columns

A capillary format was chosen as a 'column housing' for poly(AM-MBAM) based hydrophilic polyHIPE to be evaluated as stationary phases for nano-LC. Prior to the polymerization, fused silica capillaries with different internal diameters were modified with 3-(trimethoxysilyl)propyl methacrylate using a procedure previously described [48] (**Figure 3.7**).

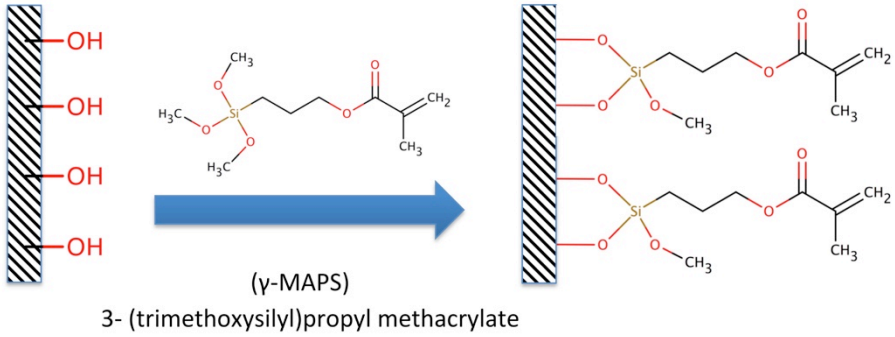

Figure 3.7. Surface modification of a fused-silica capillary surface using 3-(trimethoxysilyl)propyl methacrylate (γ -MAPS).

Using an ice bath to retard the polymerization reaction, an inverse HIPE was introduced to the capillary column using pressure of nitrogen (**Figure 3.8**). *In situ* polymerization of an inverse HIPE in a capillary was conducted using a KPS/TEMED redox couple as initiator.

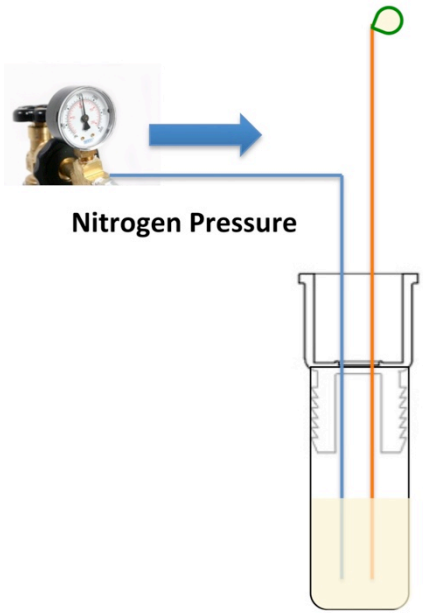

Figure 3.8. Using nitrogen pressure to fill a capillary format column with an inverse HIPE.

3.2.5 Chemical stability and swelling behavior of monolithic columns

The chemical stability of polyHIPEs in capillary formats was described by pressure drop of monolithic columns at different flow rates using pure water and acetonitrile as mobile phase. For each flow rate, the pressure values of the HPLC system were measured without and with the column, and the pressure drop across the monolith was calculated as the difference between these two values.

3.2.6 Characterization

NMR analyses was performed using a Bruker Ultra Shield Avance Spectrometer (600 MHz). For all NMR analyses deuterated solvents were used as stated. Size exclusion chromatography (SEC) was performed with a Viscotek instrument using refractive index detector (RID) and two

chromatography columns (two PSS S linear 3μm, Polymer Standard Services GmbH, PSS), THF (HPLC grade) was used as an eluent at a flow rate of 0.5 mL/min. The column oven was kept at 40 °C. The calculated molecular weights were based on a calibration curve for polystyrene (PS) standards of narrow polydispersity with a molecular weight range of 160–154000 g/mol (PSS-Polymer Laboratories). The standards were prepared (2 mg/ml) and injected, the column injection volume was 0.1 mL.

Emulsion droplets were observed by optical microscopy (Nikon, model Eclipse E200), equipped with a camera (Tucsen, model IS500). Images of the emulsions were analyzed by ImageJ (NIH image) [49]. From these, the mean droplet size and size distribution were evaluated. Three samples were analyzed for each experiment and the reported results are the average of these. More than 100 droplets were measured. PolyHIPEs were characterized by field emission gun scanning electron microscopy (FE-SEM) studies using a Hitachi SU-70 FESEM in the Central Science Laboratory, University of Tasmania. All samples were platinum coated for 15 s in an argon atmosphere (Emitech 550, Emitech Ltd., UK). The composition of the material was examined by EDX experiments where the materials were sputter-coated with carbon (Ladd 40000 carbon evaporator) before analysis. The calculation of the average voids and windows diameter (in the case of any) was performed on sets of at least 100 voids and 100 windows, respectively, using the image analysis software ImageJ (NIH image). A statistical correction was employed to obtain more accurate value, as each value was multiplied by $2/(3^{1/2})$ as described by Carnachan *et al.* [50].

The sulfur content of the polyHIPEs was determined with a Thermo Finnigan EA 1112 Series Flash Elemental Analyser. Thermogravimetric analyses were carried out using Setaram LABSYS Evo TG-DSC

Thermogravimeter in the temperature range from 30 to 600 °C at the heating rate of 5 °C min^{-1} under nitrogen atmosphere. The sample mass was about 15 mg. FTIR spectra were recorded by a Bruker Vertex 70 infrared spectrometer equipped with an ATR probe. Solid samples were pressed using a spatula before being placed on the sample holder. A CCD line detector in the exit focal plane of the monochromator was used for recording the spectra. The laser source was a Nd:YAG laser. The Brunauer–Emmett–Teller (BET) surface area and microporosity were assessed using a Tristar II analyzer for the nitrogen adsorption/desorption at 77 K (Particle and Surface Science, Gosford, AUS). The capillary liquid chromatography studies were performed using an Ultimate 3000 RS system (Dionex, Sunnyvale, CA). A 1μL sample loop was used and the system was operated with Chromeleon software. UV absorbance was monitored at 214 nm.

3.3 Results and discussion

3.3.1 Typical synthesis of the amphiphilic quasiblock macro-RAFT agent

The increasing importance and interest in macro-RAFT quasiblock copolymers arise mainly from their unique amphiphilic properties in solution, which are a direct consequence of their molecular structure and presence of the RAFT-end group [26, 27, 51].

While surfactants are selected mostly on trial and error basis for preparation of HIPEs, the hydrophilic-lipophilic balance (HLB) can indicate the capability of forming a certain preferred type of an emulsion. In case of HIPEs, surfactants with the HLB values 2-6 are used for water-in-oil and 12-16 for oil-in-water HIPEs. Specifically targeting a high HLB number (HLB ~16), amphiphilic macro-RAFT agents were synthesized to

investigate the effect of the length of the P(PEO MA) and P(Sty) of the macro-RAFT agent with regards to the stability of the inverse HIPE (See **Table 3.1**). The selection of this ratio was based on the theoretical hydrophilic-lipophilic balance (HLB) value of these macro-RAFT agents, which is suitable for the stabilization of inverse oil in water emulsions [52].

This one-pot polymerization technique has been utilized to achieve the synthesis of quasi (block-like) copolymers using sequential monomer addition [53, 54]. This approach yields quasiblock copolymers (Qb) when the conversion of monomer in the first step (e.g. PEO MA) is lower than 100% prior to a second monomer being incorporated. The low polydispersity (Đ) of macro-RAFT agent Qb-1 to Qb-3 highlights the RAFT control over the polymerization. These results confirmed that shorter chain length of PEO MA macro-RAFT agents provide high re-initiation efficiency for the polymerization of Sty, as expected based on a previous report [47].

3.3.2 Stability of oil-in-water HIPEs using PEO-based macro-RAFT agent

The preparation of a hydrophilic polyHIPE from an o/w HIPE usually requires more careful emulsion stabilization and polymerization [40]. The poly(PEO MA-qb-Sty) quasi-block copolymers prepared here are amphiphilic and can exhibit properties similar to a polymeric surfactant [55]. The use of 10 wt% of macro-RAFT agent Qb-2 resulted in the successful stabilization of HIPEs with aqueous volume fractions between 60 and 90%. The emulsion droplets were spherical but polydisperse (See **Figure 3.9** and **Figure 3.10**).

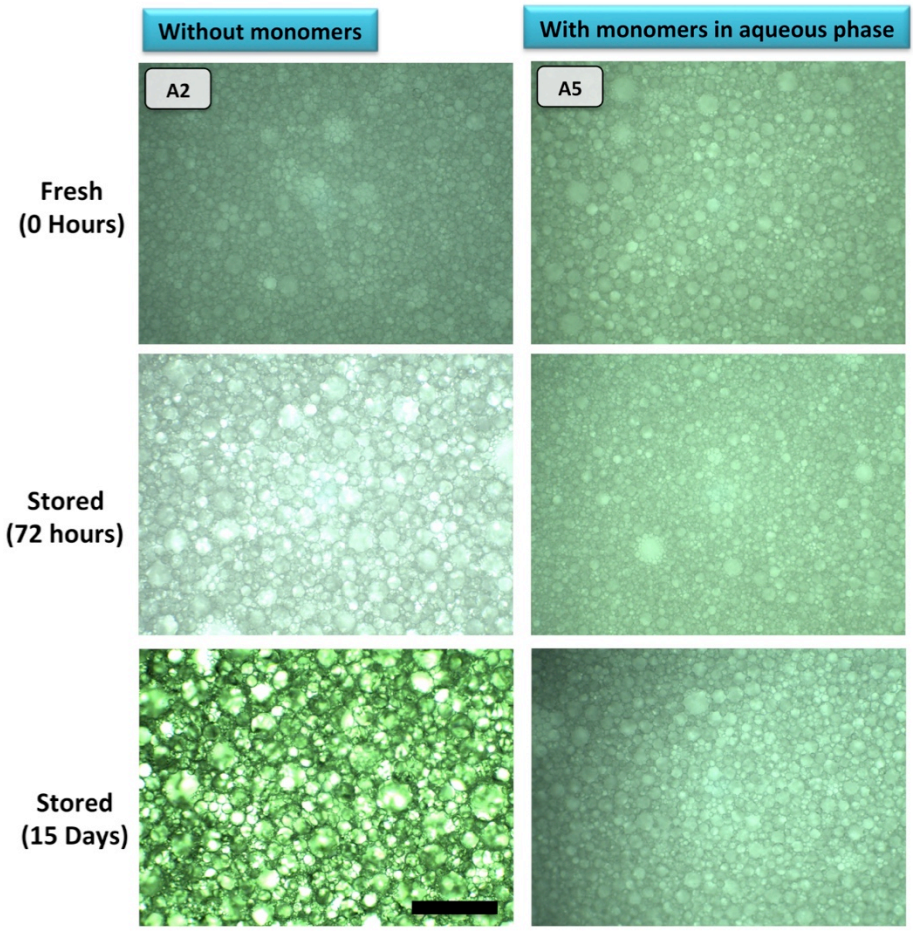

Figure 3.9. Optical microscopy of HIPEs stabilized by 10 wt% of macro-RAFT agent-Qb2 (w.r.t. the continuous phase); after preparation (0 hours), after 72 hours and after 15 days (right column (HIPE A5) has AAM and MBAM monomers in the aqueous phase). The scale bar in all cases is 600 μm.

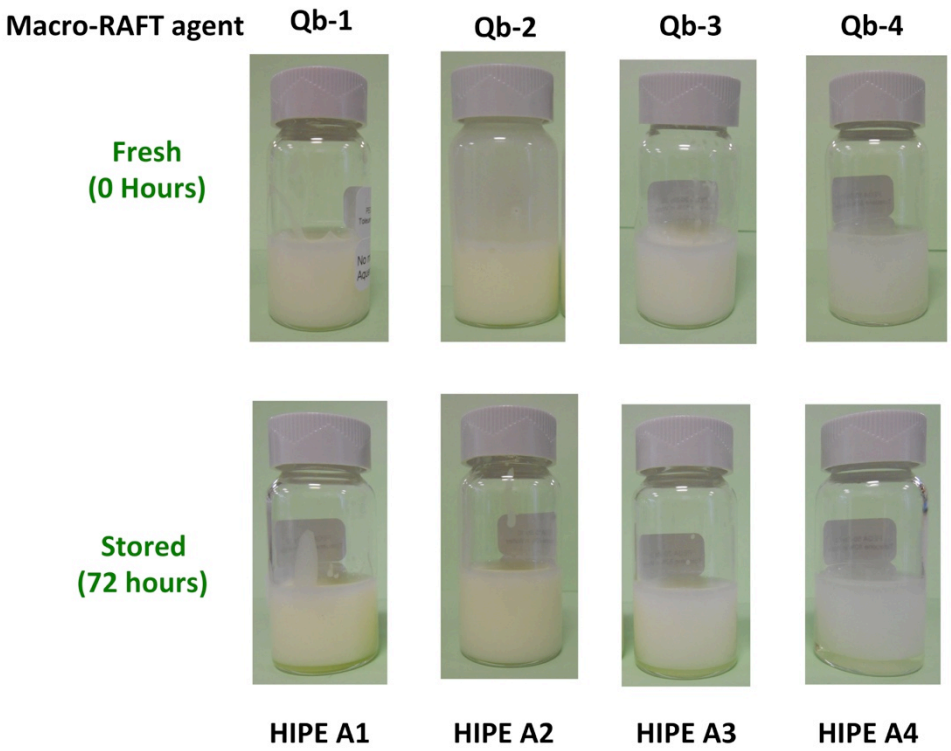

Figure 3.10. Stability of toluene in water HIPE stabilized by macro-RAFT agent. All HIPEs with 80% toluene in water solely stabilized with 10 wt % of (from the left to right): macro-RAFT agent Qb1, macro-RAFT agent Qb2, macro-RAFT agent Qb3 and macro-RAFT agent Qb4. No monomers were introduced in the HIPEs.

The drop test method indicated that the HIPE is the inverse system (o/w type) [56, 57] (**see Figure 3.11**).

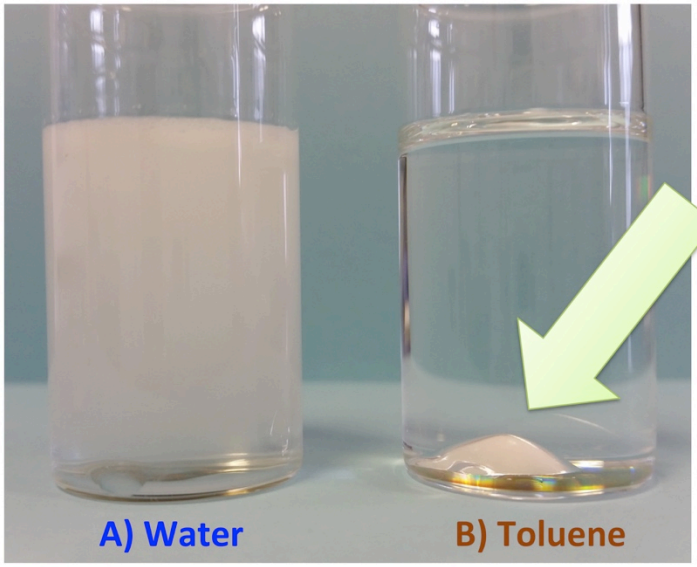

Figure 3.11. The emulsion type was determined by the drop test method. One drop of the formed HIPE with macro-RAFT agent-Qb1 was placed into (A) water and (B) toluene. The emulsion droplet was seen to disperse in the water but remained as a droplet in toluene.

Preparation of a stable HIPE requires rapid adsorption of the stabilizer at the oil-water interface to lower the interfacial tension between the phases and form a rigid interfacial film [58]. To study emulsion stability, the effect of the number of hydrophilic and hydrophobic units of the polymeric surfactant was investigated using macro-RAFT agents Qb-2 to Qb-4 (see **Figure 3.10**. The macro-RAFT agent Qb-2 proved to be sufficiently hydrophilic to stabilize o/w HIPE at least for two weeks (see **Figure 3.12**).

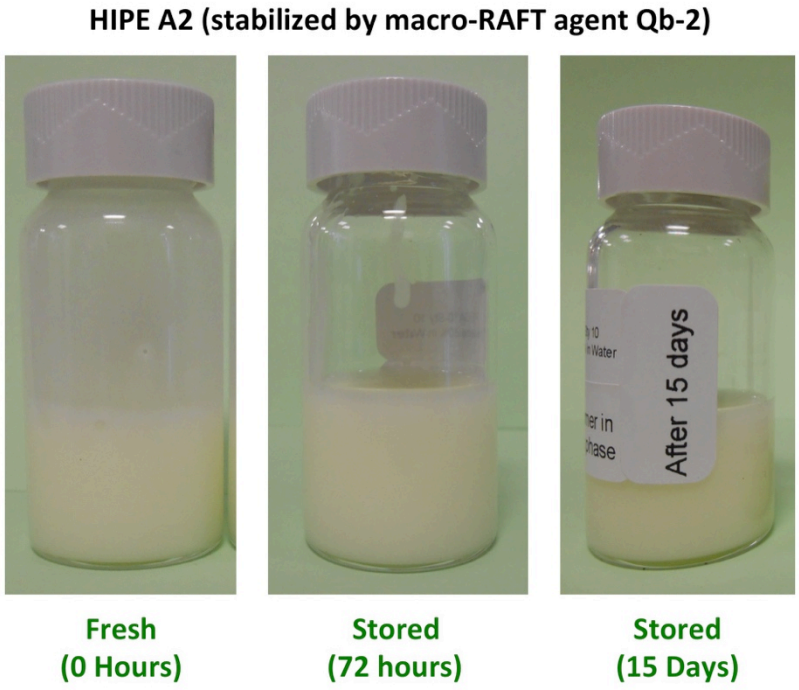

Figure 3.12. Stability of toluene in water HIPE stabilized by macro-RAFT agent-Qb-2

This long-term stability implied that this surfactant was able to suppress the coalescence and Ostwald ripening of emulsion droplets and thus, Qb-2 was selected for further studies. It is also important to mention that the absence of the PSty block (i.e. using a single block RAFT- $(PEO\ MA)_{10}$ homopolymer as sole emulsifier) resulted in rapidly unstable emulsions, demonstrating the importance of the amphiphilic nature of the stabilizer.

3.3.3 Synthesis of hydrophilic polyHIPEs

A rapid curing of a HIPE system typically locks the emulsion against Ostwald ripening and coalescence, resulting in a homogeneous polyHIPE structure. Inverse HIPEs discussed in the previous section were polymerized using a redox initiation system (TEMED/ KPS) to obtain porous polyHIPEs.

PolyHIPE A5 was obtained by using 10 wt% of macro-RAFT agent Qb-2, which retained the shape and volume of the mold. Increasing the macro-RAFT agent-Qb2 concentration from 10% wt to 50% wt had a significant effect on the morphology of the resulting polyHIPEs (e.g. on the void size [59]) as can be seen from the SEM images (**Figure 3.13**). From the SEM images, the number of "windows" per void is increasing from polyHIPE A5 to A7. A higher degree of openness is an advantage for polyHIPEs used in flow-through applications, as it decreases the backpressure of the column once the polyHIPE is introduced into a column housing.

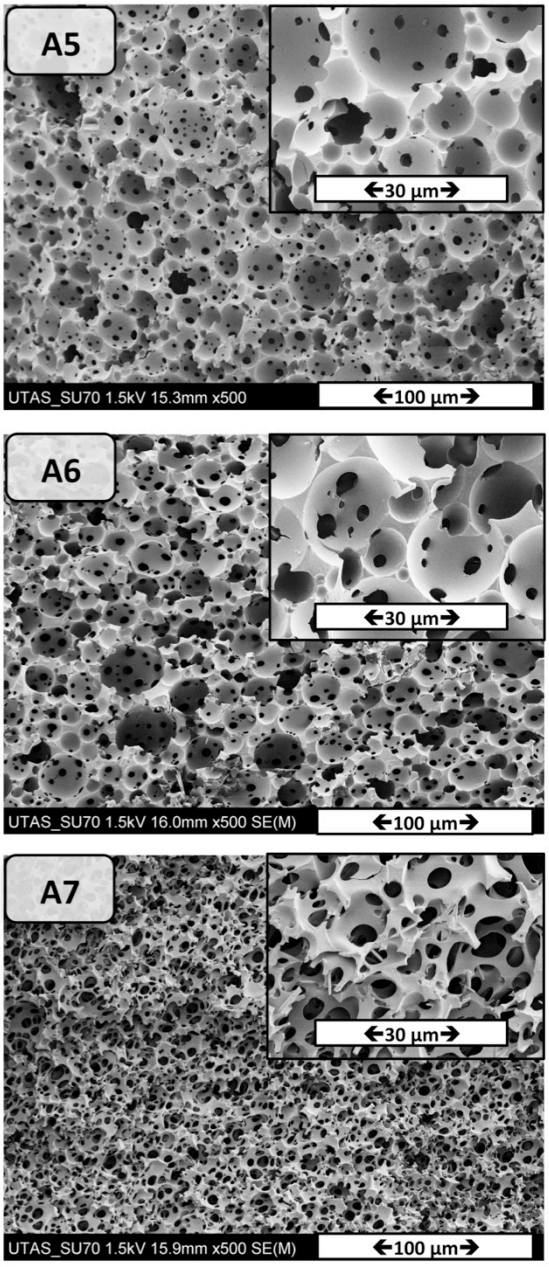

Figure 3.13. Scanning electron micrographs of emulsion templated macroporous polymer made by polymerization of HIPEs stabilized solely by different amount of macro-RAFT agent-Qb2 (10, 20 and 50 w.r.t. the continuous phase from top to bottom), polymerized at room temperature (TEMED/ KPS).

The prepared polyHIPEs retained their yellow color after washing process due to the trithiocarbonate group of the RAFT agent. Elemental analysis confirmed the amount of sulfur within the polyHIPEs (e.g. the sulfur content within polyHIPE A5 was 0.43%). Further evidence for the presence of the macro-RAFT agent on the surface of the polyHIPE was obtained from Energy Dispersive X-ray analysis (EDX), clearly indicating that sulfur was present at the surface of the polyHIPE A5 (**Figure 3.14**).

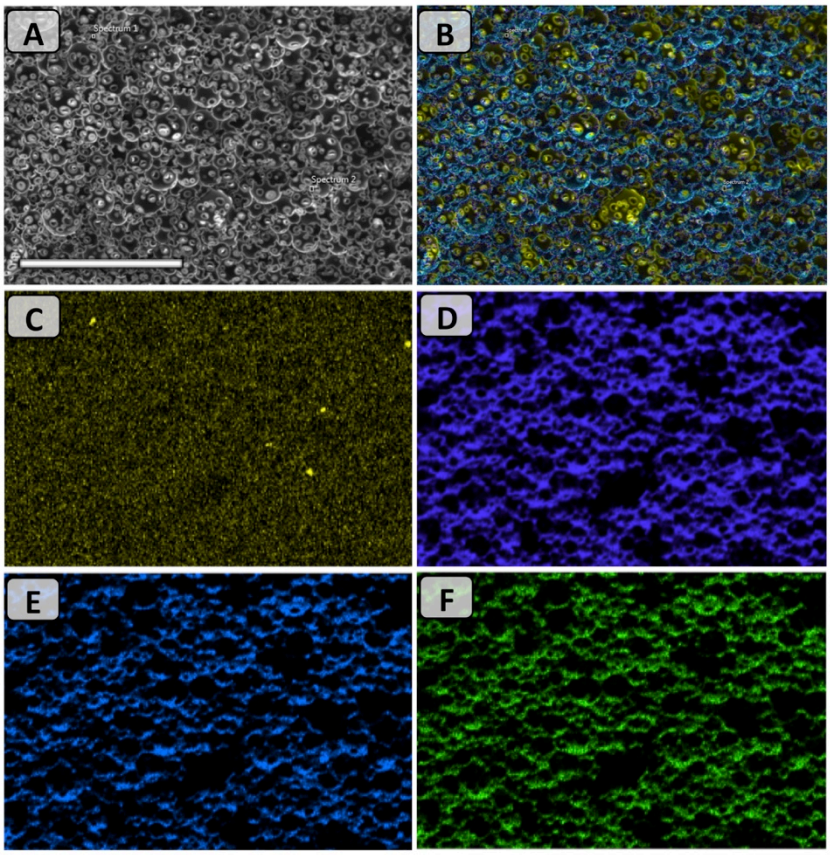

Figure 3.14. EDX mapping analysis on polyHIPE A5; (A) SEM image and (B) Overall mapping elements on the same spot: corresponding to sulfur (C), carbon (D), nitrogen (E), and oxygen (F) mapping. Scale bar is 100 μm.

To further investigate the inclusion of the macro-RAFT agent within the polyHIPE structure, FTIR analyses were performed on the resultant material, in comparison to a sample of AM-MBAM polymerized in bulk (KPS/TEMED as initiators) subjected to the same washing protocol. The FTIR spectrum of polyHIPE A5 shows the presence of an extra band at 1710 cm^{-1} with respect to bulk polymer, which is present in the FTIR spectrum of the macro-RAFT agent (**Figure 3.15**). This signal corresponds to the C=O stretching of the ester group of the PEO MA block, indicating incorporation of the macro-RAFT agent in to the polymer structure.

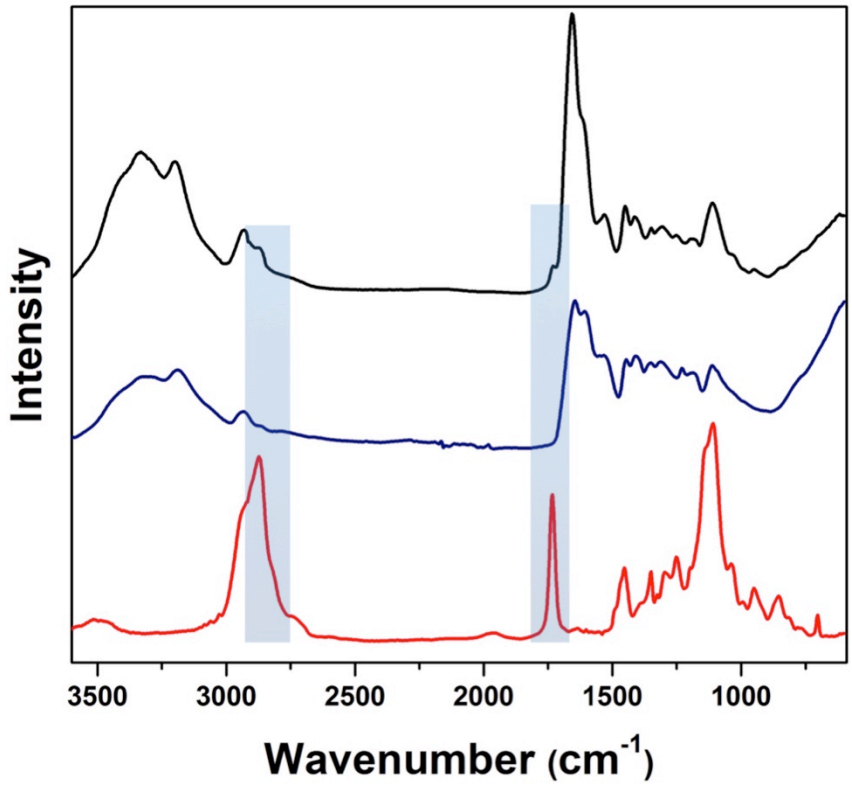

Figure 3.15. ATR-IR of macro-RAFT agent-Qb2 (red), bulk polymer (blue) and polyHIPE A5 (black). The peaks around 1700-1750 cm^{-1} (related to the C=O stretching of the ester group of the poly (PEO MA) and 2700 - 2900 cm^{-1} (related to aromatic =C-H stretching of poly(styrene)) are highlighted.

Furthermore, TGA thermograms of the macro-RAFT agent-Qb2, polyHIPE A5 and bulk polymer (**Figure 3.16**) show similarities in the decomposition profile of polyHIPE A5 and Qb-2, again indicating macro-RAFT incorporation.

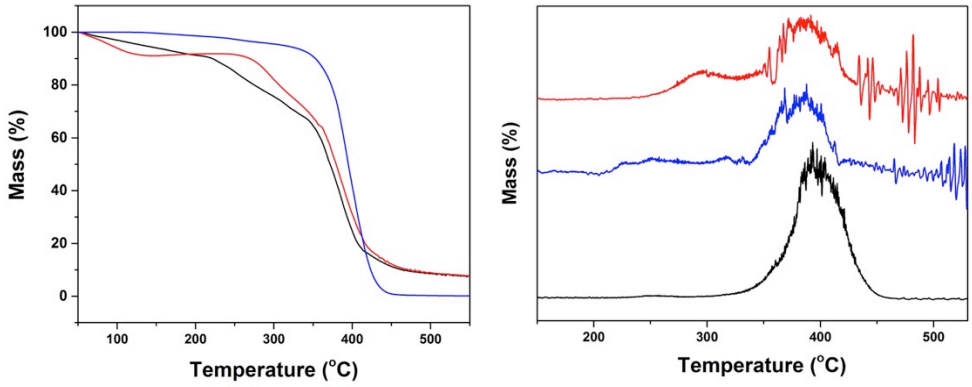

Figure 3.16. (A) TGA analysis of macro-RAFT agent-Qb2 (red), polyHIPE A5 (black) and bulk polymer (blue). B) T_{max} data.

Grafting experiments utilizing the RAFT-end groups at the polyHIPE surface were performed with an aim to demonstrate the presence of the reactive RAFT agent on the surface of voids. Adapting a procedure from Moad *et al.*[60], polyHIPE A5 was reacted at 60 °C overnight with (4-vinylphenyl) boronic acid (VPBA). Accordingly, a polyHIPE A5 was treated with a degassed solution of VPBA, RAFT agent and the initiator AIBN (molar ratios 100 : 5 : 1) in methanol–acetonitrile (volume ratio 50 : 50) at 60 °C for 22 hours. FTIR spectroscopy was used as a complementary technique to confirm the presence of poly(VPBA) on the surface, via the presence of B–O weak stretching peaks (**Figure 3.17**) [61, 62].

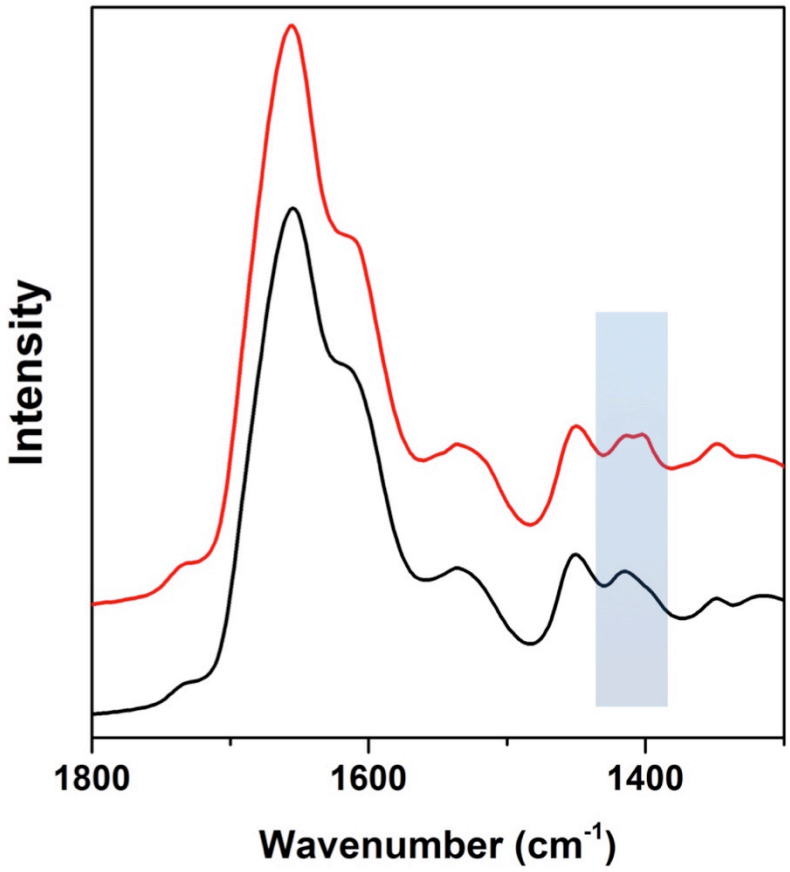

Figure 3.17. FTIR spectrum of poly(HIPE) A5 before (black) and after (red) "grafting from" polymerization of (4-vinylphenyl)boronic acid. The peak around 1375–1425 cm^{-1} is highlighted.

SEM analysis (**Figure 3.18**) demonstrated a change in surface morphology after surface grafting with VPBA where the size of the windows were decreased. These results clearly demonstrate the availability of the trithiocarbonate group (present on the surface of the functionalized polyHIPEs) for further surface modifications by grafting reactions.

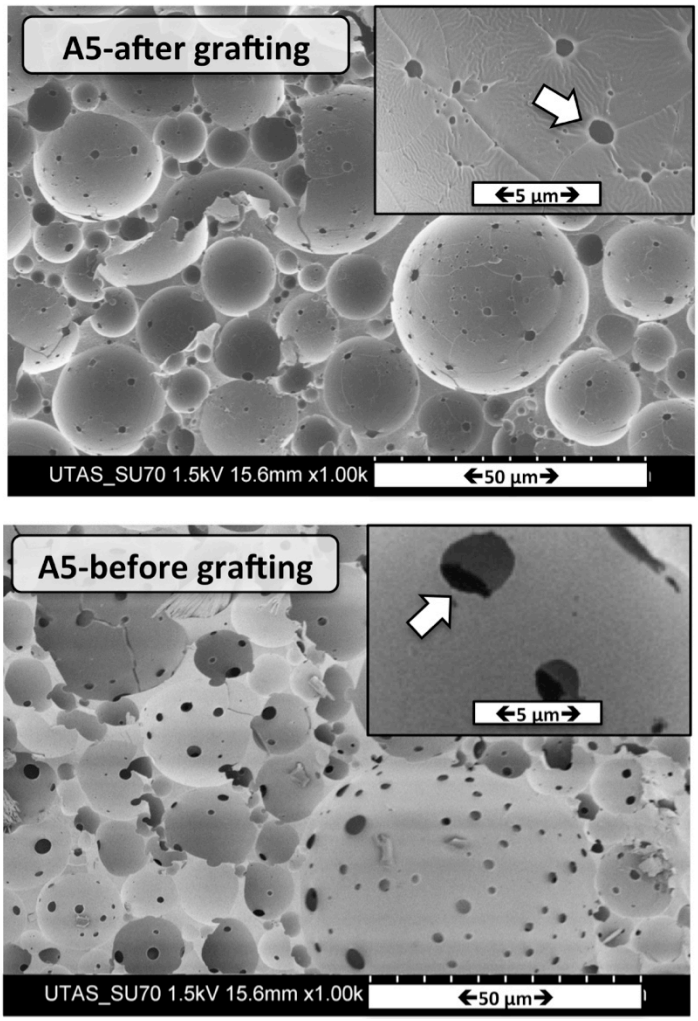

Figure 3.18. SEM images of poly(HIPE) A2 after "grafting from" polymerization of (4-vinylphenyl)boronic acid.

3.3.4. In situ synthesis of hydrophilic polyHIPEs inside a capillary format

A capillary column was chosen as the reactor for the design of hydrophilic polyHIPEs to be used as a stationary phase in chromatographic experiments. The surface of the column was chemically modified with γ-MAPS in order to ensure a covalent attachment between the polymer monolith and the walls

of the capillary, subsequently ensuring the mobile phase would flow solely through the voids of the monolith. HIPE A5 was introduced to three different ID capillaries (150, 250, and 500 μm). After preparation of the HIPE A5, the HIPE was placed in ice bath for approximately 5 minutes to lower the temperature of the emulsion. As polymerization commences upon addition of TEMED, this stage is critical with respect to retarding the polymerization of the HIPE, providing sufficient time to fill the capillary using nitrogen gas. After the pre-treated capillary was completely filled with the cold HIPE, the capillary was sealed at both ends with rubber stoppers. The sealed capillary was stored in a dark place at room temperature and allowed to react for 24 h.

As seen in **Figure 3.19**, the morphology of the resulting polyHIPE is strongly dependent on the diameter of the capillary. The morphology of the polyHIPE in the 500 μm ID capillary is most similar to the bulk structure (see **Figure 3.13**, polyHIPE A5), however there is no attachment to the capillary surface. By decreasing the size of the capillary to 150 μm ID, the polyHIPE structure is attached to the surface but the morphology of the polyHIPE changes significantly. This result may be attributed to the deformability of oil droplets when the column is filling under nitrogen pressure, by considering the increasing likelihood of deformation and or break-up of when the inner diameter is decreased.

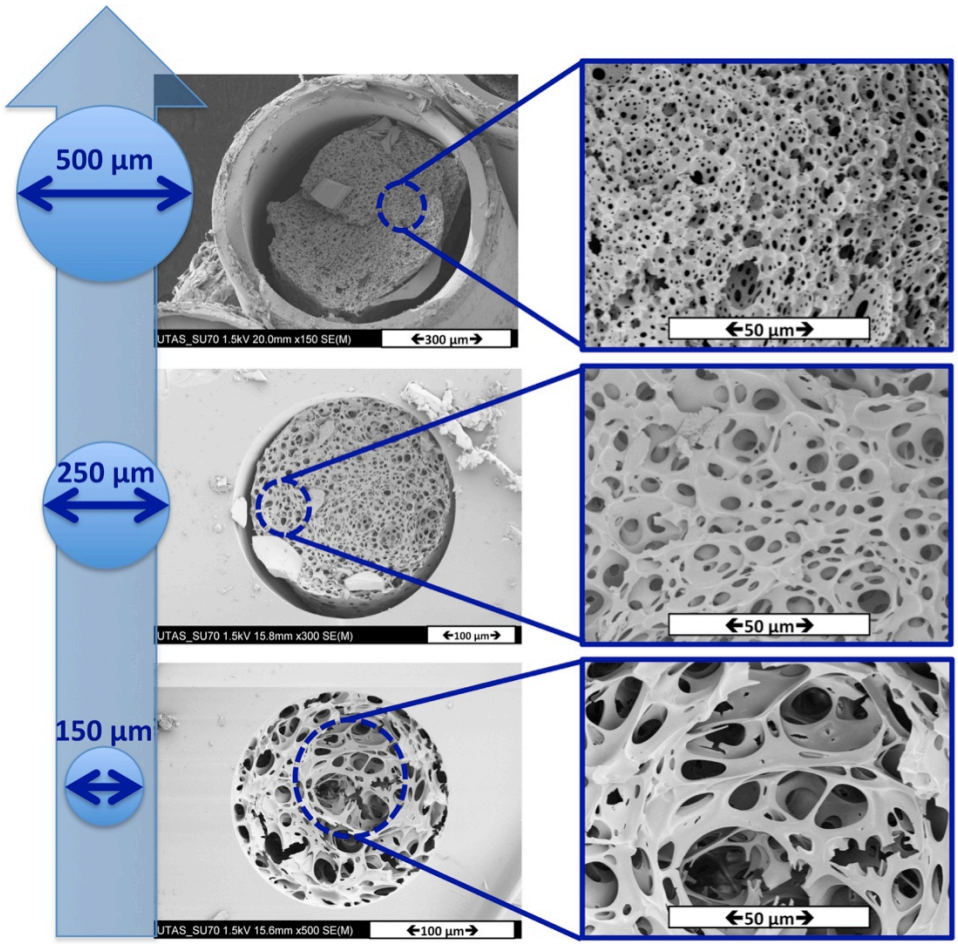

Figure 3.19. SEM images of poly(HIPE) A5: *In situ* polymerization in different ID capillaries, inner diameters from bottom to top: 150 µm, 250 µm and 500 µm.

Furthermore, the extent of polyHIPE shrinkage upon polymerization was studied (see **Figure 3.20**).

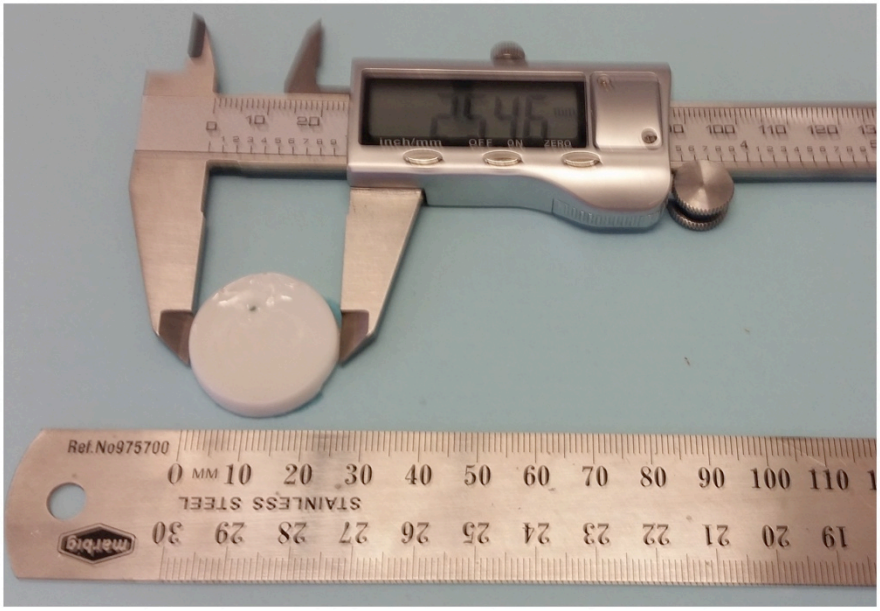

Figure 3.20. Shrinkage study on polyHIPE A5

The shrinkage of the polyHIPE structure is ~ 19% (18.95 ± 4.20%). This is an important factor respect to explaining the de-attachment of the polyHIPE to wall in a larger inner diameter capillary. When the amount of the monomer-crosslinker (AAM-MBAM) in the aqueous phase was increased by 20 % (sample A8, **Table 3.2**), SEM analysis of the resulting polymer (sample A8, **Figure 3.21**) showed a polyHIPE structure within a capillary housing similar to the bulk morphology.

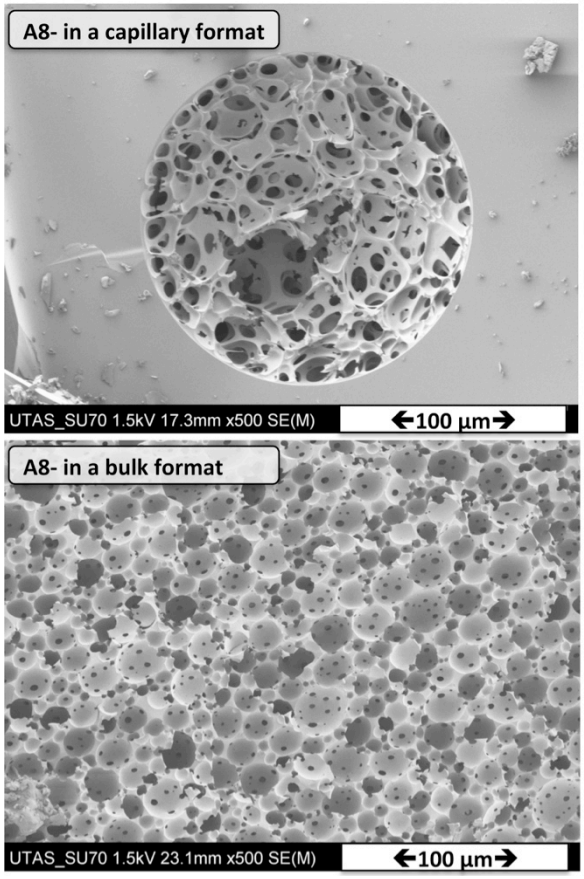

Figure 3.21. SEM images of poly(HIPE) A8: Polymerization in a bulk (bottom) and *in situ* polymerization in 150 µm ID capillary (top).

3.3.5 Evaluation of the effects of RAFT-end group of the macro-RAFT agent on polyHIPE morphology

We next turned our attention to the role of RAFT-end group of the macro-RAFT agent on polyHIPE morphology. It has been reported that the presence of the RAFT-end group in amphiphilic copolymers increases the hydrophobicity of the copolymer [51]. This influences the behavior of a diblock copolymer at an oil-water interface, as it more closely resembles and acts as triblock copolymer with hydrophobic termini, in particular when the degree of polymerization of each block is low.

To investigate this, the RAFT part of the macro-RAFT agent Qb-2 (See **Table 3.1**) was cleaved using a typical end group removing protocol with minor modifications [63]. Typical end-group removal process was applied on macro-RAFT agent Qb-2, using benzoyl peroxide as initiator. Briefly, A mixture of macro-RAFT agent Qb-2 (0.2 g, 0.13 mmol), Benzoyl peroxide (BPO) (0.5 g, 2.06 mmol), and toluene (6 g) was placed in a round-bottom flask, sealed, and degassed with argon gas for 20 minutes. 2-Propanol was degassed with argon gas in a separate sealed round-bottom flask. The 2-propanol (6 g) was removed through a syringe equipped with a long needle and injected to the mixture. The round-bottom flask containing the mixture was then heated to 100 °C for 3 h. The completion of butyl-trithiocarbonate RAFT-end group removal was determined by ^{1}H-NMR after evaporating the volatile solvents from the product in a vacuum oven at 40 °C overnight. The ^{1}H-NMR spectrum of the product demonstrated the absence of signals associated with the butyl trithiocarbonate end group at 3.3 ppm (CH_3-$(CH_2)_2$ -CH_2-S-C(S)-S-) and 4.8 ppm (the first chain length of CH oligomer backbone adjacent to the sulfur). The evaporated product was dissolved in 2-propanol and was purified by precipitation method in a cold methanol/water mixture (80/20 v/v %) to remove the unreacted BPO.

Using this copolymer as a sole stabilizer, a stable inverse HIPE (toluene in water) was obtained. The stability of the HIPE stabilizing by end group removed Qb-2 was investigated by optical microscopy. It was found that both the toluene droplet size and the morphology of the obtained polyHIPE changed. An SEM image of the obtained polyHIPE is shown in **Figure 3.22**.

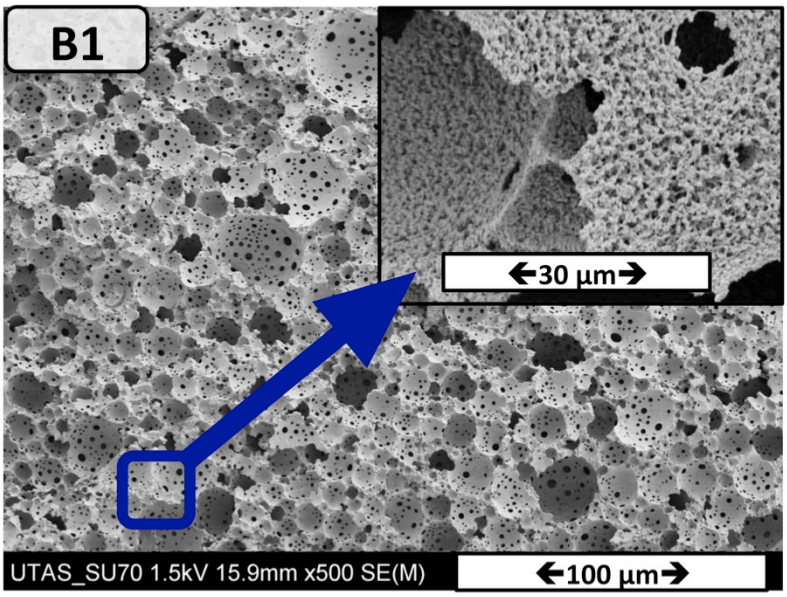

Figure 3.22. Scanning electron micrographs of emulsion templated macroporous polymer (B1) made by polymerization of HIPEs stabilized solely by end group-removed macro-RAFT agent-Qb2, polymerized at room temperature (TEMED/ KPS).

In comparison to poyHIPE A8 (**Figure 3.21**), polyHIPE B1 possess a hierarchical polyHIPE structure with an increased number of windows. This increased level of interconnectivity was demonstrated with an increase in BET specific surface area (6.75 m^2g^{-1} for B2, as opposed to 2.07 m^2g^{-1} for B1).

The elemental analysis of the obtained polyHIPE shows no sulfur and this result is confirmed by EDX-SEM mapping on the surface as well (**Figure 3.23**).

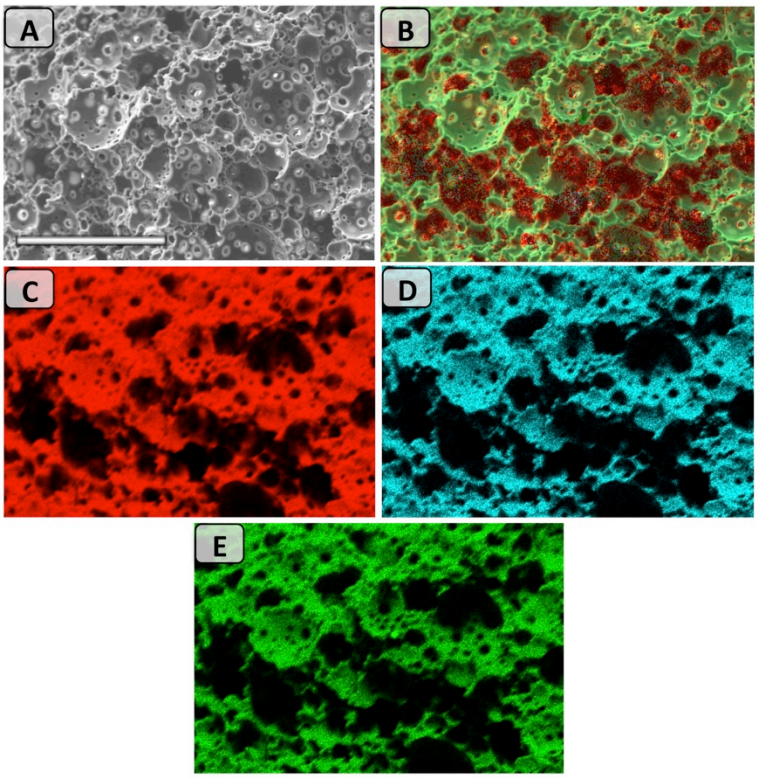

Figure 3.23. EDX mapping analysis on polyHIPE B1; (A) SEM image and (B) Overall mapping elements on the same spot: corresponding to carbon (C), nitrogen (D), and oxygen (E) mapping. Scale bar is 50 μm.

Furthermore, the incorporation of the PEO MA functionality in the obtained polyHIPE is not observed by FTIR (**Figure 3.24**).

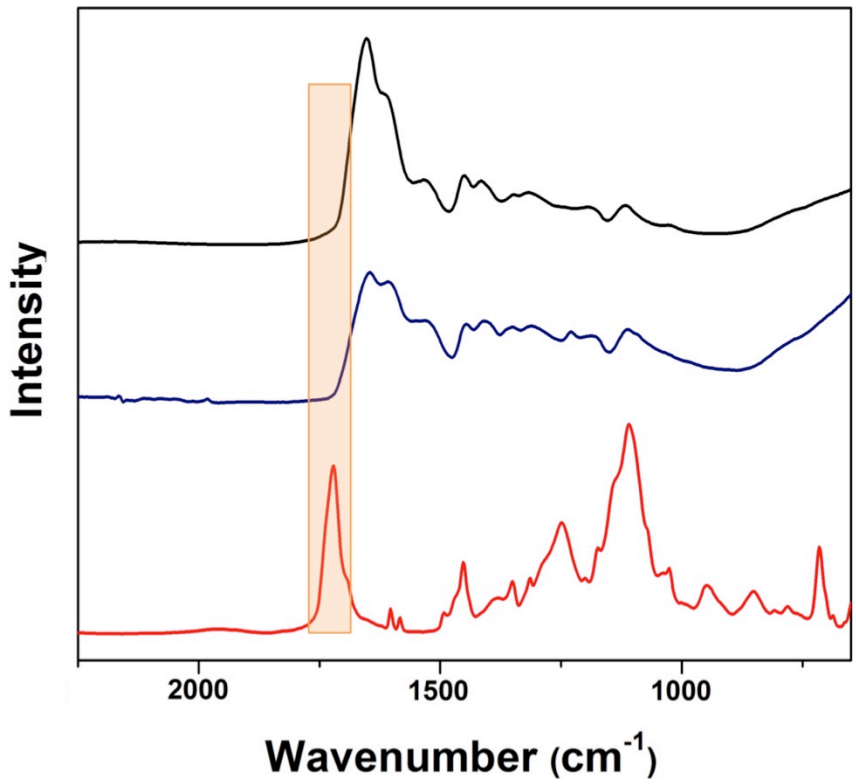

Figure 3.24. ATR-IR of end group removed copolymer-Qb2 (red line), bulk polymer (blue line) and polyHIPE B1 (black line). The peak around 1650-1850 cm^{-1} is highlighted.

Our experience with hydrophilic polyHIPEs produced via inverse HIPEs stabilized by Tween 85 (a commercially available, non-ionic surfactant) with paraffin oil as the dispersed phase showed that there is no attachment of this polyHIPE to the modified walls of a capillary format column. Similarly, no attachment of the polyHIPE B1 to the surface of the column was observed in a 150 μm ID capillary (see **Figure 3.25**).

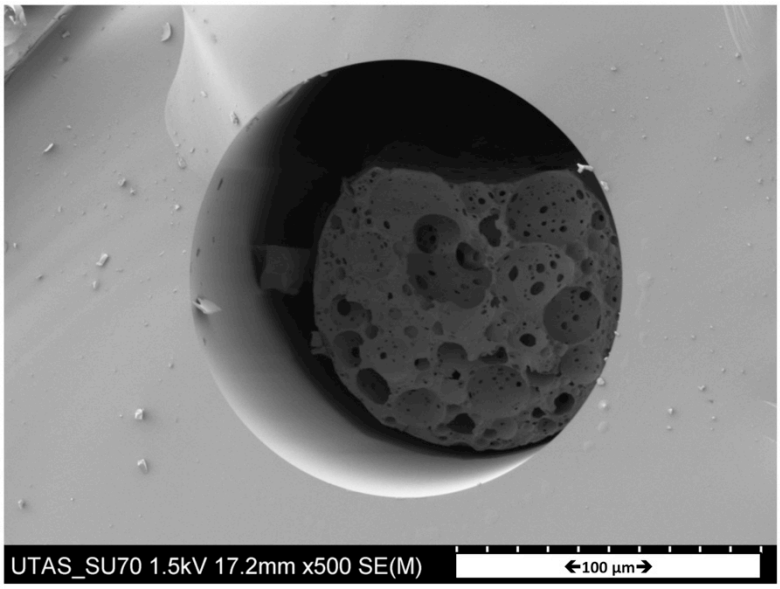

Figure 3.25. Polymerized HIPE B1 stabilized by end group removed macro-RAFT agent, in situ polymerization in 150 µm ID capillary.

The procedure was repeated in triplicate. While the polyHIPE attachment was observed in the case of sample A8, the main difference between HIPE B1 and A8 is the presence (or not) of the trithiocarbonate group in the stabilizer used. These results suggest that an end-group removed RAFT copolymer will favor the formation of a hierarchically structured polyHIPE with no attachment to the capillary format column, in comparison to the RAFT-end group enabling full attachment of the polyHIPE to the capillary wall. We believe that the RAFT-end group of the macro-RAFT agent group assures that the monolith is covalently adhered to the capillary (as the polyHIPE is remained attached to the wall after washing with a high pressure), guaranteeing the flow of liquid through the synthesized monolith. Upon removing the butyltrithiocarbonate endgroup, the anchor is changed in the way that the attachment to the capillary wall is not provided. Further investigation was performed through the preparation of the bulk polymer with and without macro-RAFT agent Qb-2 (without toluene as internal

phase). As it can be seen in **Figure 3.26**, the polymer with macro-RAFT agent is a transparent polymer, however the same recipe without the RAFT agent is forming a dispersion and the obtained polymer has a white color.

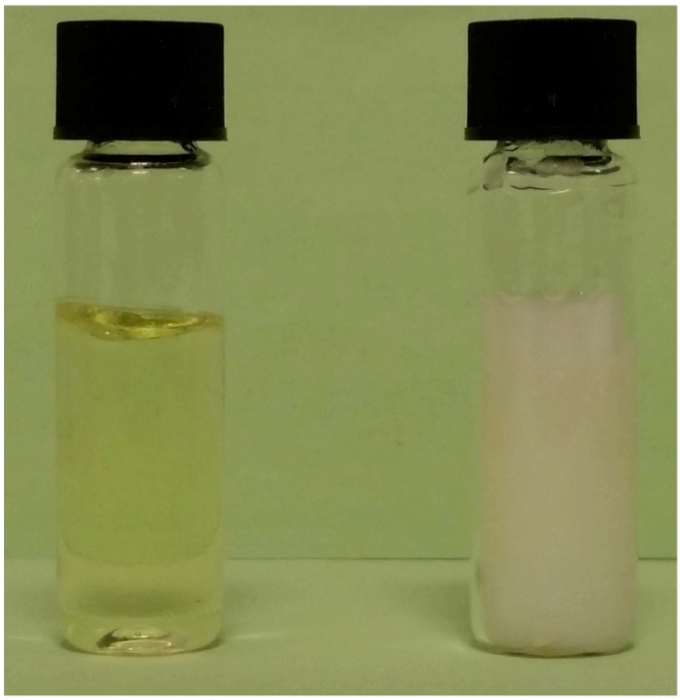

Figure 3.26. Polymerized bulk polymer in presence of macro-RAFT agent (left) and in presence of end-group removed macro-RAFT agent Qb-2 (right).

3.3.6 Evaluation of hydrophilic polyHIPE as stationary phases in HPLC

These as-prepared polymer monoliths in a capillary housing were then evaluated as stationary phases for capillary liquid chromatography. Interactions between analytes (with different polarity) and the polyHIPEs could give us information about the different microenvironments present on

the polymer surface. Two capillary columns containing polyHIPE A5 or A8 were studied. The suitability of the polyHIPE structure monoliths was assessed by measuring the backpressure of the materials at different flow rates. The backpressures obtained when both non-swelling (acetonitrile) and swelling (MilliQ-water) solvents were pumped through the polymeric monolith A8 shown in **Figure 3.27**.

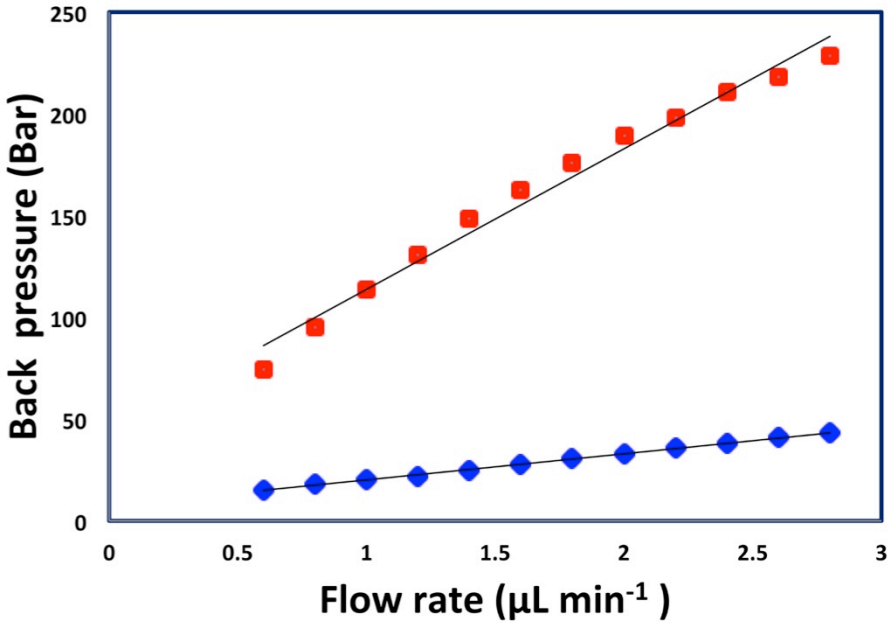

Figure 3.27. Back pressure studies on capillary A8, solvents MiliQ-water (red) and acetonitrile (blue).

Due to the poor mechanical stability of the polyHIPE A5, it is unsuitable as a stationary phase and this sample was not investigated further (**Figure 3.28**).

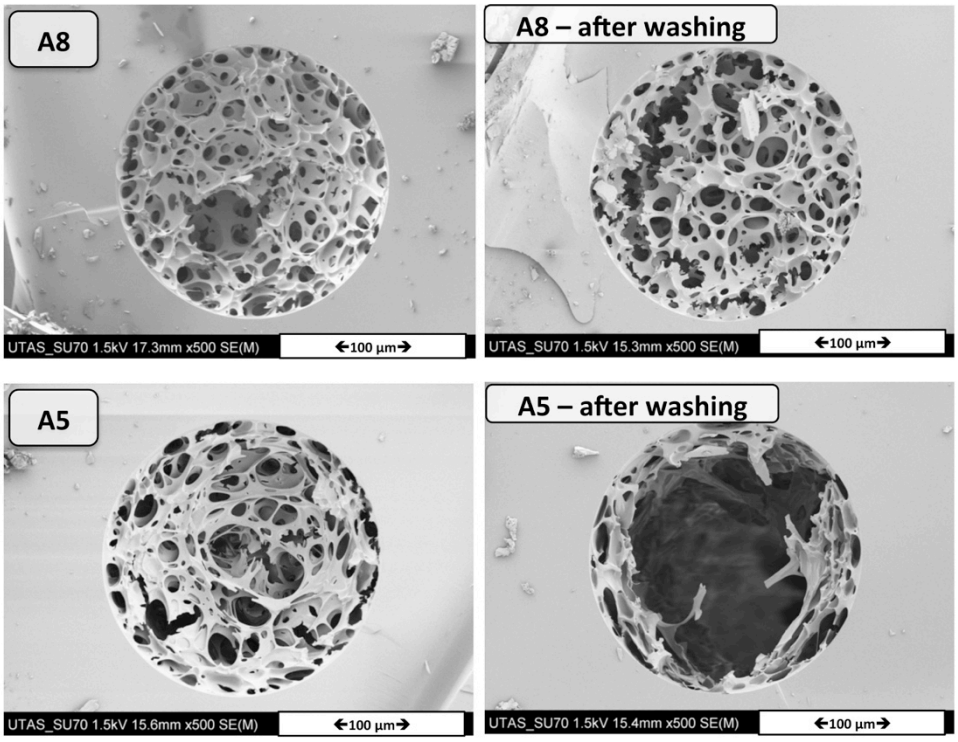

Figure 3.28. After washing of polyHIPE with water using nano-LC HPLC system

Considering the presence of amphiphilic copolymers on the surface of polyHIPEs, the materials are expected to allow the separation of both polar and non-polar analytes. The styrene part in the prepared polyHIPE induces hydrophobic interactions with nonpolar analytes while the surface coverage with PEO MA helps to retain polar analytes. The mechanism of chromatographic retention was studied using two different classes of compounds: non-polar alkylbenzenes to test for the reversed phase mode and polar hydroxybenzoic acids to test for the aqueous normal phase in hydrophilic interaction liquid chromatography (HILIC). Upon injecting the alkylbenzene mixture, the following elution order was observed:

Toluene < ethylbenzene < propylbenzene < butylbenzene < pentylbenzene

Although this order is typical for reversed phase mode, the relationship between the length of the aliphatic chain (nc) and the logarithm of the retention factor was nonlinear as shown in **Figure 3.29A**. This can be explained if another mechanism is contributing to the retention. To investigate further, a mixture of 3-hydroxybenzoic acid, 3,5 dihydroxybenzoic acid, and 3,4,5 trihydroxybenzoic acid was injected using a 80:20 ACN:Water mixture as the mobile phase. Surprisingly, the least polar analyte; 3-hydroxybenzoic acid was the first to elute followed by 3,5 dihdroxybenzoic acid, followed by 3,4,5 trihydroxybenzoic acid which is the most polar. This order clarifies that another mechanism such as HILIC, is also involved in the separation process.

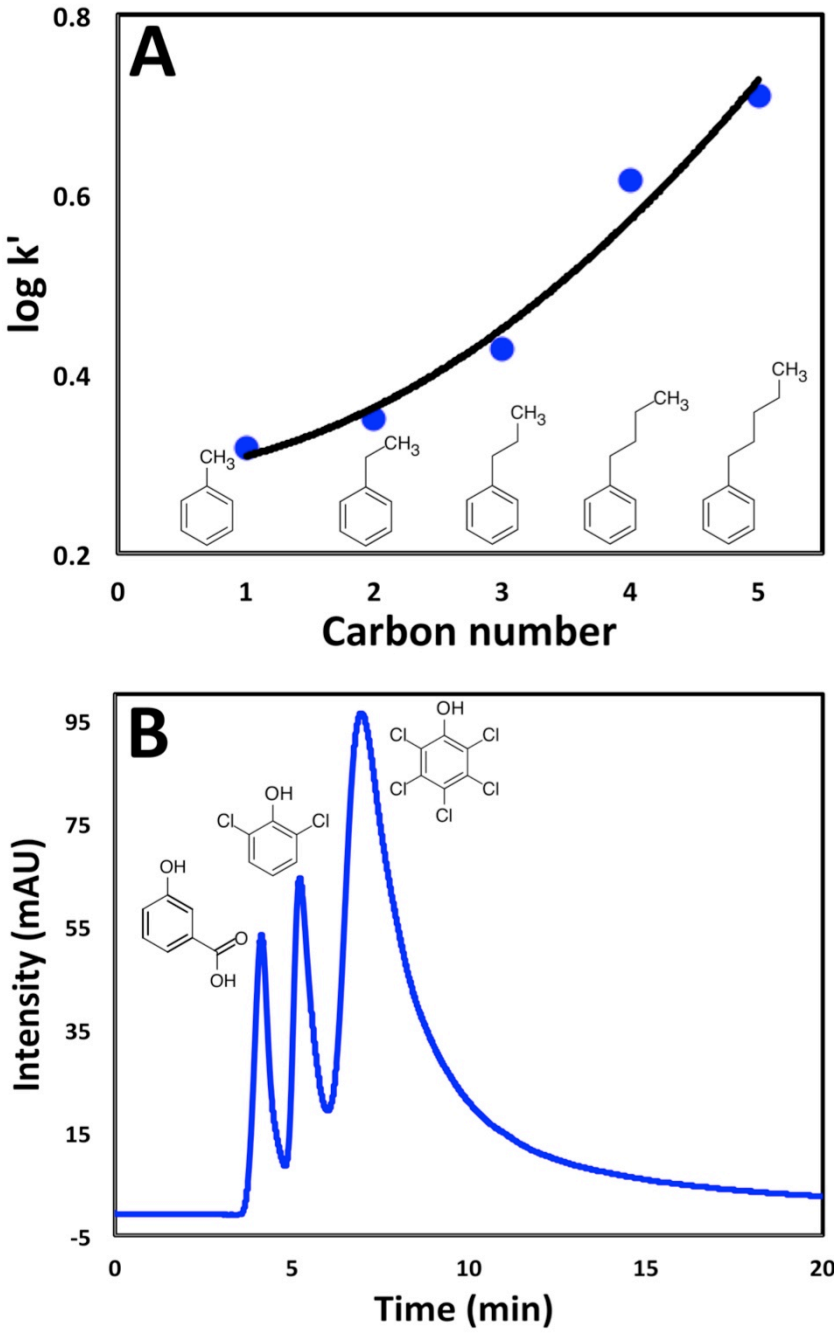

Figure 3.29. A) Methylene selectivity of the benzene derivatives (toluene, ethylbenzene, propylbenzene, butylbenzene, Pentylbenzene). B) Separation of small molecules in a mixture, from left to right: 3-hydroxybenzoic acid, 2,6-dichlorophenol and pentachlorophenol.

It is also worth mentioning that uracil, a nucleobase which normally elutes unretained in the reversed phase mode was retained to a greater extent than 3-hydroxybenzoic acid, further demonstrating the presence of hydrophilic interactions between polar analytes and the PEO patches on the stationary phase. To determine the predominant mode, the effect of mass fraction of acetonitrile (%ACN) in the mobile phase on the retention time was studied using toluene and 3-hydroxybenzoic acid; an inconsistent change in the retention time was obtained when %ACN was increased which again indicates the existence of Reversed Phase/ Hydrophilic Interaction Liquid Chromatography (RP/HILIC) mixed mode. It is important to mention here that the elution order of the two analytes was reversed at high %ACN. That means reversed phase was dominant at low %ACN while HILIC was predominant at high %ACN. The mechanical stability and efficiency of the column were also studied. The column was stable to the increasing flow rates up to 3.0 μL min^{-1} using aqueous and organic mobile phases. The column efficiency was studied by measuring the height equivalent to theoretical plates at different mobile phase velocities.

The maximum efficiency obtained was 2500 plates m^{-1}. The column permeability (K) was calculated using Darcy's law (Equation 3.1):

$$K = \frac{F \times \eta \times L}{\Delta P \times \pi \times r^2} \qquad (3.1)$$

where F is the volume flow rate of the mobile phase ($m^3.s^{-1}$) , η is the dynamic viscosity of the mobile phase (Pa.s), L is the column length (m), ΔP is the column back pressure (Pa), and r the inner radius of the column (m). The dynamic viscosity of water mobile phase at 30°C was 0.798×10^{-3} Pa.s. The calculated column permeability was found to be 3.34×10^{-14} m^2. This high permeability enables for increasing the column length and allows for further modification of the column.

As an example of applying this material to the separation of small molecules, a mixture of three analytes (3-hydroxybenzoic acid, 2,6-dichlorophenol and pentachlorophenol) was injected using 20%ACN. As shown in **Figure 3.29B**, a reasonable separation was obtained which proves that this type of stationary phases could be promising for various applications of chromatographic retention, especially under mixed mode.

3.4 Concluding remarks

PEO-based, brush-like amphiphilic macro-RAFT agent with a specific HLB value act in the same fashion as common surfactants for the stabilization of oil in water emulsions. As a result, these polymeric stabilizers can be used as a sole stabilizer of an inverse HIPE system to directly prepare hydrophilic polyHIPEs, consisting of cross-linked acrylamide in the continuous phase. The innovative nature of this approach is further illustrated by the high degree of spatial control for placement of functionalities within the monolithic structure.

Several important parameters have been identified to take into consideration for *in situ* polymerization of polyHIPE within a capillary column. Furthermore, these columns were investigated as stationary phase for high-pressure liquid chromatography. Using capillary liquid chromatography it has been shown that the polyHIPE are decorated with different microenvironments amongst the voids or domains of the monolithic structure and the result suggests the existence of RP/HILIC mixed mode with promising performance for separation of small molecules. In addition to the applied context of these materials, this work also serves as the first demonstration of the role of the RAFT group of the emulsifier in the attachment of the obtained polyHIPE to the surface of a column.

3.5 References

1. Wu, D., et al., *Design and preparation of porous polymers.* Chem Rev, 2012. **112**(7): p. 3959-4015.
2. Bartle, H. and W. v. Bonin, Makromol. Chem., 1962. **57**: p. 74-95.
3. Bartle, H. and W. v. Bonin, Makromol. Chem., 1963. **66**: p. 151-156.
4. Lissant, K.J. and K.G. Mayhan, *A study of medium and high internal phase ratio water/polymer emulsions.* Journal of Colloid and Interface Science, 1973. **42**(1): p. 201-208.
5. Barby, D. and Z. Haq, EP0060138, 1982.
6. Williams, J.M., *High internal phase water-in-oil emulsions: influence of surfactants and cosurfactants on emulsion stability and foam quality.* Langmui, 1991. **7**(7): p. 1370-1377.
7. Barbetta, A. and N.R. Cameron, *Morphology and Surface Area of Emulsion-Derived (PolyHIPE) Solid Foams Prepared with Oil-Phase Soluble Porogenic Solvents: Three-Component Surfactant System.* Macromolecules, 2004. **37**(9): p. 3202-3213.
8. Kircher, L., P. Theato, and N.R. Cameron, *Functionalization of Porous Polymers from High-Internal-Phase Emulsions and Their Applications*, in *Functional Polymers by Post-Polymerization Modification*. 2012, Wiley-VCH Verlag GmbH & Co. KGaA. p. 333-352.
9. Kovacic, S., et al., *The use of an emulsion templated microcellular poly(dicyclopentadiene-co-norbornene) membrane as a separator in lithium-ion batteries.* Macromol Rapid Commun, 2013. **34**(7): p. 581-7.
10. Shirshova, N., et al., *Polymerised high internal phase ionic liquid-in-oil emulsions as potential separators for lithium ion batteries.* Journal of Materials Chemistry A, 2013. **1**(34): p. 9612.

11. Asfaw, H.D., et al., *Emulsion-templated bicontinuous carbon network electrodes for use in 3D microstructured batteries.* Journal of Materials Chemistry A, 2013. **1**(44): p. 13750.
12. Asfaw, H.D., et al., *Nanosized LiFePO4-decorated emulsion-templated carbon foam for 3D micro batteries: a study of structure and electrochemical performance.* Nanoscale, 2014. **6**(15): p. 8804-13.
13. Zhao, C., et al., *Emulsion-templated porous materials (PolyHIPEs) for selective ion and molecular recognition and transport: applications in electrochemical sensing.* Journal of Materials Chemistry, 2007. **17**(23): p. 2446.
14. Nalawade, A.C., et al., *Inverse high internal phase emulsion polymerization (i-HIPE) of GMMA, HEMA and GDMA for the preparation of superporous hydrogels as a tissue engineering scaffold.* J. Mater. Chem. B, 2016. **4**(3): p. 450-460.
15. Hayward, A.S., et al., *Acrylic-Acid-Functionalized PolyHIPE Scaffolds for Use in 3D Cell Culture.* Macromol Rapid Commun, 2013. **34**(23-24): p. 1844-9.
16. Zhou, S., A. Bismarck, and J.H.G. Steinke, *Ion-responsive alginate based macroporous injectable hydrogel scaffolds prepared by emulsion templating.* Journal of Materials Chemistry B, 2013. **1**(37): p. 4736.
17. Oh, B.H., A. Bismarck, and M.B. Chan-Park, *High internal phase emulsion templating with self-emulsifying and thermoresponsive chitosan-graft-PNIPAM-graft-oligoproline.* Biomacromolecules, 2014. **15**(5): p. 1777-87.
18. Liu, H., et al., *Dendritic Amphiphile Mediated One-Pot Preparation of 3D Pt Nanoparticles-Decorated PolyHIPE as a Durable and*

Well-Recyclable Catalyst. ACS Appl Mater Interfaces, 2015. **7**(37): p. 20885-92.

19. Pulko, I., M. Kolar, and P. Krajnc, *Atrazine removal by covalent bonding to piperazine functionalized PolyHIPEs.* Sci Total Environ, 2007. **386**(1-3): p. 114-23.
20. Hus, S., M. Kolar, and P. Krajnc, *Separation of heavy metals from water by functionalized glycidyl methacrylate poly (high internal phase emulsions).* J Chromatogr A, 2016. **1437**: p. 168-75.
21. Barlık, N., et al., *Surface modification of monolithic PolyHIPE Polymers for anionic functionality and their ion exchange behavior.* Journal of Applied Polymer Science, 2015. **132**(29): p. DOI: 10.1002/app.42286.
22. Du, F., et al., *High-internal-phase-emulsion polymeric monolith coupled with liquid chromatography-electrospray tandem mass spectrometry for enrichment and sensitive detection of trace cytokinins in plant samples.* Anal Bioanal Chem, 2015. **407**(20): p. 6071-6079.
23. Tebboth, M., A. Kogelbauer, and A. Bismarck, *Effectiveness of Emulsion-Templated Macroporous Polymer Micromixers Characterized by the Bourne Reaction.* Industrial & Engineering Chemistry Research, 2015. **54**(22): p. 5974-5981.
24. Tebboth, M., A. Kogelbauer, and A. Bismarck, *Liquid–Liquid Extraction within Emulsion Templated Macroporous Polymers.* Industrial & Engineering Chemistry Research, 2015. **54**(29): p. 7284-7291.
25. Arrua, R.D., T.J. Causon, and E.F. Hilder, *Recent developments and future possibilities for polymer monoliths in separation science.* Analyst, 2012. **137**(22): p. 5179-89.

26. Khodabandeh, A., et al., *Preparation of inverse polymerized high internal phase emulsions using an amphiphilic macro-RAFT agent as sole stabilizer.* Polymer Chemistry, 2016. **7**(9): p. 1803-1812.
27. Mathieu, K., C. Jerome, and A. Debuigne, *Influence of the Macromolecular Surfactant Features and Reactivity on Morphology and Surface Properties of Emulsion-Templated Porous Polymers.* Macromolecules, 2015. **48**(18): p. 6489-6498.
28. Cameron, N.R., *High internal phase emulsion templating as a route to well-defined porous polymers.* Polymer, 2005. **46**(5): p. 1439-1449.
29. Livshin, S. and M.S. Silverstein, *Enhancing hydrophilicity in a hydrophobic porous emulsion-templated polyacrylate.* Journal of Polymer Science Part A: Polymer Chemistry, 2009. **47**(18): p. 4840-4845.
30. Cohen, N. and M.S. Silverstein, *One-Pot Emulsion-Templated Synthesis of an Elastomer-Filled Hydrogel Framework.* Macromolecules, 2012. **45**(3): p. 1612-1621.
31. Park, J.S. and E. Ruckenstein, *Selective permeation through hydrophobic–hydrophilic membranes.* Journal of Applied Polymer Science, 1989. **38**(3): p. 453-461.
32. Kulygin, O. and M.S. Silverstein, *Porous poly(2-hydroxyethyl methacrylate) hydrogels synthesized within high internal phase emulsions.* Soft Matter, 2007. **3**(12): p. 1525.
33. Zhang, H. and A.I. Cooper, *Synthesis of Monodisperse Emulsion-Templated Polymer Beads by Oil-in-Water-in-Oil (O/W/O) Sedimentation Polymerization.* Chemistry of Materials, 2002. **14**(10): p. 4017-4020.

34. Krajnc, P., D. Štefanec, and I. Pulko, *Acrylic Acid "Reversed" PolyHIPEs.* Macromolecular Rapid Communications, 2005. **26**(16): p. 1289-1293.
35. Ruckenstein, E. and J.S. Park, *The separation of water–ethanol mixtures by pervaporation through hydrophilic—hydrophobic composite membranes.* Journal of Applied Polymer Science, 1990. **40**(12): p. 213-220.
36. Gitli, T. and M.S. Silverstein, *Bicontinuous hydrogel–hydrophobic polymer systems through emulsion templated simultaneous polymerizations.* Soft Matter, 2008. **4**(12): p. 2475.
37. Gitli, T. and M.S. Silverstein, *Emulsion templated bicontinuous hydrophobic-hydrophilic polymers: Loading and release.* Polymer, 2011. **52**(1): p. 107-115.
38. Kovačič, S., K. Jeřabek, and P. Krajnc, *Responsive Poly(acrylic acid) and Poly(N-isopropylacrylamide) Monoliths by High Internal Phase Emulsion (HIPE) Templating.* Macromolecular Chemistry and Physics, 2011. **212**(19): p. 2151-2158.
39. Viswanathan, P., et al., *3D Surface Functionalization of Emulsion-Templated Polymeric Foams.* Macromolecules, 2014. **47**(20): p. 7091-7098.
40. Kovačič, S., D. Štefanec, and P. Krajnc, *Highly Porous Open-Cellular Monoliths from 2-Hydroxyethyl Methacrylate Based High Internal Phase Emulsions (HIPEs): Preparation and Void Size Tuning.* Macromolecules, 2007. **40**(22): p. 8056-8060.
41. Bozukova, D., et al., *Imparting antifouling properties of poly(2-hydroxyethyl methacrylate) hydrogels by grafting poly(oligoethylene glycol methyl ether acrylate).* Langmuir, 2008. **24**(13): p. 6649-6658.

42. Li, W., et al., *PEO-Based Star Copolymers as Stabilizers for Water-in-Oil or Oil-in-Water Emulsions.* Macromolecules, 2012. **45**(23): p. 9419-9426.
43. Lee, J.H. and S.H. Oh, *MMA/MPEOMA/VSA copolymer as a novel blood-compatible material: effect of PEO and negatively charged side chains on protein adsorption and platelet adhesion.* J Biomed Mater Res, 2002. **60**(1): p. 44-52.
44. Riess, G. and C. Labbe, *Block Copolymers in Emulsion and Dispersion Polymerization.* Macromolecular Rapid Communications, 2004. **25**(2): p. 401-435.
45. Siouffi, A.M., *About the C term in the van Deemter's equation of plate height in monoliths.* J Chromatogr A, 2006. **1126**(1-2): p. 86-94.
46. Ferguson, C.J., et al., *Ab Initio Emulsion Polymerization by RAFT-Controlled Self-Assembly.* Macromolecules, 2005. **38**(6): p. 2191-2204.
47. Zhao, W., et al., *Optimization of the RAFT polymerization conditions for the in situ formation of nano-objects via dispersion polymerization in alcoholic medium.* Polymer Chemistry, 2014. **5**(24): p. 6990-7003.
48. Dario Arrua, R., et al., *Monolithic cryopolymers with embedded nanoparticles. I. Capillary liquid chromatography of proteins using neutral embedded nanoparticles.* J Chromatogr A, 2013. **1273**: p. 26-33.
49. Schneider, C.A., W.S. Rasband, and K.W. Eliceiri, *NIH Image to ImageJ: 25 years of image analysis.* Nature Methods, 2012. **9**(7): p. 671-675.
50. Carnachan, R.J., et al., *Tailoring the morphology of emulsion-templated porous polymers.* Soft Matter, 2006. **2**(7): p. 608-616.

51. Chong, J.Y.T., et al., *RAFT preparation and the aqueous self-assembly of amphiphilic poly(octadecyl acrylate)-block-poly(polyethylene glycol methyl ether acrylate) copolymers.* Colloids and Surfaces A: Physicochemical and Engineering Aspects, 2015. **470**: p. 60-69.
52. Utama, R.H., M.H. Stenzel, and P.B. Zetterlund, *Inverse Miniemulsion Periphery RAFT Polymerization: A Convenient Route to Hollow Polymeric Nanoparticles with an Aqueous Core.* Macromolecules, 2013. **46**(6): p. 2118-2127.
53. Haven, J.J., et al., *One pot synthesis of higher order quasi-block copolymer libraries via sequential RAFT polymerization in an automated synthesizer.* Polymer Chemistry, 2014. **5**(18): p. 5236-5246.
54. Guerrero-Sanchez, C., et al., *Quasi-block copolymer libraries on demand via sequential RAFT polymerization in an automated parallel synthesizer.* Polymer Chemistry, 2013. **4**(6): p. 1857-1862.
55. Raffa, P., et al., *Polymeric Surfactants: Synthesis, Properties, and Links to Applications.* Chem Rev, 2015. **115**(16): p. 8504-63.
56. Binks, B.P. and S.O. Lumsdon, *Influence of particle wettability on the type and stability of surfactant-free emulsions.* Langmuir, 2000. **16**(23): p. 8622-8631.
57. Zhou, S., A. Bismarck, and J.H.G. Steinke, *Interconnected macroporous glycidyl methacrylate-grafted dextran hydrogels synthesised from hydroxyapatite nanoparticle stabilised high internal phase emulsion templates.* Journal of Materials Chemistry, 2012. **22**(36): p. 18824-18829.
58. Ford, R.E. and C.G. Furmidge, *Studies at Phase Interfaces .2. Stabilization of Water-in-Oil Emulsions Using Oil-Soluble*

Emulsifiers. Journal of Colloid and Interface Science, 1966. **22**(4): p. 331-341.

59. Cameron, N.R. and A. Barbetta, *The influence of porogen type on the porosity, surface area and morphology of poly(divinylbenzene) PolyHIPE foams.* Journal of Materials Chemistry, 2000. **10**(11): p. 2466-2471.
60. Barlow, K.J., et al., *Porous, functional, poly(styrene-co-divinylbenzene) monoliths by RAFT polymerization.* Polymer Chemistry, 2014. **5**(3): p. 722-732.
61. Ishi-i, T., et al., *Structure determination of a 1:2 threitol-boronic acid complex: Comments on the structural controversy between 5,5- and 6,6-membered rings.* Tetrahedron, 1998. **54**(30): p. 8679-8686.
62. Qu, Y., et al., *Glycoprotein recognition by water-compatible core–shell polymeric submicron particles.* J. Mater. Chem. B, 2015. **3**(19): p. 3927-3930.
63. Siauw, M., B.S. Hawkett, and S. Perrier, *RAFT Polymerization: A Powerful Tool for the Synthesis and Study of Oligomers*, in *Progress in Controlled Radical Polymerization: Materials and Applications*. 2012. p. 13-25.

4. One-pot synthesis of hydrophobic polyHIPE structure with a hydrophilic surface functionalization: Visualizing surface chemistry

4.1 Introduction

Polymerized high internal phase emulsions (polyHIPEs) are a representative type of macroporous polymer material, often with a highly interconnected structure [1-3]. Following the development of various new polyHIPE materials using amphiphilic macro-RAFT agents in chapter two and three, this chapter will investigate the influence of the RAFT end-group of a macro-RAFT agent on the morphology of the poly (styrene-*co*-divinylbenzene) foams.

Polymer porosity, homogeneity and functionality are key factors for materials to be considered as potential separation media. However, such properties are not well-defined in styrene-based polyHIPEs, in particular surface chemistry [4, 5]. As mentioned in chapter 2, a new approach for the preparation of such monoliths, which is referred to as "polymeric surfactant-assisted functionalization" has been established to offer a relatively higher control over the porosity of the obtained monolith. Compared to conventional surfactants, such polyHIPE syntheses allow preparation of a homogeneous functionalized porous monolith while the desired functionality is placed on the surface [6]. This strategy involves using reversible addition−fragmentation chain transfer (RAFT) polymerization for the preparation of polymeric surfactants as mentioned in chapter 1.

Using macro-RAFT agents has been demonstrated in the synthesis of

hydrophilic surface-modified styrene-based polyHIPEs by Debuigne *et al*. [6]. Within the same group, a series of polymerized medium internal phase emulsions (polyMIPEs) were stabilized by using the same macro-RAFT agent. The polyMIPE structure was studied in order to find the main parameters that influence the size of the voids and the windows of the porous monolith [7]. For understanding the surface chemistry, they used an indirect method, static water contact angles, which depends on the interfacial energies between the water droplet and the surface of the polyHIPE. Another example of using poly(styrene)-b-poly(acrylic acid)- macro-RAFT agent in polyHIPE was demonstrated by Luo *et al.* In this work the hydrophilic block of the macro-RAFT agent (acrylic acid) on the surface of polyHIPE was characterized by X-ray photoelectron spectroscopy (XPS) [8]. XPS analysis is widely used for surface characterization of polyHIPEs [9-15]. While this technique provides chemical information of the surface, the spatial resolution of the technique is only slightly better than fluorescence microscopy [16].

In chapter 2, a macro-RAFT agent was used as an anionic emulsifier in an inverse HIPE approach [17]. The surface chemistry of the obtained polyHIPE was mapped using RAMAN spectroscopy. In this chapter, the ability to control the morphology and functionality of the porous monolith has been targeted, while ensuring the obtained polymers possess a homogeneous structure [18, 19]. For characterization of such porous monoliths, while many of the components exist in the bulk, visualizing surface chemistry at the nanoscale is imperative.

During polyHIPE formation, it is hypothesized that quasi-block

copolymers remain on the surface of the polyHIPE structure either through physi- or chemisorption (**Figure 4.1**). Using synchrotron-based scanning transmission X-ray microscopy (STXM) as a new technique for the characterization of polyHIPE monolith with a surface spatial resolution on the order of 30-100 nm, in this chapter I test this hypothesis and report our findings.

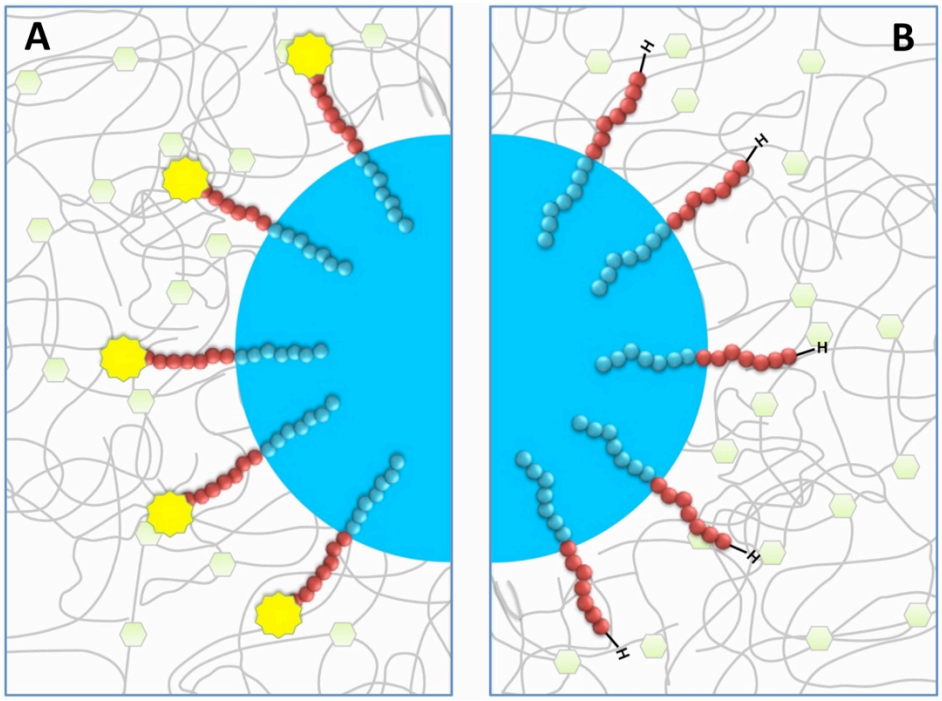

Figure 4.1. Schematic representation of the HIPE polymerization approach towards straightforward surface functionalization by acrylic acid (AA). A) Using a macro-RAFT agent and B) Using an end-group removed macro-RAFT agent as sole emulsifier (Blue circle is AA units, Red circle is styrene units and yellow star is presenting the RAFT moiety of the macro-RAFT agent).

4.2 Experimental Section

4.2.1 Materials

Styrene (Sty, Aldrich, 99%) was passed through a column of Al_2O_3 to remove the inhibitor. Acrylic acid (AA, Merck, ≥99%) was purified by distillation under reduced pressure. The RAFT agent, 2-[[(butylsulfanyl)-carbonothioyl]sulfanyl] propanoic acid (PABTC), was synthesized as described in Ref. [20]. Methanol (Fluka), basic alumina (Al_2O_3, Brockman activity I, 60-325 mesh), calcium chloride dihydrate ($CaCl_2$, APS Ajax Finechem, 98%), 4,4′-azobis(4-cyanovaleric acid) (V501, >98%, Aldrich) were all used as received. 2, 2′-azobis(isobutyronitrile) (AIBN, MP Biomedicals, Eschwege, Germany) was recrystallized from methanol.

4.2.2 Synthesis of amphiphilic surfactant by RAFT technology

A series of amphiphilic quasi-block macro-RAFT agents (Qb) consisting of AA and Sty were synthesized by some modification as reported in the literature [8]. A typical polymerization protocol that was adopted is summarized: In first step, 1 g (4.20×10^{-3} mol) of PABTC, 0.12 g (4.20×10^{-4} mol) of V501 and 1,3,5-trioxane (53 mg, 0.586 mmol) as an internal reference were introduced to a round-bottom flask which was then sealed with a rubber septum, and solids were purged with argon for 10 min. In a second step, 1.82 g (2.52×10^{-2} mol) of acrylic acid (AA) was then dissolved in 50 mL of dioxane before addition to a flask to obtain a solution. This was purged with argon for 10 min. The reaction was allowed to proceed at 80°C for 3 h under constant stirring.

After quenching the reaction in an ice bath, a small aliquot of the solution was removed for ^{1}H NMR analysis. Styrene (Sty) and V501 were then added to the round bottom flask at a molar ratio (relative to the initial chain

transfer agent concentration) equal to the desired number of monomer repeat units per macro-RAFT agent. The mixture was further purged with argon for 10 min and further polymerization for 12 h at 80°C was performed, after which a small aliquot of the solution was removed for SEC and ^{1}H NMR analysis. The product macro-RAFT agent was collected by precipitation of the above mixture in water and then water was removed via freeze-drying of the macro-RAFT agents at -30 °C under reduced pressure for at least 100 hours (**Figure 4.2**).

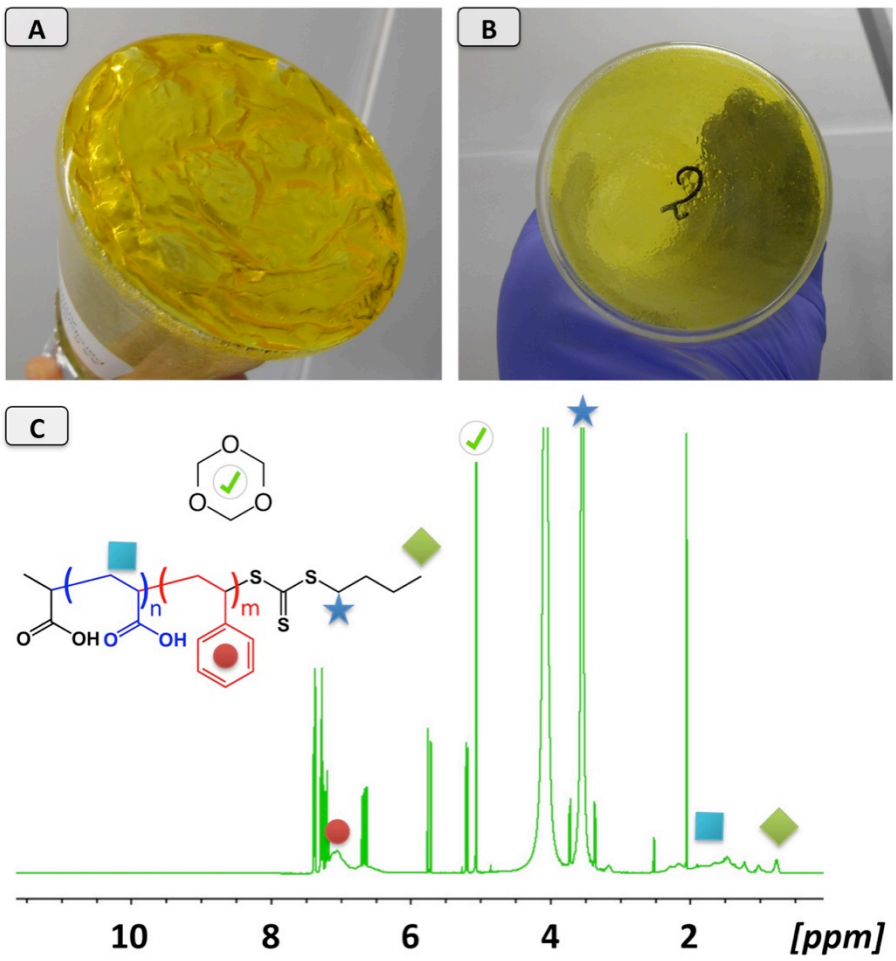

Figure 4.2. A) Macro-RAFT agent Qb-1 B) Macro-RAFT agent Qb-2. C) ^{1}HNMR spectra of macro-RAFT agent Qb-1 (DMSO-d6).

To investigate the effect of the RAFT moiety, the RAFT end group of the macro-RAFT agents were cleaved using a typical protocol with minor modifications (see Chapter 3). The polymer was then stored at 4 °C until use. **Table 1** shows the characteristic data for the P(AA)-qb-P(Sty) diblock copolymers synthesized in this study. **Figure 4.3** shows the general synthesis of AA_m-b-Sty_n quasi-block copolymers.

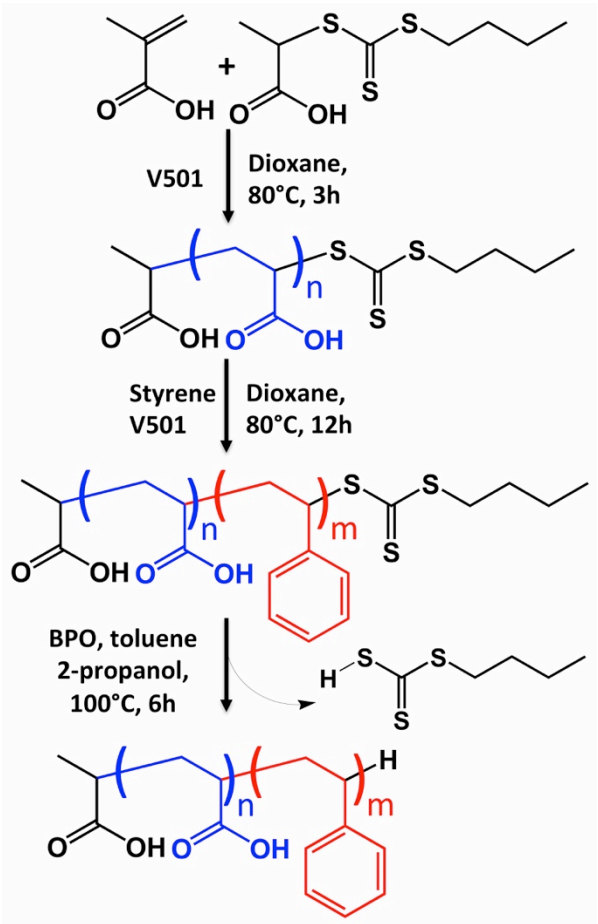

Figure 4.3. General synthesis of the P(AA)-qb-P(Sty) amphiphilic quasi-block copolymers

Table 4.1. Amphiphilic surfactant synthesized in this study

$(AA)_X$-qb-$(Sty)_Y$	X (feed) (AA)[a]	Y (feed) (Sty)[a]	$M_{n,\,SEC}$ (g mol^{-1}) [1]	Đ
Qb-1	6	12	1291	1.19
Qb-2	3	6	1015	1.12
End group removed-Qb-1	6	12	1245	1.19
End group removed-Qb-2	3	6	902	1.12

[1] Determined by SEC in THF (Calibration Sty).

4.2.3 Polymerization of styrene-based polyHIPEs

The quasi-block copolymer and AIBN as initiator were dissolved in styrene and divinylbenzene and an aqueous phase containing calcium chloride (to suppress the Ostwald ripening) was added drop-wise to an aqueous solution of macro-RAFT agent with a desired concentration at a rate of 0.8 mL min^{-1} with constant stirring (magnetic stirrer) at 1000 rpm. The emulsion was then stirred at 14000 rpm using a homogenizer for 2 minutes (Ultra Turrax T 25 IKA, 7.5 mm rotor, Germany). The emulsion was transferred to a mold (a glass container) and cured in a water bath at 65 °C for 24 h. The resulting polyHIPE was purified via Soxhlet extraction with methanol for 48 hours as well as 48 hours with water. The purified monolith was dried under vacuum oven for at least 72 h to constant weight under vacuum at 30 °C. Four different types of polyHIPEs were prepared by varying the type of quasi-block copolymers used in the polymerization process. **Table 4.2** lists the structural properties of different polyHIPEs prepared in this chapter.

Table 4.2. Morphological features of polyHIPE samples.

Sample code	macro-RAFT agent	%wt	**(SEM) (µm)**	
			<D> (1)	<d> (1)
A1	Qb-1	10	5.35	-
A2	Qb-2	10	4.39	-
A3	End group removed Qb-1	10	-	-
A4	End group removed Qb-2	10	4.65	0.81

A void describes the pores of the PolyHIPE and <D> is average size of voids. Window refers to the interconnecting pores between two adjacent droplets and <d> is average size of windows.

4.2.4 Characterization techniques

NMR analyses was performed using a Bruker Ultra Shield Avance Spectrometers (600 MHz). For all NMR analyses deuterated solvents were used as stated. Size exclusion chromatography (SEC) was performed using a Viscotec instrument using a refractive index detector (RID) and two chromatography columns (two PSS S linear 3 µm, Polymer Standard Services GmbH, PSS) and THF (HPLC grade) as eluent (flow rate 0.5 mL min^{-1}). The column oven was kept at 40 °C. All polymer samples were dissolved overnight in the eluent at a concentration ~ 2 mg mL^{-1}, then filtered through a 450 nm Nylon filter. The calculated molecular weights were based on calibration with respect to polystyrene (PSt) standards spanning a mass range of 160 to 154000 g mol^{-1} (PSS-Polymer Laboratories). The standards were prepared (2 mg mL^{-1}) and injected.

PolyHIPEs were characterized by field emission gun scanning electron microscopy (FE-SEM) studies using a Hitachi SU-70 FESEM in the Central Science Laboratory, University of Tasmania. All samples were platinum coated for 15 s in an argon atmosphere (Emitech 550,

Emitech Ltd., UK). The calculation of the average voids and windows diameter (in the case of any) was performed on sets of at least 100 voids and 100 windows, respectively, using the image analysis software ImageJ (NIH image) [21]. A statistical correction was employed to obtain more accurate value by using a correction factor of $2/(3^{1/2})$, as described by Carnachan *et al.*[22].

The composition of the material was examined by EDX experiments where the materials were sputter-coated with carbon (Ladd 40000 carbon evaporator) before analysis. Sulfur content was analyzed using CHNS elemental analyzes using a Thermo Finnigan EA 1112 Series Flash Elemental Analyser. The sample mass was about 15 mg. FTIR spectra were recorded using a Bruker Vertex 70 infrared spectrometer equipped with an ATR probe coupled with a Hyperion 3000 (FPA - microscope). X-ray photoelectron spectroscopy (XPS) was performed on a Kratos Axis Ultra DLD equipped with a monochromatic Al Kα source (1486.6 eV). Each sample was analyzed at an emission angle normal to the sample surface. Wide-scan spectra (1100 – 0 eV) were acquired at a pass energy of 160 eV and high resolution C 1s spectra were acquired at 20 eV. Data were processed with CasaXPS (ver.2.3.16 Pre rel. 1.6, Casa Software Ltd). Bright field TEM images were obtained at the McMaster Faculty of Health Sciences electron microscopy facility using a JEOL 1200EX operating at 80 kV.

STXM measurements were performed using the STXM at the BL4U beamline at the UVSOR Synchrotron (Okazaki, Japan). This instrument has been described previously in Ref. [23]. After introducing the sample into the main STXM chamber, the chamber was evacuated and was filled with helium gas to 60 mbar. The STXM measurements in this case required ~ 2 h of beamtime and a further 2 h of data analysis. The transmitted intensity (I) of the particles or

reference materials was normalized by the transmitted intensity (I_0) through Si_3N_4 windows without the sample to yield the optical density OD = -ln(I/I_0). All STXM data analysis was performed using the aXis2000 software provided by Prof. Adam Hitchcock, McMaster University, Canada [24].

Techniques for preparing the thin section samples are similar to those used for transmission electron microscopy (TEM). Briefly, the polyHIPE was embedded with an aliphatic epoxy resin consisting of a 1:1 mixture of trimethylolpropane triglycidyl ether (TTE) and an alicyclic amine, 4,4′ -methylene bis (2-methylcyclohexylamine) (MMCA), and was cured overnight at 60 °C. The embedded sample was then ultramicrotomed at room temperature into ~100 nm thin sections which were floated on distilled water and picked up onto Formvar-coated 100 mesh Cu TEM grids.

4.3 Results and discussion

4.3.1 Morphology control in polyHIPEs via macro-RAFT agent composition

In order to determine the influence of the RAFT moiety of the macro-RAFT agents on the morphology and the surface chemistry, control polyHIPEs A1 and A2 were synthesized using the macro-RAFT agent Qb-1 and Qb-2 (10% w.r.t. the continuous phase), respectively. Both polyHIPEs A1 and A2 possess closed morphology with average void diameters of 5.35 μm and 4.39 μm, respectively (**Figure 4.4** and **Table 4.2**). This confirmed that while the HLB number (hydrophilic-lipophilic balance [11]) of both macro-RAFT agent is the same, the

lower molecular weight macro-RAFT agent was able to stabilize HIPE with a smaller average droplet size and as result smaller voids in the obtained polyHIPE A2.

Furthermore, by using the end group removed-Qb-1 (10 wt%) as a sole stabilizer the successful stabilization of HIPE (A3) was obtained. It was found that both the water droplet size and the morphology of the obtained polyHIPE was different to that of A1. An SEM image of the obtained polyHIPE is shown in **Figure 4.4**. In comparison to poyHIPE A1, polyHIPE A3 possess an interconnected polyHIPE structure with an increased number of windows.

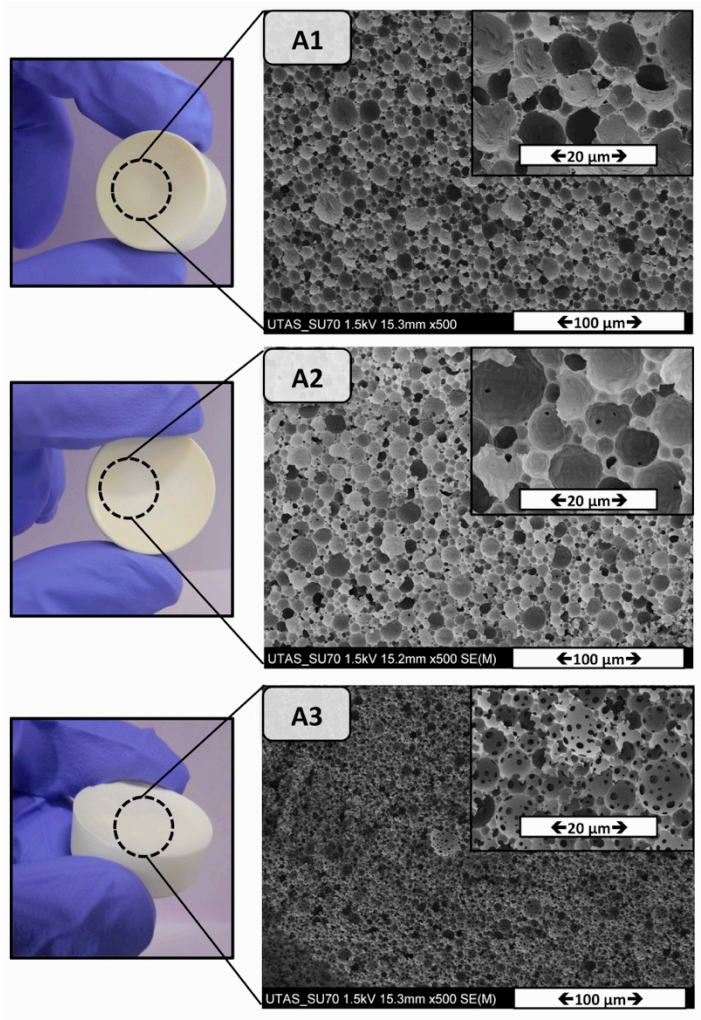

Figure 4.4. Scanning electron micrographs of emulsion template macroporous polymer made by polymerization of HIPEs stabilized solely by A1) macro-RAFT agent-Qb1, A2) macro-RAFT agent-Qb2, and A3) end group removed-Qb-1 at 65 °C in presence of AIBN as initiator.

The end group removed-Qb-2 (10 wt%) was also used as sole stabilizer but there was rapid phase separation, indicating the importance of the RAFT moiety for stabilizing the system (**Figure 4.5**).

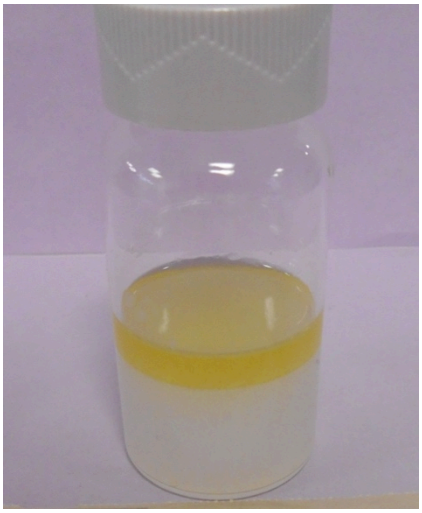

Figure 4.5. Phase separation after preparation of HIPE A4 formulation.

It has been shown previously that reducing the possibility of interfacial initiation of the emulsion templated polymerization by removing the RAFT moiety has a significant effect on porosity of the resultant polyHIPE [6]. It was observed that removing the RAFT moiety of a nonionic polymeric surfactant resulted in materials with an open structure; here we demonstrate the same trend with an anionic polymeric surfactant.

4.3.2 Compositions of polyHIPE containing quasi-block copolymers

It has been reported that the presence of the RAFT-end group in amphiphilic copolymers increases the hydrophobicity of the copolymer [25]. To further investigate the inclusion of the quasi-block copolymer within the polyHIPE structure, FTIR analyses were performed on the resultant materials, in comparison to a sample of poly (styrene-*co*-divinylbenzene) polymerized in bulk (AIBN as initiator) subjected to the same washing protocol. A difference

between the bulk polymer and polyHIPE A1 and A3 was found (**Figure 4.6A**). This result confirmed the presence of the carbonyl group in both polyHIPEs A1 and A3. Further, the FTIR mapping technique confirmed the presence of the C=O groups in the same physical location as the walls of the polyHIPE voids, which are due to the carboxylic group of the acrylic acid segment (**Figure 4.6B**).

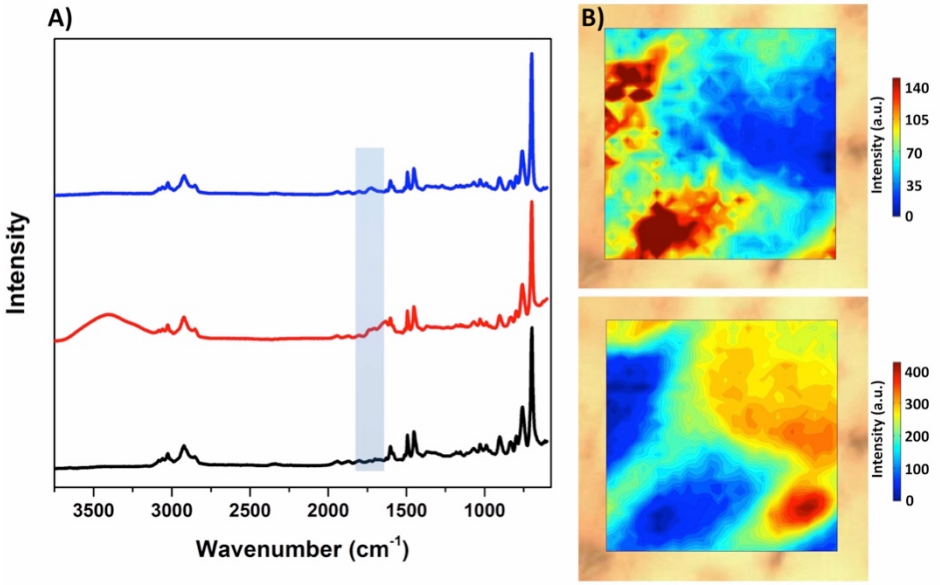

Figure 4.6. A) ATR-IR of bulk polymer (black line), polyHIPE A1 (red line), and polyHIPE A3 (blue line) (from bottom to top). The peak around 1650- 1850 cm^{-1} is highlighted. B) FTIR mapping (upper) is based on the normalized carboxylic peak: (C=O/C=C) (1725 – 1770 cm^{-1}) peak area divided on aromatic carbon-carbon double bond peak area (2800 – 3000 cm^{-1}). FTIR mapping (bottom) based on signal to baseline from 2800 to 3000 cm^{-1} at the same area (Dark blue regions in the lower image are void locations within the polyHIPE. The size of the image of the FTIR maps is 30×30 μm).

The FTIR spectra of the polyHIPE A3 is very similar to the polyHIPE A1. So, the same protocol for FTIR mapping characterization was

applied in polyHIPE A3. Unfortunately the attachment of the scanning probe to the surface of the polyHIPE A3 was not successful and the results lacking the necessary chemical sensitivity (as in the case of scanning probe technologies).

Further evidence for the presence of the macro-RAFT agent on the surface of the polyHIPE was obtained from Energy Dispersive X-ray analysis (EDX), clearly indicating that oxygen was present at the surface of the polyHIPE A3 (**Figure 4.7**).

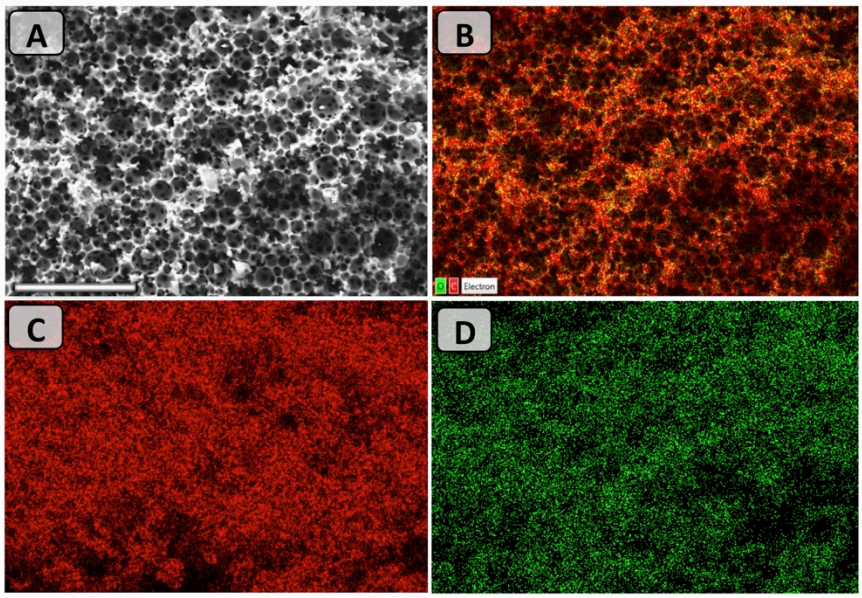

Figure 4.7. EDX mapping analysis on polyHIPE A3; (A) SEM image and (B) Overall mapping elements on the same spot: corresponding to carbon (C), and oxygen (D) mapping. Scale bar is 50 μm.

The most likely explanation for this observation is that the quasi-block copolymer (or end-group removed Qb-1) is adsorbed to the surface of the polyHIPE A3. For polyHIPE A1, sulfur and oxygen were revealed which are come from macro-RAFT agent Qb-1. Calcium and chloride (from $CaCl_2$) were also present on the surface. This shows that the

washing protocol for the closed-structure polyHIPE A1 was not able to wash out the co-stabilizer (**Figure 4.8**).

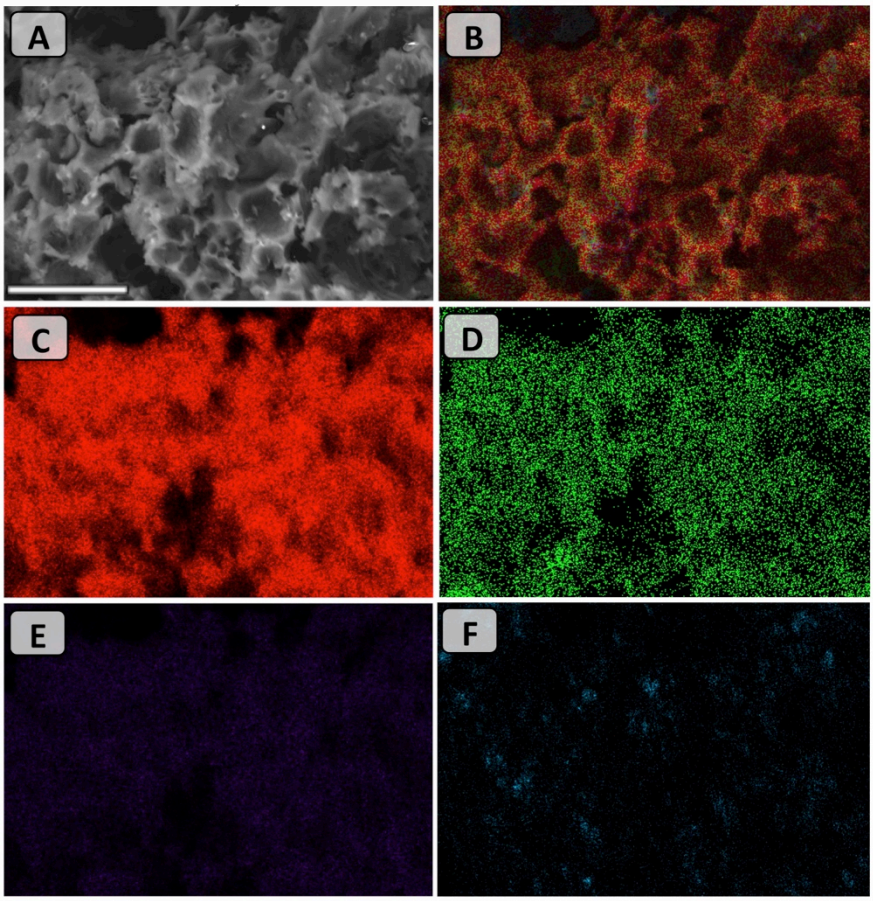

Figure 4.8. EDX mapping analysis on polyHIPE A1; (A) SEM image and (B) Overall mapping elements on the same spot: corresponding to carbon (C), oxygen (D), calcium (E), and chloride (F) mapping. Scale bar is 10 μm.

Elemental analysis also confirmed the presence of sulfur amount within the polyHIPE A1 (see **Table 4.3**.).

Table 4.3. Elemental analysis data

Sample ID	N%	C%	H%	S%
Bulk polymer	0.17	90.76	8.23	0.00
PolyHIPE A1	0.18	80.56	7.79	0.69
PolyHIPE A3	0.09	85.72	8.41	0.00

In addition to the EDX-SEM and elemental analysis results, which show evidence for presence of the quasi-block copolymer on the surface of polyHIPEs, polyHIPEs A1 and A3, and poly (styrene-*co*-divinylbenzene) were further evaluated by X-ray Photoelectron Spectroscopy (XPS). The high-resolution C 1s spectrum for polyHIPE A1 is shown in **Figure 4.9** with the quantification results of wide-scan relative elemental composition shown in the inset.

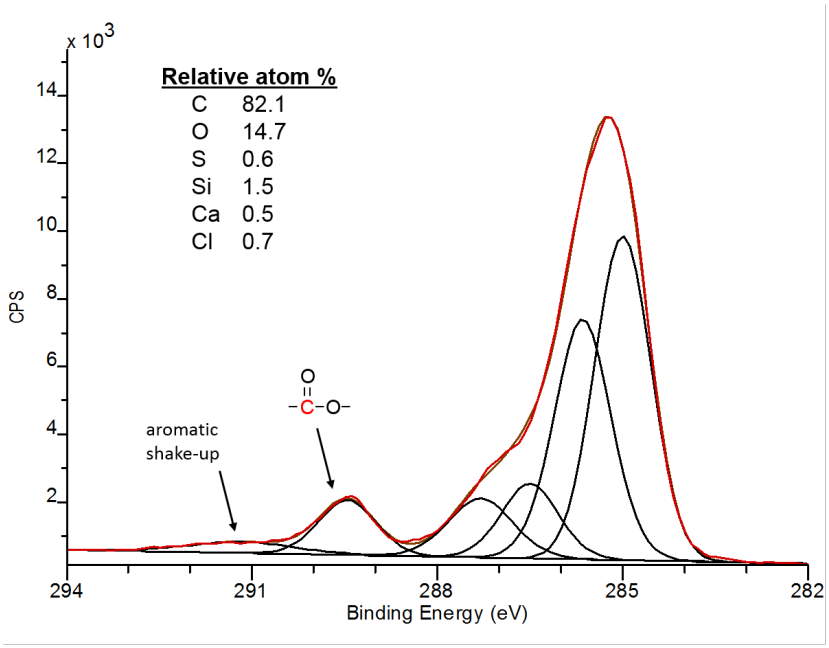

Figure 4.9. High-resolution C 1s spectrum for polyHIPE A1 with quantification of wide-scan data inset. Carbon binding environments (in black) were fit to the spectrum envelope (red).

Table 4.4. XPS analysis data

Sample ID	C%	O%	S%	Si%	Ca%[1]	Cl%[1]
RAFT Agent	72.8	18.5	5.9	2.8		
Poly HIPE A1	82.1	14.7	0.6	1.5	0.5	0.7
Poly HIPE A3	95.4	3.9	0.7			
Poly (styrene-*co*-DVB) Bulk polymer	96.5	2.9	0.7			

Calcium Chloride was dissolved in aqueous phase to suppress the Ostwald ripening.

In addition to the large abundance of C and O, a small amount of S was present as expected. Additionally, there was evidence of trace amounts of Ca, Cl and Si from the synthesis and contamination. Component peak fitting of the C 1s spectrum shows evidence for carboxylic acid and aromatic functionalities consistent with the polymer structure. In contrast, the polyHIPE A3 spectrum had a higher abundance of carbon, and lower abundance of oxygen (C = 95.4 %, O = 3.9 %) which was quantitatively and qualitatively similar to the spectrum for bulk poly (styrene-*co*-divinylbenzene) (Table 4.4). As ejected photoelectrons originate from the outermost 10 nm of the sample, XPS analysis indicates a higher surface presentation of aromatic groups in the A3 sample compared to the A1 sample.

4.3.3 PolyHIPE Characterization by Scanning Transmission X-ray Microscopy (STXM)

There is a drawback in all the above characterization methods for revealing the surface chemistry, mainly related to the resolution of these techniques. While all above characterization methods are powerful analytical techniques, the ability of these techniques to deliver the chemical composition distribution of polyHIPE A3 are limited.

In our group, scanning transmission X-ray microscopy (STXM) has been shown to be a powerful imaging technique that provides chemical selectivity and high spatial resolution of ~35 nm for the characterization of monoliths as support phases for liquid chromatography [19]. STXM is basically a synchrotron-based technique which combines near edge X-ray absorption fine structure (NEXAFS) spectroscopy and soft X-ray scanning microscopy. Chemical contrast is obtained from differences in NEXAFS carbon K-edge spectra, which arise due to differences in the π* anti-bonding orbitals of the blend materials [26]. This powerful technique provides a relatively rapid chemical imaging of polymer using a sequence of highly resolved X-ray photon, enabling an excellent spatial resolution and a possibility for quantitative analysis [27-29].

STXM imaging was conducted by focusing on the C 1s core-line signal in NEXAFS. This region was selected because the chemical environment of the carbon atoms (such as aromatic carbon-carbon double bond) is of particular interest for the present systems. In this technique spectra can be acquired over a small region. **Figure 4.10** shows the C 1s NEXAFS spectra obtained for the cross-linked styrene network area of both polyHIPEs (A1 and A3). Reference spectra of the pure polymeric components were also recorded with the same instrument: macro-RAFT agent Qb-1, RAFT agent (PABTC) and the epoxy which was used to embed the polyHIPEs.

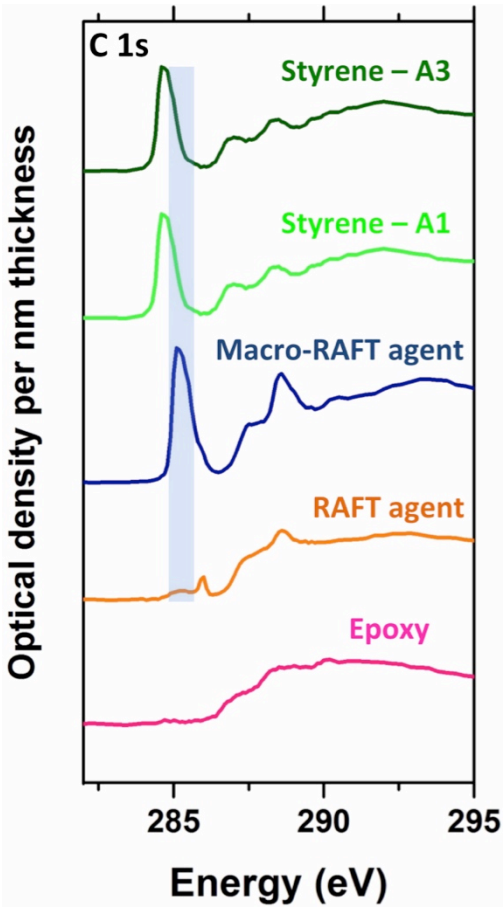

Figure 4.10. NEXAFS reference spectra of the epoxy (embedding matrix), RAFT agent, macro-RAFT agent, and polystyrene cross-linked polyHIPEs that correspond to 1 nm thickness of each component.

The spectrum for the cross-linked styrene-based scaffold has a strong peak at 284.6 eV, which is characteristic of C 1s → π*C=C transition in phenyl ring. The macro-RAFT agent spectrum shows two peaks: a strong peak at 284.9 eV, which corresponds to the C 1s → π*C=C transition of the phenyl ring (styrene of macro-RAFT agent) and a peak at 288.9 eV, which is characteristic of C 1s → π*C=O transition in esters. In comparison to the RAFT agent spectrum, the intensity of peak at 288.9 eV has been increased due to acrylic acid incorporation

to the macro-RAFT agent. It is also important to mention that the epoxy resin has little or no absorption at these energies and therefore there is excellent contrast between the resin, the scaffold, and the macro-RAFT agent.

TEM images of the polyHIPEs A1 and A3 are shown in **Figure 4.11.** This technique gives information about the inner cross-sectional area of the polyHIPE.

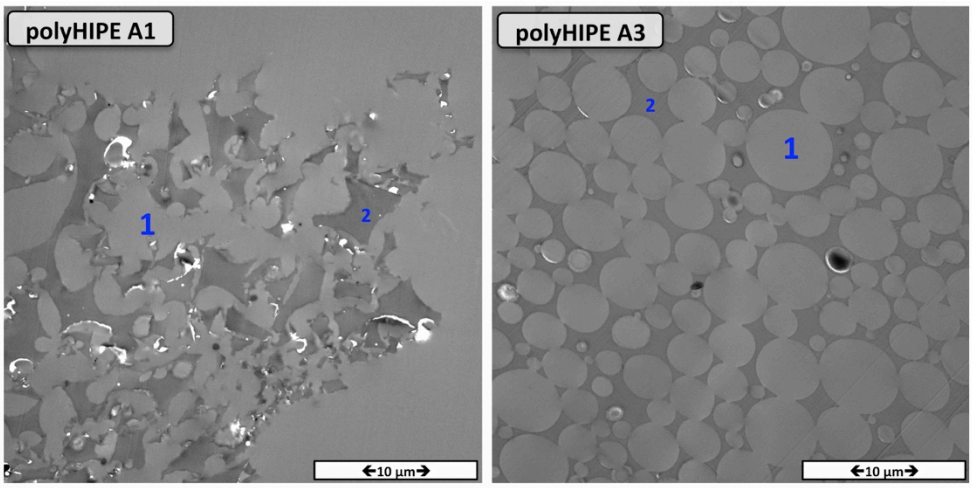

Figure 4.11. TEM images of polyHIPEs: (a) polyHIPE A1 and (b) polyHIPE A3 embedded in epoxy. The zones are: the epoxy embedding materials (1), the cross-linked poly (styrene-*co*-divinylbenzene) (2). The scale bar is 10 µm.

Using a sequence of highly resolved X-ray photon energies covering the C 1s spectral region (280 to 320eV), successive images were obtained for polyHIPE A1 and A3. A STXM composite component map of polyHIPE A3 was created (**Figure 4.12**) with respect to the corresponding X-ray spectra of reference materials; the macro-RAFT agent Qb1, poly (styrene-*co*-divinylbenzene) crosslinked polymer

network and epoxy components are shown in blue, green, and red, respectively.

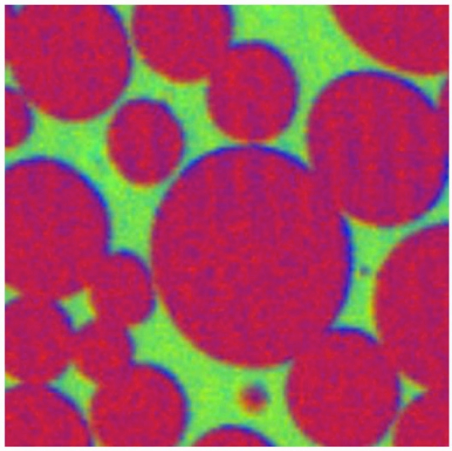

Figure 4.12. STXM color coded composite map (red=epoxy, green=PSty, blue=macro-RAFT agent on the surface of polyHIPE A3).

The following features can be noticed in the representative selection of micrographs reported in **Figure 4.12**: (i) it can be seen clearly that the macro-RAFT agents fully cover the interface between void and scaffold (blue). (ii) The data from inside the void has been masked by epoxy which was used embedded polyHIPEs (red). For polyHIPE A1, STXM composite component map is shown in **Figure 4.13**. The same features as polyHIPE A3 were observed in STXM map.

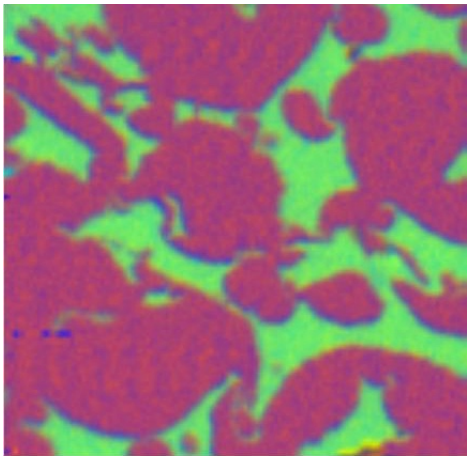

Figure 4.13. STXM color coded composite map of polyHIPE A1 (red=epoxy, green=PSty, blue=macro-RAFT agent).

4.4 Concluding remarks

A hydrophilic coating is introduced to the poly (styrene-*co*-divinylbenzene) by using a straight forward strategy in order to anchoring poly(acrylate) to the surface. The void size of the polyHIPEs was tunable by tailoring the macro-RAFT agent composition: Possess closed structure when HIPE stabilized by macro-RAFT agent and possess open homogenous template polyHIPE when the RAFT agent of the amphiphilic macro-RAFT agent has been cleaved prior stabilizing the HIPE. The surface chemistry of the polyHIPE has been revealed by FTIR mapping, EDX-SEM, XPS as well as STXM.

Soft X-ray microscopy images recorded at multiple wavelengths have been used to qualify the chemical composition in polyHIPE. This capability is being used for mapping of the surface of polyHIPE. This methodology was found to be effective in spectroscopically mapping the distribution of macro-RAFT agent on the surface of macroporous polyHIPE monolith. The results shown in this work clearly

demonstrate how STXM analysis can reveal chemical information for these materials.

4.5 References

1. Cameron, N.R. and D.C. Sherrington, *High internal phase emulsions (HIPEs) — Structure, properties and use in polymer preparation.* Adv. Polym. Sci., 1996. **126**: p. 163-214.
2. Silverstein, M.S., *Emulsion-templated porous polymers: A retrospective perspective.* Polymer, 2014. **55**(1): p. 304-320.
3. Silverstein, M.S., *PolyHIPEs: Recent advances in emulsion-templated porous polymers.* Prog. Polym. Sci., 2014. **39**(1): p. 199-234.
4. Wu, D., et al., *Design and preparation of porous polymers.* Chem. Rev., 2012. **112**(7): p. 3959-4015.
5. Arrua, R.D., T.J. Causon, and E.F. Hilder, *Recent developments and future possibilities for polymer monoliths in separation science.* Analyst, 2012. **137**(22): p. 5179-5189.
6. Mathieu, K., C. Jerome, and A. Debuigne, *Influence of the Macromolecular Surfactant Features and Reactivity on Morphology and Surface Properties of Emulsion-Templated Porous Polymers.* Macromolecules, 2015. **48**(18): p. 6489-6498.
7. Mathieu, K., C. Jérôme, and A. Debuigne, *Macro- and near-mesoporous monoliths by medium internal phase emulsion polymerization: A systematic study.* Polymer, 2016. **99**: p. 157-165.
8. Luo, Y., A.-N. Wang, and X. Gao, *One-pot interfacial polymerization to prepare PolyHIPEs with functional surface.* Colloid and Polymer Science, 2015. **293**(6): p. 1767-1779.
9. Zhang, Y., et al., *HIPEs template: Towards the synthesis of polymeric catalysts with adjustable porous structure, acid–base*

strength and wettability for biomass energy conversation. Chemical Engineering Journal, 2016. **283**: p. 956-970.

10. Zhang, Y., et al., *Hierarchically Macro-/Mesoporous Polymer Foam as an Enhanced and Recyclable Catalyst System for the Sustainable Synthesis of 5-Hydroxymethylfurfural from Renewable Carbohydrates.* ChemPlusChem, 2016. **81**(1): p. 108-118.
11. Viswanathan, P., et al., *3D Surface Functionalization of Emulsion-Templated Polymeric Foams.* Macromolecules, 2014. **47**(20): p. 7091-7098.
12. Langford, C.R., D.W. Johnson, and N.R. Cameron, *Chemical functionalization of emulsion-templated porous polymers by thiol–ene "click" chemistry.* Polym. Chem., 2014. **5**(21): p. 6200-6206.
13. Hayward, A.S., et al., *Acrylic-Acid-Functionalized PolyHIPE Scaffolds for Use in 3D Cell Culture.* Macromol Rapid Commun, 2013. **34**(23-24): p. 1844-9.
14. Hayward, A.S., et al., *Galactose-Functionalized PolyHIPE Scaffolds for Use in Routine Three Dimensional Culture of Mammalian Hepatocytes.* Biomacromolecules, 2013. **14**(12): p. 4271-7.
15. Ungureanu, S., et al., *One-Pot Syntheses of the First Series of Emulsion Based Hierarchical Hybrid Organic−Inorganic Open-Cell Monoliths Possessing Tunable Functionality (Organo−Si(HIPE) Series).* Chemistry of Materials, 2007. **19**(23): p. 5786-5796.
16. Hitchcock, A.P., et al., *Soft X-Ray Microscopy of Soft Matter — Hard Information from Two Softs.* Surface Review and Letters, 2002. **09**(01): p. 193-201.
17. Khodabandeh, A., et al., *Preparation of inverse polymerized high internal phase emulsions using an amphiphilic macro-RAFT agent as sole stabilizer.* Polymer Chemistry, 2016. **7**(9): p. 1803-1812.

18. Dario Arrua, R. and E.F. Hilder, *Highly ordered monolithic structures by directional freezing and UV-initiated cryopolymerisation. Evaluation as stationary phases in high performance liquid chromatography.* RSC Adv., 2015. **5**(87): p. 71131-71138.
19. Arrua, R.D., et al., *Characterization of polymer monoliths containing embedded nanoparticles by scanning transmission X-ray microscopy (STXM).* Anal Chem, 2014. **86**(6): p. 2876-81.
20. Ferguson, C.J., et al., *Ab Initio Emulsion Polymerization by RAFT-Controlled Self-Assembly.* Macromolecules, 2005. **38**(6): p. 2191-2204.
21. Schneider, C.A., W.S. Rasband, and K.W. Eliceiri, *NIH Image to ImageJ: 25 years of image analysis.* Nature Methods, 2012. **9**(7): p. 671-675.
22. Carnachan, R.J., et al., *Tailoring the morphology of emulsion-templated porous polymers.* Soft Matter, 2006. **2**(7): p. 608-616.
23. Ohigashi, T., et al., *Construction of the Scanning Transmission X-ray Microscope Beamline at UVSOR.* Journal of Physics: Conference Series, 2013. **463**: p. 012006.
24. Hitchcock, A.P., *aXis 2000 is written in Interactive Data Language (IDL), 2015. It is available free for non-commercial use from,* http://unicorn.mcmaster.ca/.
25. Chong, J.Y.T., et al., *RAFT preparation and the aqueous self-assembly of amphiphilic poly(octadecyl acrylate)-block-poly(polyethylene glycol methyl ether acrylate) copolymers.* Colloids and Surfaces A: Physicochemical and Engineering Aspects, 2015. **470**: p. 60-69.
26. Stöhr, J., *NEXAFS Spectroscopy*. 1992, Berlin: Springer.

27. Urquhart, S.G., et al., *NEXAFS spectromicroscopy of polymers: overview and quantitative analysis of polyurethane polymers.* Journal of Electron Spectroscopy and Related Phenomena, 1999. **100**(1-3): p. 119-135.
28. McNeill, C.R., et al., *Nanoscale quantitative chemical mapping of conjugated polymer blends.* Nano Lett, 2006. **6**(6): p. 1202-6.
29. Hitchcock, A.P., et al., *Chemical Mapping of Polymer Microstructure Using Soft X-ray Spectromicroscopy.* Australian Journal of Chemistry, 2005. **58**(6): p. 423.

5. General conclusions and future perspectives

The following general conclusions summarise the main findings of this thesis which explores a novel method for the synthesis of porous polymeric monolith materials, with potential further applications as a stationary phase in separation science.

As mentioned in the Preface, the structural inhomogeneity of polymer-based monoliths can adversely affect their separation efficiency. More homogeneous structures can be obtained by polymerising high internal phase emulsions (HIPEs), which consist of a highly porous structure with interconnected spherical voids (known as polyHIPEs).

Chapter 2 investigated the preparation of an inverse (oil-in-water) HIPE, using an amphiphilic macro-RAFT agent with toluene as the internal dispersed phase and an aqueous monomer solution as the continuous phase. The presence of this amphiphilic polymeric surfactant allowed the successful preparation of a polyHIPE upon polymerization. Varying the lengths of the hydrophilic and hydrophobic blocks of the macro-RAFT agent resulted in polyHIPEs with different porous structures. The presence of RAFT functionality in the polyHIPE was confirmed by a combination of characterisation techniques used to improve the understanding of the surface chemistry. In particular, Raman mapping revealed full coverage of the void walls with trithiocarbonate groups.

As mentioned in Chapter 2, by using a KPS/TEMED redox couple as the initiating system, a polyHIPE with a regular porous structure was obtained via polymerization at room temperature. While I demonstrated the synthesis of polyHIPE at room temperature is essential with respect to the

homogeneity of the structure, the presence of KPS is a source of sulfur in the subsequent analysis of the material. Considering the sulfur amount from macro-RAFT agent, it would be interesting to utilize initiating systems by γ-ray radiation method at room temperature. In such a case elemental analysis will directly quantify the macro-RAFT agent incorporation into the material. The use of radiation methods for polymerization of polyHIPE would be also be of interest.

Radiation-based methods offer additional control over the polymerisation of polyHIPE. In this case, the mechanism of the attachment of the macro-RAFT agent on the surface of the polyHIPE (physic- or chemisorption) could be studied in detail, especially respect to understanding the presence of two extra peaks (observed at ~985 and 1000 cm^{-1}) in the RAMAN spectrum of the polyHIPE which were not seen in either bulk or macro-RAFT agent spectra (**Figure 5.1**). The identity of these peaks is unknown and could be attributed to species formed via traditional chemical initiation.

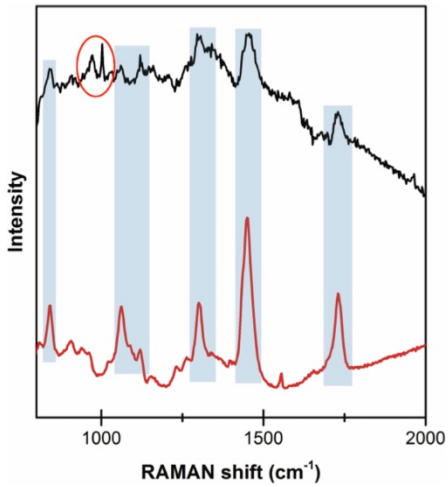

Figure 5.1. Raman spectra of macro-RAFT agent-Qb1 (Red line), difference between polyHIPE A3 and bulk polymer (Black line) (Reprint from Chapter 2).

Chapter 3 described the application of hydrophilic polyHIPEs as a possible stationary phase in High Performance Liquid Chromatography (HPLC). The functionalized polyHIPE was prepared in a capillary column based on the method that was developed in Chapter 2. The amphiphilic brush copolymers of Poly(poly(ethylene glycol) methyl ether acrylate)-qb-Poly(Styrene) were produced to use as stabilizer. The PEO-based "brush-like" monomers were used in order to increase stabilization due to a larger surface area occupied per chain and the higher surface mobility of this block. While all demonstrated polyHIPE examples in separation science consist of polymers that are hydrophobic in nature, which limits their applications in separation science, this work represents (to the best of our knowledge) the first hydrophilic polyHIPE prepared inside a capillary column.

A capillary format was chosen as a 'column housing' for hydrophilic polyHIPE to be evaluated as stationary phases for nano-Liquid chromatography. I systematically studied the effect of concentration, monomer amount in the aqueous phase and capillary internal diameter as a "column housing" in order to prepare high interconnected, hydrophilic polyHIPE monoliths. We also showed that the RAFT functionality on the surface of the polyHIPE materials provide a powerful substrate for subsequent surface chemistry reactions and that this offers exciting possibilities for future applications of materials prepared in this way. Further, the importance of the RAFT moiety of the macro-RAFT agent on the attachment of the polyHIPE to the inner surface of column was highlighted. The surface chemistry of obtained polyHIPE was studied by liquid chromatography with respect to the retention time of different compounds in different modes of chromatography such as reversed phase (RP) and hydrophilic interaction liquid chromatographic (HILIC).

An investigation on the macro-RAFT composition on the stability of HIPEs would be interesting, especially by using a random block copolymer, which is expected to improve the stability and as a result, a more homogeneous polyHIPE structure. Further investigation into decorating these materials with different functional groups would be of great interest. This could be achieved by using different hydrophobic monomers followed by investigation of different hydrophilic monomers and number of units to determine the effect of the polymeric surfactant on void size and their surface chemistry. The suggested future work would be decorated these materials with different functional groups. Hence, a range of well-defined polyHIPE columns with almost any functionality on the surface can be accessed including ion-exchange, affinity, chiral, and mixed-mode.

The applications described in this chapter lay the groundwork for other potential research that could be performed with polyHIPE. While it has been shown that the polyHIPE monolith can separate small molecules with a reasonable performance, there is still significant work to be done improving column performance. For example, optimization of flow rates, column lengths, injection volumes, and on column pressures would allow improvements in chromatographic performance. As stationary phase materials, the future of polyHIPE monolithic for use in separation science holds exciting prospects for fast sample preparation as well as for liquid-liquid extraction. Also, the obtained polyHIPE appears to offer new opportunities for use as supports in batch or flow-through chemical reactions, which can be targeted for future investigations.

Chapter 4 investigated the synthesis and surface characterization of “normal,” styrene-based polyHIPEs where the macro-RAFT agent (Poly(styrene)-Qb-Poly(acrylic acid)) used as sole stabilizer. As a result, a hydrophilic coating was

introduced to the styrene-based polyHIPE through a straight forward strategy in order to anchoring poly(acrylic acid) to the surface. FTIR surface mapping confirmed the presence of the carbonyl groups in the same physical location as the walls of the polyHIPE voids, solely due to the carboxylic group of the poly(acrylic acid) segment of the stabilizer.

I further explored the effect of the RAFT moiety of the macro-RAFT agent on the morphology of the obtained polyHIPEs. In the absence of RAFT moiety, an open porous structure was formed. This interconnectivity is essential for considering materials for flow-through application such as separation science. The surface chemistry of the open structure is similarly important. In this case, prepared polyHIPEs were fully characterized by FTIR spectroscopy, FTIR mapping, SEM, SEM-EDX, TEM, XPS as well as synchrotron-based scanning transmission X-ray microscopy (STXM). The latter technique was particularly informative, revealing the surface chemistry of the obtained polyHIPEs and macro-RAFT agent multicomponent with an excellent surface spatial resolution. These series of the powerful characterisation techniques are essential to understand the surface chemistry of obtained polyHIPEs.

This work highlights that there is still a considerable need to gain a broader understanding of polyHIPE surface chemistry. While these findings demonstrated the suitability of the obtained functionalized polyHIPE to be considered as a separation media, further work is necessary to gain a precise insight into the limitations of surface area.

In summary, this thesis documents the development of a novel technology to allow straightforward functionalization of obtained polyHIPEs via a

surfactant-assisted functionalization strategy, to create new classes functionalized porous media. A series of advanced characterization techniques were utilized to understand the surface chemistry of the resulting polyHIPEs. The application of hydrophilic-based polyHIPE was evaluated as a stationary phase for nano-Liquid Chromatography, with exciting potential applications into the future.